Amino-, Amido- and Oxy-bipyridyl Complexes of Copper, Ruthenium, Molybdenum and Rhodium

by

Francesco Luigi Bernardis B.Sc. (Hons.), (Natal)

A thesis submitted in partial fulfilment of the requirements for the degree of Master of Science in the Faculty of Science, University of Natal, Pietermaritzburg

Department of Chemistry
University of Natal
Pietermaritzburg
December 1996

Declaration

I hereby certify that this research is the result of my own investigation which has not already been accepted in substance for any degree and is not being submitted in candature for any other degree.

Signed:.....

F. Bernardis

I hereby certify that this statement is correct.

Signed:.....

Professor R.J. Haines

(Supervisor)

Signed:.....

Professor J.S. Field

(Co-supervisor)

Department of Chemistry

University of Natal

Pietermaritzburg

December 1996

Dedico quest'opera alla memoria dei miei nonni.

Contents

Acknowledgements

I wish to thank Professors **R.J. Haines** and **J.S. Field** for their guidance and input throughout the course of this investigation.

I am also grateful to the following persons:

Mr Martin Watson and **Mrs Zöe Hall** for the recording of NMR spectra, the running of GCMS samples and for their assistance and training in the operation of these instruments;

Miss Niyum Ramesar for her contribution to all X-ray crystal structure determinations with regard to data collection and computation;

Mr James Ryan for elemental analysis;

Mr Paul Forder for the construction and repair of glassware;

Mr Dave Crawley for technical assistance;

Mssrs. Chris Morewood, Les Mayne, Dave Gregory, Roelie Hendriks, Darrel Leibbrandt and **James Ryan** from the Faculty of Science Mechanical Instrument workshop for the repair and construction of various instruments and for their contribution towards keeping my Alfa Romeo on the road;

My research colleagues for their advice;

The **Foundation for Research and Development** and the **University of Natal** for financial support;

My family for their support.

Abbreviations and Symbols

Å	Angstrom
abipy	anion of 6-anilino-2,2'-bipyridine
ap	anion of 2-anilinopyridine
BAII	bis (pyridylimino) isoindoline
bipy	2,2'-bipyridine
bmanapy	2-benzylamido-7-methyl-1,8-naphthyridine
bpnp	bis 2-(2-parietal)-1,8-naphthyridine
C	Celsius
chp	anion of 6-chloro-2-hydroxypyridine
δ	chemical shift in parts per million
DH	monoanion of dimethylglyoxime
fhp	anion of 2-hydroxy-6-fluoropyridine
g	gram
Habipy	6-anilino-2,2'-bipyridine
Hap	6-anilinopyridine
Hhp	2-hydroxypyridine
Hmhp	2-hydroxy-6-methylpyridine
Hobipy	2,2'-bipyridin-6-one
hp	anion of 2-hydroxypyridine
I	iso
Im	imidazole
IR	infrared
L	ligand
M	transition metal
mabipy	6-N-methylanilino-2,2'-bipyridine
map	anion of 2-amino-6-methylpyridine
mg	milligram
mhp	anion of 2-hydroxy-6-methylpyridine
mmol	millimol

ν	frequency
napy	1,8-naphthyridine
Nhpy	2-aminopyridine
obipy	anion of 2,2'-bypyridin-6-one
Ph_2Pbipy	6-diphenylphosphino-2,2'-bipyridine
pipbipy	6-piperidino-2,2'-bipyridine
py	pyridine
pynp	2-(2-pyridyl)-1,8-naphthyridine
Rap	2-aminopyridyl ligands
THF	tetrahydrofuran
tbp	tris (pyrazoyl) borate
TsO	tosylate

List of Complexes Synthesised

$[Cu(\eta^2\text{-mabipy})_2](PF_6)$	**1**
$[Cu(\eta^2\text{-pipbipy})_2](PF_6)$	**2**
$[Cu(\eta^2\text{-Habipy})_2](PF_6)$	**3**
$[Cu(\eta^2\text{-mabipy})_2](ClO_4)_2$	**4**
$[Ru_2(\mu\text{-abipy})_2(CO)_4]$	**5**
$[Ru_2(\mu\text{-obipy})_2(CO)_4]$	**6**
$[Ru_2(\mu\text{-abipy})(O_2CCH_3)_3Cl]$	**7**
$[Mo_2(\mu\text{-abipy})(O_2CCH_3)_3]$	**8**
$[Rh_2(\mu\text{-abipy})(O_2CCH_3)_3(H_2O)]$	**9**

Summary

The work described in this thesis concerns the synthesis and study of the coordination behaviour of the 6-anilino-2,2'-bipyridyl (Habipy), 6-N-methylanilino-2,2'-bipyridyl (mabipy), 6-piperidyl-2,2'-bipyridyl (pipbipy) and 2,2'-bipyridin-6-one (Hobipy) ligands.

Chapter one reviews the coordination chemistry of the 2-aminopyridyl (Rap), 2-hydroxypyridyl (Hhp) and the 2-(2-pyridyl)-1,8-naphthyridine (pynp) ligands. These ligands are closely related to Habipy, mabipy, pipbipy and Hobipy in that they share a common NCN or NCO fragment. Thus the review of their coordination behaviour provides insight into the expected coordination of the Habipy, mabipy, pipbipy and Hobipy ligands.

The synthesis and characteristaion of the novel Habipy, mabipy and pipbipy ligands are reported in Chapter two. X-ray crystal structure determinations of mabipy and pipbipy reveal that the geometry about the exocyclic nitrogen atom in both ligands is nearly planer, suggesting substantial overlap of the nitrogen lone pair orbital with the π electron system of the bipyridyl rings. In both mabipy and pipbipy the N3-C10 bond lengths are shorter then normal N-C single bonds.

In Chapter three the synthesis and characterisation of copper(I) complexes containing mabipy, pipbipy and Habipy, and a copper(II) complex containing mabipy are reported. The copper(I) complexes have the general formula $[Cu(\eta^2\text{-}L)_2]^+$, where L= mabipy **1**, pipbipy **2** or Habipy **3**. The structures of complexes **1** and **2** are determined by X-ray crystallography. In complexes **1- 3** the bipyridyl fragments of mabipy, pipbipy and Habipy chelate while the exocyclic nitrogen atoms remain free. The crystal structures of **1** and **2** reveal that the exocyclic nitrogens have a planar geometry as was the case in the uncoordinated ligand. The crystal structure of $[Cu(\eta^2\text{-mabipy})_2]^{2+}$ (**4**) is determined by X-ray crystallography and is very similar to that of the copper(I) species. Coordination of the mabipy ligand in **4** is the same as that in **1** and the exocyclic nitrogen in **4** is also planar. The redox couple **4/1** is shown to be electrochemically reversible with $E_{1/2}$= 0.45 V.

In Chapter four the synthesis and chararcterisation of dinuclear complexes containing the Ru_2^{2+}, Ru_2^{5+}, Mo_2^{4+} and Rh_2^{4+} cores are reported in which the abipy ligand bridges two metal centres.

The complexes $[Ru_2(\mu\text{-}L)_2(CO)_4]$, where L= abipy **5** or obipy **6**, were synthesised by the reaction of the free ligands with $[\{Ru_2(CO)_4(O_2CCH_3)_2\}_n]$ in toluene. The structures of **5** and **6** are determined by X-ray crystallography and show the ligands bridging the Ru(I) atoms in a head to tail fashion and occupy mutually *cis* positions about the octahedral Ru(I) atoms. The Ru-Ru separations in **5** and **6** are 2.668(1) and 2.671(1) Å respectively. The reaction of Habipy with $[Ru_2(O_2CCH_3)_4Cl]_n$ was found to afford the mixed valence species $[Ru_2(\mu\text{-abipy})(O_2CCH_3)_3Cl]$ (**7**), the structure of which is determined by X-ray diffraction methods. The structure of **7** reveals one abipy ligand bridging the two ruthenium atoms as in **5**. The Ru-Ru separation in **7** is 2.294(2) Å. The reaction of $[Mo_2(O_2CCH_3)_4]$ with habipy in methanol affords $[Mo_2(\mu\text{-abipy})(O_2CCH_3)_3]$ (**8**). The structure of **8** is determined by X-ray diffraction methods and reveals one abipy ligand bridging two quadruply bonded molybdenum atoms which have a Mo-Mo separation of 2.094(2) Å. The $[Rh_2(\mu\text{-abipy})(O_2CCH_3)_3(H_2O)]$ (**9**) is formed from the reaction of $[Rh_2(O_2CCH_3)_4]$ with Habipy in methanol. The structure of $[Rh_2(\mu\text{-abipy})(O_2CCH_3)_3(NCPh)]$ is determined by X-ray diffraction methods and shows the abipy ligand bridging two Rh(II) atoms which are separated by 2.399(1) Å. This chapter is concluded with a discussion of the possiblity of substitution of more than one acetate ligand by the abipy ligand in terms of 'hard' and 'soft' acid-base theory and synthetic methods.

Chapter one

The coordination chemistry of 2-amino and 2-hydroxy substituted pyridyl ligands and of the 2-(2-pyridyl)-1,8-naphthyridyl ligand

The work described in this thesis concerns the synthesis and the study of the coordination behaviour of the 6-anilino-2,2'-bipyridyl (Habipy), 6-N-methylanilino-2,2'-bipyridyl (mabipy), 6-piperidyl-2,2'-bipyridyl (pipbipy) and 2,2'-bipyridyl-6-one (Hobipy) ligands. The first three ligands are new whereas the last mentioned ligand, though known, has not as yet been studied with regard to its coordination behaviour. This chapter reviews the coordination chemistry of a selection of closely-related ligands with a view to providing insight into the expected coordination behaviour of the Habipy, mabipy, pipbipy, and Hobipy ligands. The ligands selected are: the 2-aminopyridyl (Rap), 2-hydroxypyridyl (Hhp) and the 2-(2-pyridyl)-1,8-naphthyridyl (pynp) ligands.

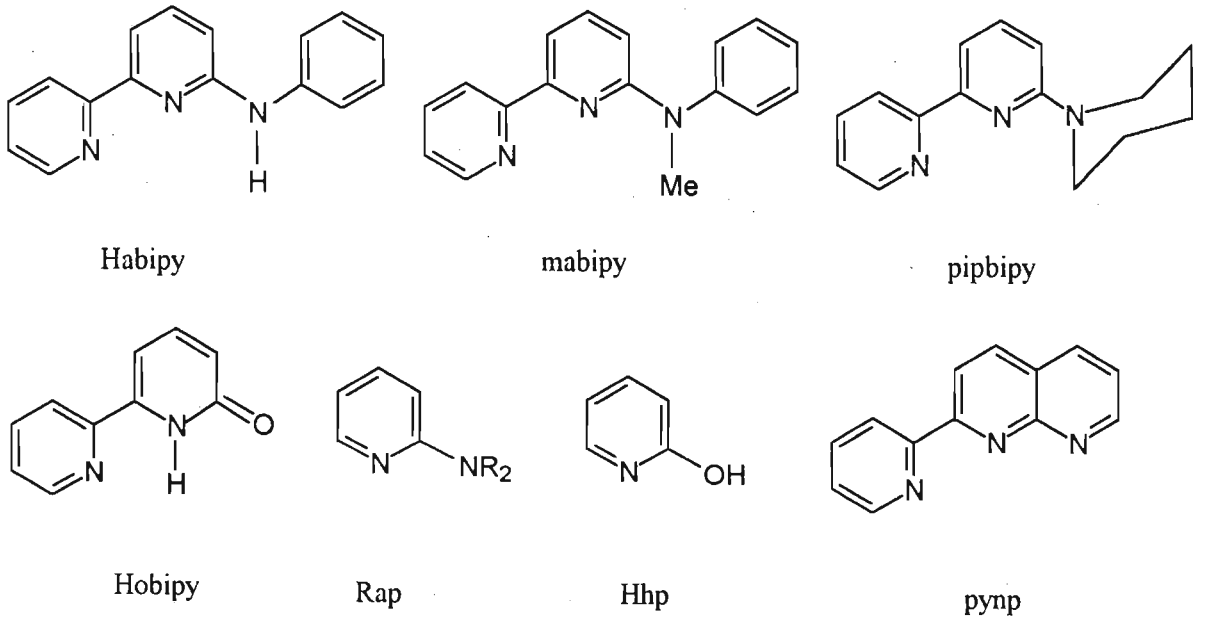

Fig. 1.1 : Structural formulae of the ligands studied and reviewed in this thesis

The 2-amino and 2-hydroxypyridyl ligands are similar to their bipyridyl analogues in that a common NCN or NCO fragment is shared. However, whereas the amino and hydroxy substituted bipyridyl ligands are potentially tridentate ligands, their pyridyl analogues are potentially bidentate.

The potentially tridentate 2-(2-pyridyl)-1,8-naphthyridyl ligand is more closely related to the 6-aminobipyridyl ligands in this respect.

In view of the many similarities between the amino and hydroxypyridyl ligands with regard to their structures and coordination chemistry, these ligands will be discussed together.

1.1 2-Amino and 2-hydroxypyridyl ligands

One important feature of the primary or secondary aminopyridyl ligands on the one hand and hydroxypyridyl ligands on the other, is the presence of a relatively acidic proton on the exocyclic amino or hydroxy group respectively. These acidic protons can be abstracted to yield anionic ligands capable of assuming two resonance forms:

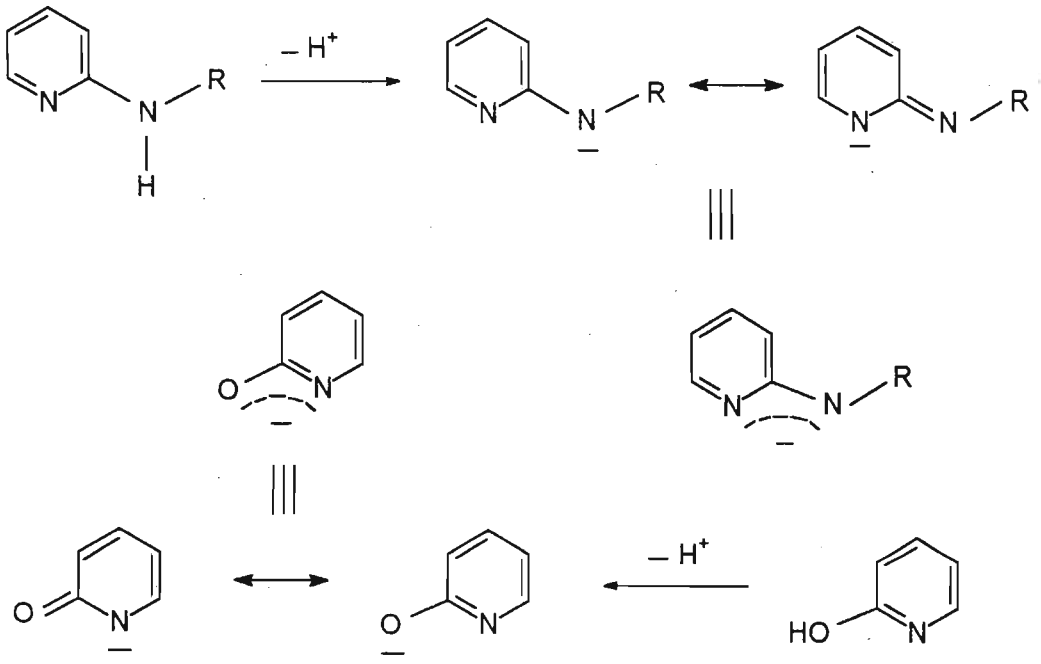

Fig. 1.2 : Resonance forms of 2-amino and 2-hydroxypyridine

Extensive work has been carried out regarding the coordination of these anionic ligands[1] which warrants their separate discussion from the neutral ligands.

1.1.1 The anionic form of the 2-aminopyridyl and 2-hydroxypyridyl ligands

These ligands have thus far been reported to coordinate to transition metals, alkali and alkali earth metals in a variety of fashions. These include behaviour as bridging ligands, terminally coordinating ligands bound to the metal through one donor atom only and as chelating ligands. Of these coordination modes, the most widely studied and structurally important mode has been the bridging mode where the metal centres are bridged by either NCN^- or NCO^- chains. Interest in this mode stems from the capacity of these ligands to bridge particularly short metal-metal bonds. It is probably true to mention that most of the complexes displaying the other modes were products of serendipity, gleaned from attempts to synthesise these structurally important complexes.

1.1.1.1 The bridging mode of coordination

Three different bridging modes have been reported, all of which have been verified by X-ray crystallography.

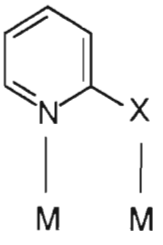

I

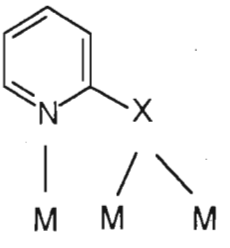

II

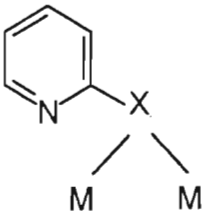

III

X = NR, O

Mode I coordination

In mode **I** coordination an unsymmetrical sp^2 bonded NCN^- or NCO^- chain forms a five membered ring with the two metal centres. Metal-metal bond orders in these complexes have been found to vary from one to four. The first reported complexes of this type were the

tetrasubstituted, quadruply bonded dimers of the Group VI metals, Cr, Mo and W having the general formula $[M_2(\mu\text{-}L)_4]$. Their study was prompted by the existence of quadruply bonded complexes containing the stereoelectronically similar carboxylate ligands[2].

Two routes have been successfully followed for the synthesis of these dinuclear species: these involve either the reaction of the lithium or sodium salt of the ligand with the metal precursor in THF, or the reaction of the free ligand with the metal precursor at high temperatures (molten state). In most cases the metal precursor has been the appropriate metal carboxylate.

$$[M_2(O_2CCH_3)_4] + NaL \xrightarrow{THF} [M_2(L)_4] + NaO_2CCH_3$$

$$[M_2(O_2CCH_3)_4] + HL \longrightarrow [M_2(L)_4] + HO_2CCH_3$$

Due to the unsymmetrical nature of these ligands, four different coordination arrangements for the tetrasubstituted complexes are possible:

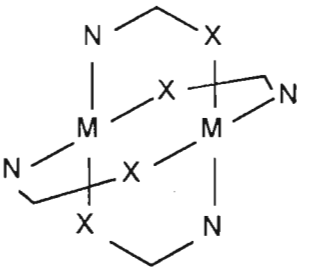

cis

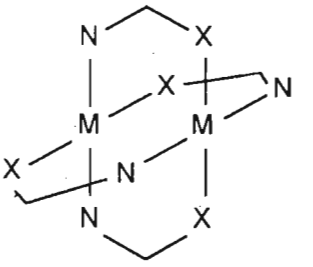

trans

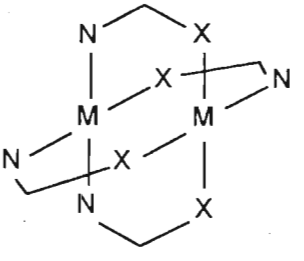

unsymmetrical polar

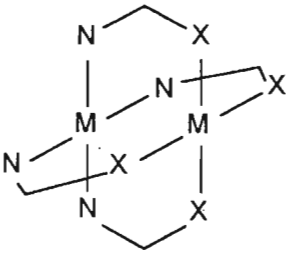

polar

X = NR , O

The *cis* arrangement has thus far only been reported for the anilinopyridyl ligand and only for molybdenum and tungsten (Fig. 1.2)[2]. In this mode the pairs of nitrogen donor atoms are *cis* to one another, about the metal atoms.

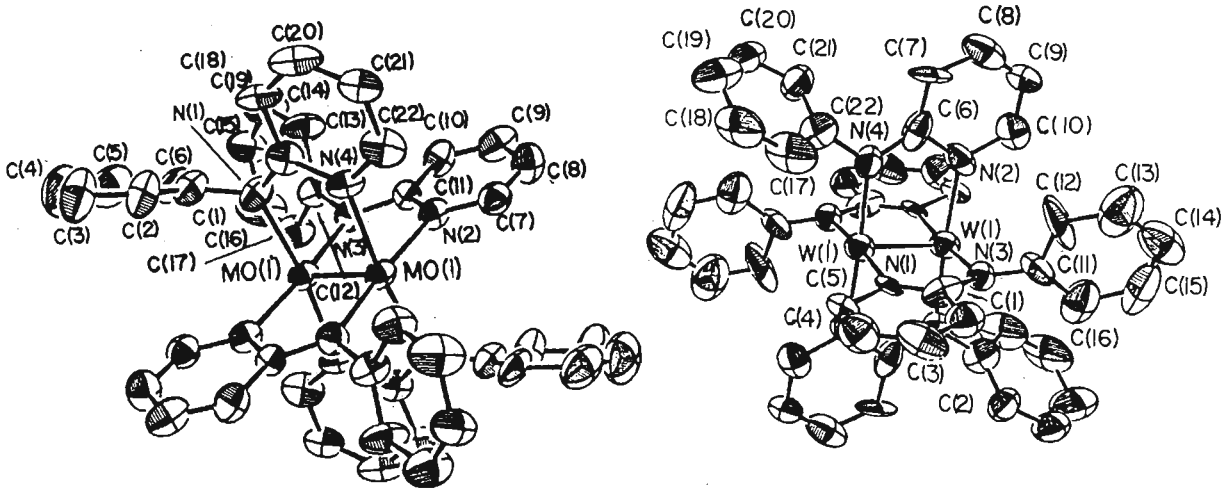

Fig. 1.2 : Structures of $[Mo_2(ap)_4]$ and $[W_2(ap)_4]$

The Mo-Mo and W-W separations for these complexes are 2.071(2) and 2.165(2) Å respectively, which together with bond order calculations suggest quadruple bonding between the metals. In both cases the metal-metal distance is ca. 0.02 Å shorter than that for the corresponding metal carboxylate. Although these are the only examples of complexes that exhibit the *cis* arrangement, the yields for these reactions are high thus excluding the possibility of isomer formation.

A more frequently reported arrangement is the *trans* arrangement of these ligands about the metal atoms. Examples of this arrangement are found in $[M_2(map)_4]$ and $[M_2(mhp)_4]$ (M= Cr, Mo, W; map = the anion of 2-amino-6-methylpyridine; mhp = the anion of 2-hydroxy-6-methylpyridine). The Cr-Cr bond length in $[Cr_2(map)_4]$, illustrated in Fig. 1.3, is 1.870(3) Å [3]. Metal-metal bond lengths of this magnitude are referred to as "super short", which by definition for the Cr-Cr bond implies bond lengths of less than 1.900 Å. Interestingly, the Cr-Cr distance in $[Cr_2(O_2CCH_3)_4]$ in the solid state [4] is found to be 2.288(3) Å which is 0.4 Å longer than in $[Cr_2(map)_4]$.

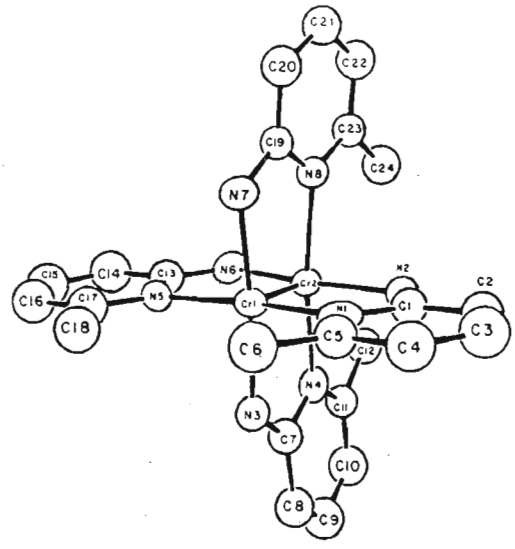

Fig. 1.3 : Structure of $[Cr_2(map)_4]$

In endeavouring to explain why these ligands afford dimers which have super short metal-metal bonds which are significantly shorter than their parent carboxylates, Cotton and Walton[1] cited an observed consistent trend: in all the super short bonded species there is an absence of axial bonding. It is generally understood that axial bonding enables population of orbitals which have some antibonding character thus disrupting the metal-metal bonds. The vast difference in Cr-Cr bond lengths between $[Cr_2(O_2CCH_3)_4]$ and $[Cr_2(map)_4]$ can be explained by this effect. In $[Cr_2(O_2CCH_3)_4]$ the lone pairs on the oxygen atoms of the bridging acetates coordinate axially to metal atoms of adjacent dimers thus forming chains of dimeric units. Electron diffraction studies of $[Cr_2(O_2CCH_3)_4]$ in the gas phase[5] (where this phenomenon is not possible) reveal a remarkably shorter Cr-Cr bond distance of 1.966(14) Å . The absence of intermolecular axial coordination in $[Cr_2(map)_4]$ due to obvious steric factors must surely contribute to Cr-Cr bond shortening.

In other studies, attempts have been made to establish any correlation between the basicity of the bridging ligand donor atoms and M-M bond lengths and, although uncertainty prevails, it would appear that the more basic the donor atoms, the shorter the metal -metal bonds.

Table 1.1: Ligand arrangement and M-M bond lengths of selected complexes containing amido or hydroxypyridinate ligands.

complex	ligand arrangement	M-M (Å)	ref.
$[Mo_2(ap)_4]$	*cis*	2.071(2)	2
$[W_2(ap)_4]\cdot 2/3\ (THF)$	*cis*	2.165(2)	2
$[Mo_2(map)_4]$	*trans*	2.070(1)	3
$[Mo_2(mhp)_4]$	*trans*	2.067(1)	7
$[W_2(map)_4]$	*trans*	2.164(1)	3
$[W_2(mhp)_4]\cdot (THF)$	*trans*	2.161(1)	6
$[Cr_2(map)_4]$	*trans*	1.870(3)	3
$[Cr_2(mhp)_4]$	*trans*	1.889(1)	6
$[Mo_2(fhp)_4]\cdot (THF)_{ax}$	polar	2.092(1)	8
$[W_2(fhp)_4]\cdot (THF)_{ax}$	polar	2.185(2)	8
$[Cr_2(fhp)_4]\cdot (THF)_{ax}$	polar	2.150(2)	8
$[Ru_2Cl(ap)_4]$	polar	2.275(3)	11
$[Ru_2Cl(hp)_4(Hhp)]$	polar	2.286(1)	11
$[Rh_2(ap)_4Cl]$	polar	2.406(1)	10
$[Rh_2(mhp)_4(MeCN)]$	unsymmetrical polar	2.372(1)	9

map = the anion of 2-amino-6-methylpyridine; mhp = the anion of 2-hydroxy-6-methylpyridine fhp = the anion of 2-hydroxy-6-fluoropyridine; ap = the anion of 2-anilinopyridine; hp = the anion of 2-hydroxypyridine

In the so-called unsymmetrical polar arrangement, two ligands adopt a *trans* arrangement while the other two are *cis*. The only example of a complex with this arrangement is $[Rh_2(mhp)_4(MeCN)]$[9] depicted in Fig. 1.4.

A polar arrangement of ligands about the metal atoms is displayed by mixed valence amino pyridyl complexes of Ru and Rh, and by fhp (fhp = the anion of 2-hydroxy-6-fluoropyridine) complexes of the Group VI metals [8, 11, 9]. In $[Rh_2Cl(ap)_4]$ depicted in Fig. 1.5 one rhodium atom Rh1 is

axially bound by one chlorine atom and equatorially bound by four pyridyl nitrogens[10].

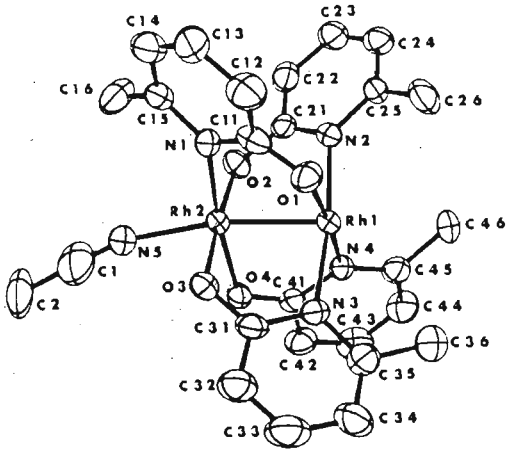

Fig. 1.4 : Structure of $[Rh_2(mhp)_4(MeCN)]$

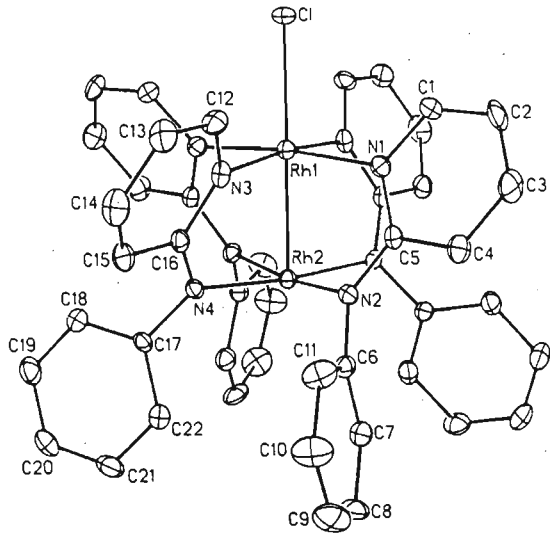

Fig. 1.5 : Structure of $[Rh_2Cl(ap)_4]$

The second rhodium atom Rh2 is bound equatorially to four anilino nitrogens and is sterically prevented from undergoing any axial ligation. On average the Rh-N bonds are longer for the pyridyl nitrogen which is consistent with the adoption of the resonance form in which the negative charge is formally on the anilino nitrogen. Significantly a large average N-Rh-Rh-N torsion angle of 23° is observed in $[Rh_2Cl(ap)_4]$[10], whereas the equivalent torsion angle in $[Mo_2(fhp)_4]\cdot(THF)$ is 0° [8].

Generally the reasons for the stability of certain arrangements over others in complexes containing these ligands are not understood, although explanations based on steric or electronic grounds are possible.

Complexes in which only partial substitution of carboxylate groups by these ligands occurs have been reported for Rh, Ru, Mo and Cr. Replacement of three carboxylate groups is displayed by $[Ru_2(O_2CCH_3)(map)_3]$[12], whereas $[Rh_2(O_2CCH_3)_2(mhp)_2(Im)]$ [9] is the product of substitution of only two carboxylate groups.

Mode II coordination

In coordination mode **II** the exocyclic donor atom bridges two metal centres while the pyridyl nitrogen bonds to a third metal atom. In the case of amino pyridyl ligands the resulting cluster complexes have thus far been confined to ruthenium and osmium while for the hydroxypyridyl ligands the only example of a complex containing the ligand bonded in mode **II** is a rhodium "dimer of dimers" $[Rh_2(mhp)_3(TsO)]_2$.

Reaction of excess anilino pyridine with $[Ru_3(CO)_{12}]$ in refluxing toluene affords the metal cluster hydride $[Ru_3(\mu\text{-}H)(\mu_3\text{-}ap)(CO)_9]$ without detectable side reactions[13]. An X-ray crystallographic study reveals a nearly equilateral triangle of ruthenium atoms bonded to nine carbonyl groups (three to each metal atom), as depicted in Fig. 1.6. The Ru(2)-Ru(3) edge is bridged by a hydride ligand. The 2-anilinopyridinate ligand is bonded to Ru(1) through the pyridinic nitrogen while the exocyclic nitrogen bridges the other two ruthenium atoms, the Ru(2)-N(2)-Ru(3) plane being nearly perpendicular to the Ru(1)-Ru(2)-Ru(3) plane.

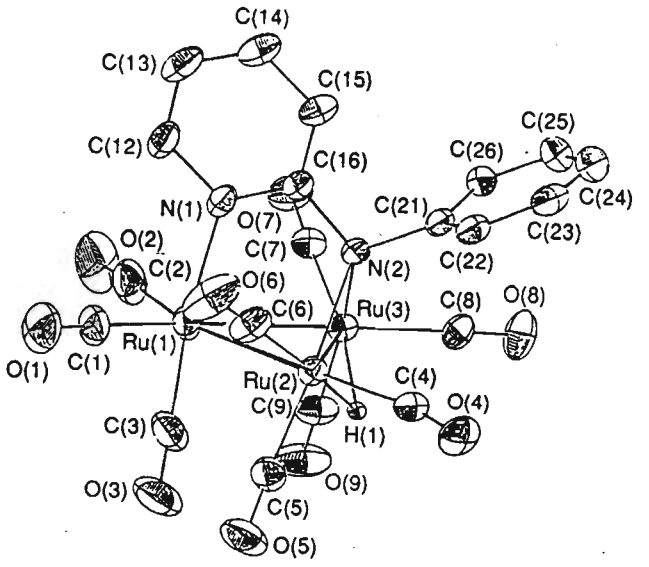

Fig. 1.6 : Structure of $[Ru_3(\mu\text{-}H)(\mu_3\text{-}ap)(CO)_9]$

Reaction of $[Rh_2(mhp)_4]$ with toluene sulphonic acid results in the replacement of a bridging mhp ligand with a bridging TsO^- ligand and subsequent dimerisation of the dimers[14] depicted in Fig.

1.7. The Rh-O bonds bridging the dimers are 2.24(1) and 2.30(2) Å , being only 0.2 Å longer then the equatorial Rh-O bonds.

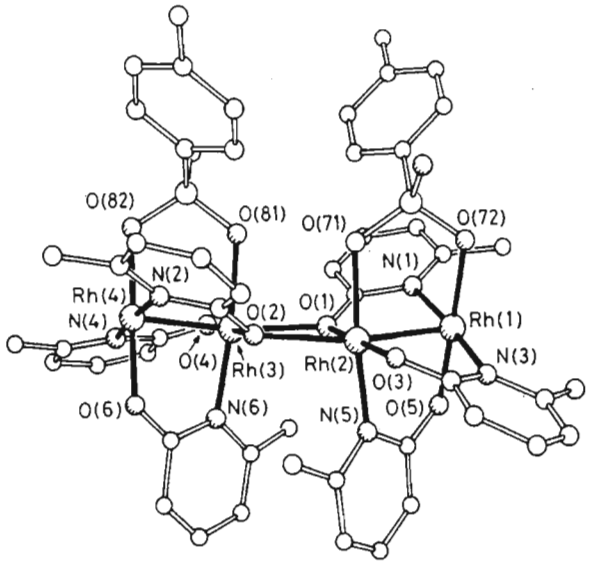

Fig. 1.7 : Structure of $[Rh_2(mhp)_3(TsO)]_2$

Mode III coordination

In mode **III**, bridging is only displayed by the anionic exocyclic nitrogen or oxygen atom. In the $[\{Cu(chp)_2(bipy)\}_2]$ (chp = the anion of 6-chloro-2-hydroxypyridine) complex, depicted in Fig. 1.8, both bridging and terminal coordination of the ligand is evident[15]. The copper atoms are held together through two μ-pyridone oxygen bridges which consist of long and short Cu-O bonds [1.942(2) and 2.339(2) Å respectively]. The Cu...Cu distance is 3.3295(4) Å.

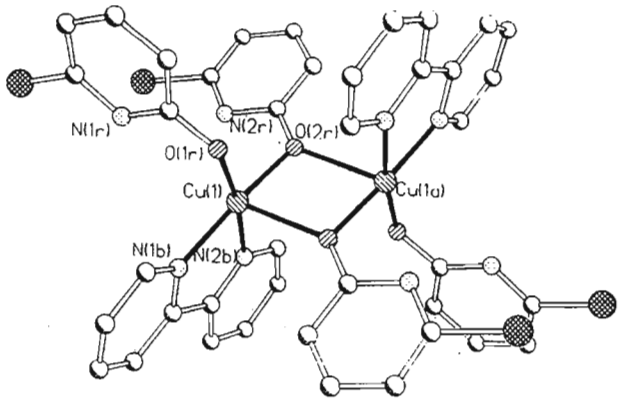

Fig. 1.8 : Structure of $[Cu(chp)_2(bipy)_2]_2$

The first reported edge sharing bioctahedral complex of Ru(III), $[Ru_2(C_5NH_4NH)_6(PMe_2Ph)_2]$, shown in Fig. 1.9, displays three different modes of coordination of the 2-pyridinamide ligand[16]. It was isolated in 15% yield after attempting to synthesise a multiply bonded binuclear species displaying bridging mode **I** exclusively. Instead, the resulting complex has the 2-pyridinamide ligand serving as a terminal ligand as well as a bridging ligand adopting both modes **I** and **III**. In the later mode the amido nitrogen gives rise to symmetrical Ru-N bonds averaging 2.094 Å. The Ru-Ru distance is 2.573(2) Å and may formally be regarded as a single bond.

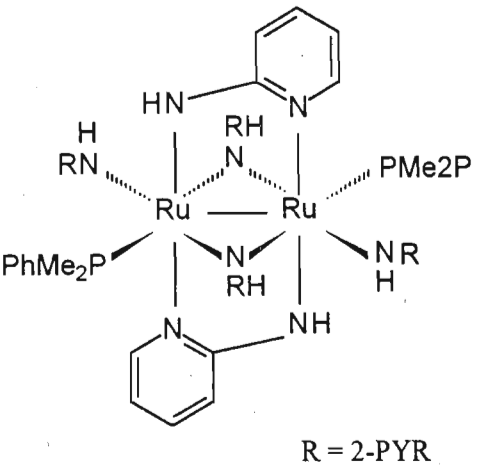

Fig. 1.9 : Structure of $[Ru_2(C_5NH_4NH)_6(PMe_2Ph)_2]$

1.1.1.2 The terminal mode of coordination

For the anionic form of these ligands there are two possible terminal modes of coordination. Coordination to metals can either occur through the pyridyl nitrogen or the exocyclic donor atom where the negative charge can fromally lie on ether of the donor atoms. The already mentioned complexes $[Ru_2(C_5NH_4NH)_6(PMe_2Ph)_2]$ and $[\{Cu(chp)_2(bipy)\}_2]$ exemplify the later possibility. So far the only examples of complexes that exhibit coordination of the ligand through the pyridyl nitrogen have been the Pt (IV) complexes of α pyridone. Deprotonation of the α pyridone ligand in the formation of $[Pt(NH_3)_2(C_5H_4NO)Cl_3]$, depicted in Fig. 1.10, is believed to be promoted by the high electrostatic Lewis acid strength of Pt (IV)[17].

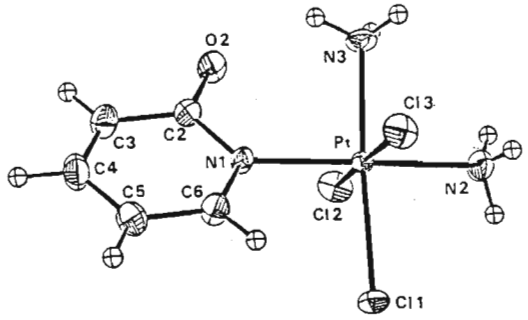

Fig. 1.10 : Structure of $[Pt(NH_3)_2(C_5H_4NO)Cl_3]$

1.1.1.3 The chelating mode of coordination

Examples of 2-aminopyridinate and its oxygen analogue forming chelates with single metal atom centres are relatively few. This is probably due to the closeness of the donor atoms to one another and the fact that the donor atom orbitals are directed along approximately parallel lines. The four membered rings formed by the chelate are thus rather strained. An interesting example is the bis amido complex $[Mg(ap)_2(THF)_2]$ in which magnesium uncharacteristically displays an octahedral geometry[18].

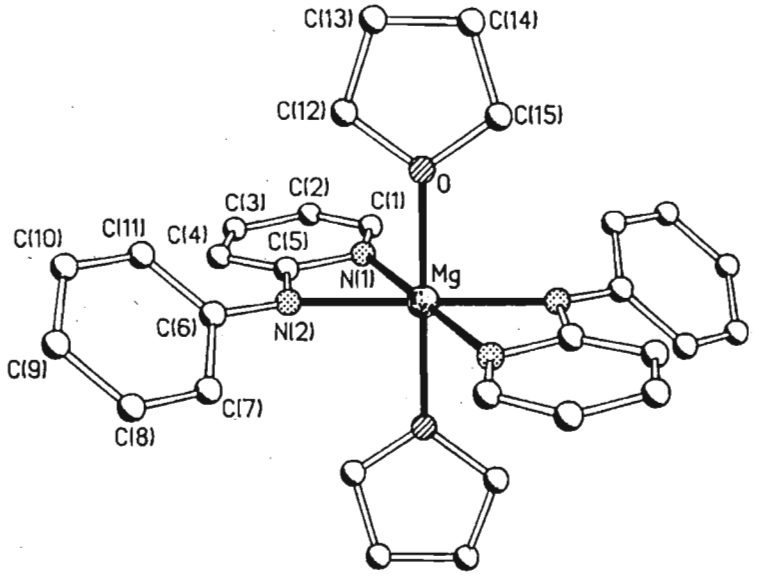

Fig. 1.11 : Structure of $[Mg(ap)_2(THF)_2]$

The mhp and ap ligands in $[Ru(\eta\text{-}C_6H_6)Cl(mhp)]$ [19] and $[Ru\ (ap)_2(PPh_3)_2]$ [20] are also bound to the metal via this mode of coordination.

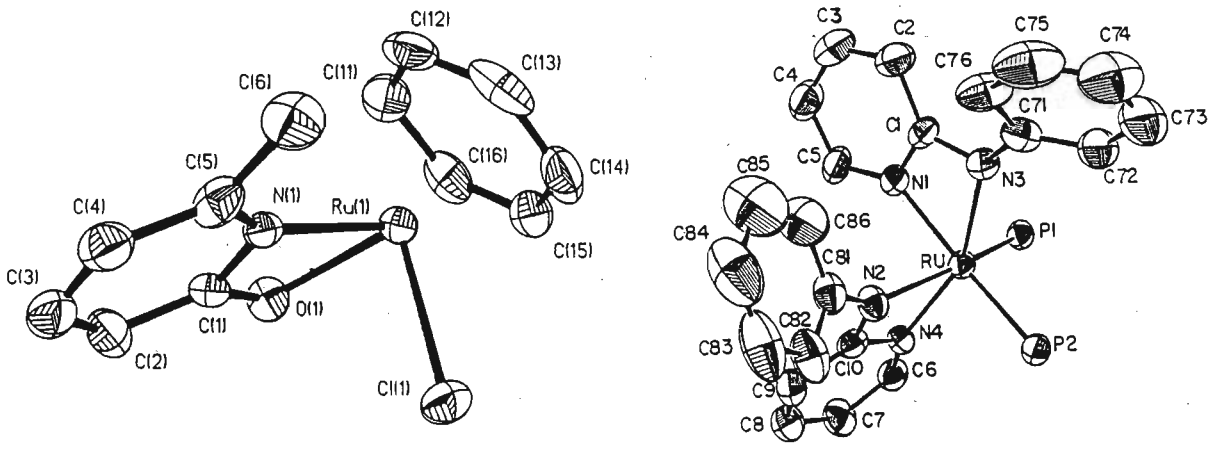

Fig. 1.12 : Structures of $[Ru(\eta\text{-}C_6H_6)Cl(mhp)]$ and $[Ru(ap)_2(PPh_3)_2]$

1.1.2 The neutral form of the 2-aminopyridyl and 2-hydroxypyridyl ligands

The neutral form of the 2-amino and 2-hydroxypyridyl ligands which includes the tertiary amino pyridyl ligands (which do not have any acidic protons) have been shown to display bridging, terminal, and even, in the case of aryl substituted amino groups, orthometalating modes of coordination.

1.1.2.1 The bridging mode of coordination

Only two bridging modes are known. Due to the presence of acidic protons on primary or secondary amino as well as hydroxy pyridyl ligands, neutral bridges formed by three atom NCN chains are confined to those formed by tertiary amino pyridyl ligands. The only example of a complex containing this mode is the unstable species $[Ru_3(\mu\text{-dmap})(\mu\text{-}CO)_3(CO)_7]$ shown in Fig.

1.13. The structure of this complex is tentatively assigned on the basis of its IR spectroscopic data, and is similar to that of $[Ru_3(\mu\text{-napy})(\mu\text{-CO})_3(CO)_7]$ [13].

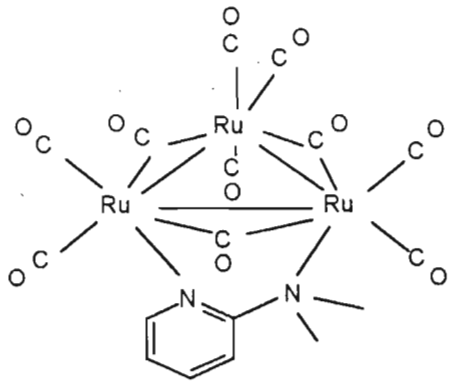

Fig. 1.13 : Structure of $[Ru_3(\mu\text{-dmap})(\mu\text{-CO})_3(CO)_7]$

In the other neutral bridging mode, the exocyclic donor atom bridges two metal centres. This mode is confined to α pyridones only, since only oxygen has two lone pairs available for this purpose. The complex $[V_2O_2Cl_4(\mu\text{-Hmhp})_3]$ contains three neutral ligands bridging in this fashion[21].

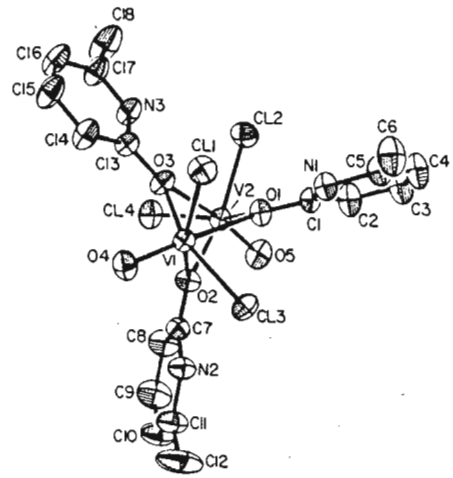

Fig. 1.14 : Structure of $[V_2O_2Cl_4(\mu\text{-Hmhp})_3]$

1.1.2.2 The terminal mode of coordination

The neutral ligands may coordinate in a terminal fashion either through the pyridyl nitrogen or the exocyclic donor atom. Thus far examples of the latter option are only provided by examples of the α pyridone ligands.

The Hap and Hhp ligands in $[Ru_2Cl(O_2CCH_3)_2(ap)_2(Hap)]$ [22] and $[Ru_2Cl(hp)_4(Hhp)]$[11] shown in Fig. 1.15, both display axial terminal coordination. In the anilinopyridyl complex axial coordination is via the pyridyl nitrogen, while in the α pyridone complex it is via the oxygen atom. This difference is due to the stability of the keto form of the 2-hydroxypyridyl ligand, the analogous imino form in the amino pyridyl ligand being unstable.

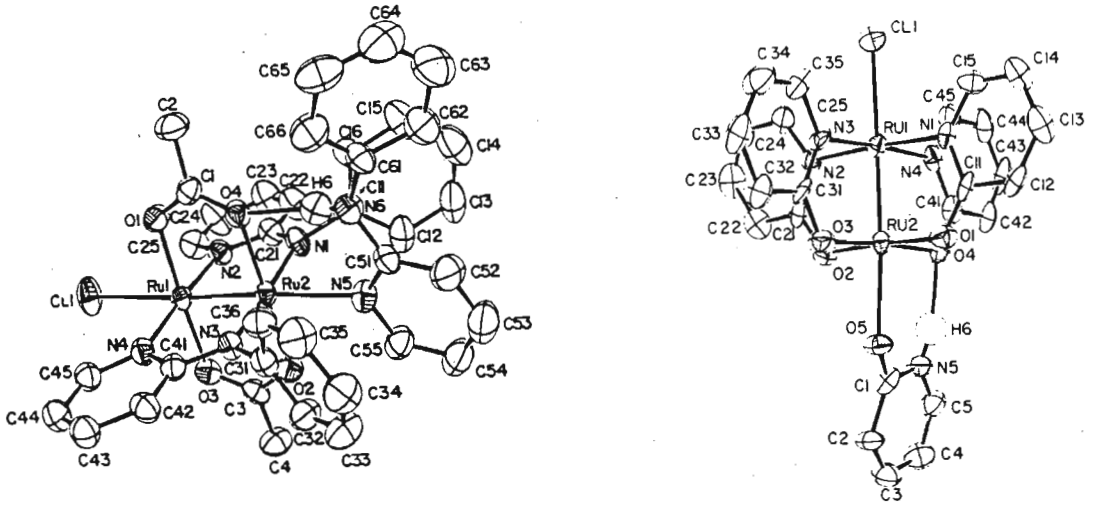

Fig. 1.15 : Structures of $[RuCl_2(O_2CCH_3)_2(ap)_2(Hap)]$ and $[Ru_2Cl(hp)_4(Hhp)]$

Other examples of complexes that contain terminally coordinated ligands include $[Pt(NH_3)_2(Hhp)_2]^{2+}$ [17] where the hydroxypyridyl ligand coordinates through the pyridyl nitrogen, and [(Nhpy)Co $(DH)_2iC_3H_7$] which has a relatively long Co-N_5 bond mimicking coenzyme B_{12} [23].

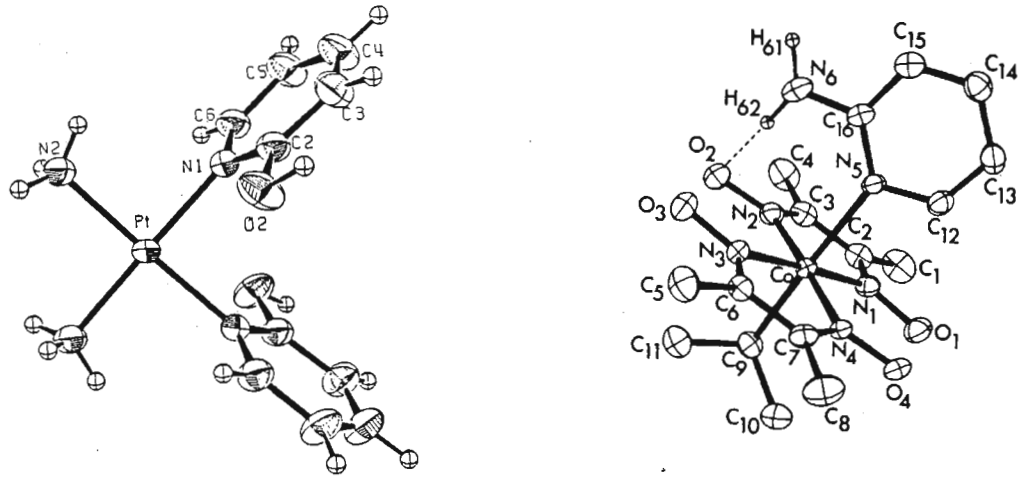

Fig. 1.16 : Structures of $[Pt(NH_3)_2(Hhp)_2]^{2+}$ and $[(Nhpy)Co(DH)_2iC_3H_7]$

1.1.2.3 The chelating mode of coordination

No examples of the neutral ligands adopting the chelating mode of coordination are known. This is probably due to the relatively poor donor ability of the exocyclic donor atom not being able to overcome the strain produced by the chelate. Chelates of the N-oxides of the amino pyridyl ligands are known. The stability of these chelates is as a consequence of the alleviation of ring strain brought about by the formation of a five membered ring due to the presence of the extra O atom. The bis (2-dimethylaminopyridine 1-oxide) copper(II) cation, shown in Fig. 1.17, displays this coordination mode[24].

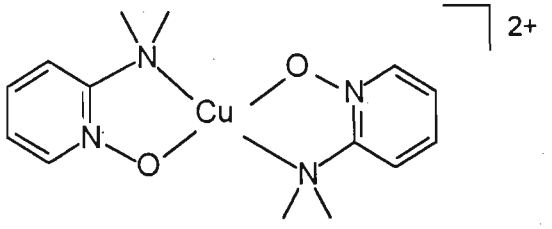

Fig. 1.17 : Structure of the bis (2-dimethylaminopyridine 1-oxide) copper(II) cation

1.1.2.4 Orthometallation

Consideration of the geometry of aryl N-substituted amino pyridyl ligands leads to the conclusion that it is not inconceivable that metalation could occur at the ortho-carbon atom of the aryl substituent with simultaneous coordination of the pyridyl nitrogen. This occurs in fact in the complex $[RhCl_2(py)_2[(C_6H_4)NHpy]$ shown in Fig. 1.18, isolated in good yield from the reaction of $[RhCl_3]\cdot 3H_2O$ with 2-anilinopyridine in the presence of sodium metal [25]. A crystal structure determination reveals coordination of the anilino pyridine ligand to the metal through the pyridyl nitrogen and C1 of the phenyl ring to form a six membered metallocycle; the anilino nitrogen remains uncoordinated.

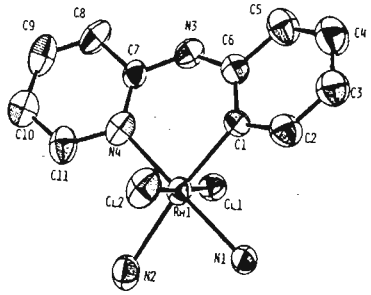

Fig. 1.18 : Structure of $[RhCl_2(py)_2[(C_6H_4)NH(py)]$

1.2 The 2-(2-pyridyl)-1,8-naphthyridine ligand (pynp)

The 2-(2-pyridyl)-1,8-naphthyridine ligand is a tridentate ligand possessing three donor pyridyl nitrogens. This crescent shaped ligand appears to be a unique hybrid of the ubiquitous 2,2'-bipyridyl ligand and the equally ubiquitous 1,8-naphthyridyl ligand. As a result, the tridentate ligand has potentially chelating and potentially bridging fragments, an ideal setup for maintaining a dimeric framework in transition metal complexes. In addition the ligand possesses an extended π system, a feature which has proven useful with regard to electrochemical processes.

Considering that the preferred coordination modes for the bipyridyl and 1,8-naphthyridlyl ligands are chelating and bridging respectively, only two modes of coordination of the pynp ligand seem likely. Chelation can occur through the bipyridyl fragment only (**I**), or simultaneous chelation and bridging could occur (**II**). A bridging-only mode is not likely to occur considering that the likelihood of the bipyridyl fragment coordinating terminally is not great.

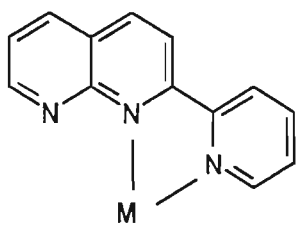

I

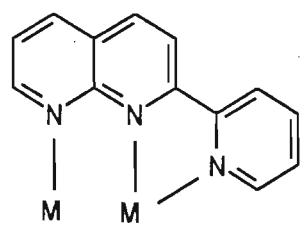

II

Both modes **I** and **III** are displayed by the pynp ligands in $[Rh_2(pynp)_3Cl_2](PF_6)_2 \cdot CH_3CN$ [26], shown in Fig. 1.19. In this complex two of the pynp ligands bridge in a head to tail fashion, *cis* to one another, while a third pynp ligand chelates equatorially through its bipyridyl fragment. The Rh-Rh bond length is 2.5668(7) Å.

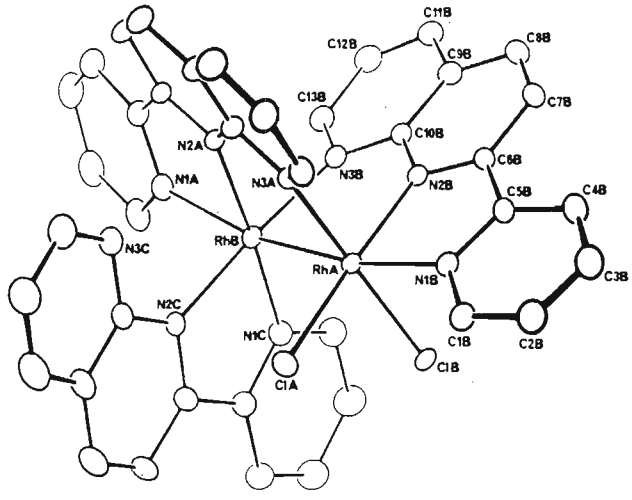

Fig. 1.19 : Structure of $[Rh_2(pynp)_3Cl_2]^{2+}$

The only other complexes of the pynp ligand are the tris pynp complex $[Ru(pynp)_3](PF_6)_2$ [27], in which all three pynp ligands display mode **I** coordination, and the pynp- and acetate-bridged rhodium complexes $[Rh_2(OAc)_3(pynp)](PF_6)$ and $[Rh_2(OAc)_2(pynp)_2](PF_6)_2$. The structures of the latter complexes are depicted in Fig 1.20, the structure of the $[Rh_2(OAc)_2(pynp)_2](PF_6)_2$ complex having been proposed on the basis of its H^1 NMR spectroscopic data.

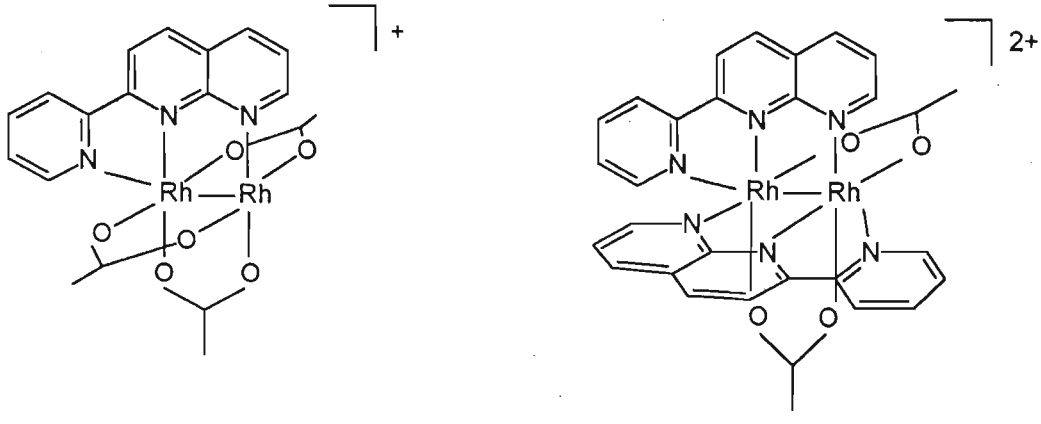

Fig. 1.20 : Structures of $[Rh_2(OAc)_3(pynp)]^+$ and $[Rh_2(OAc)_2(pynp)_2]^{2+}$

1.3 Potential coordination modes of the 6-aminobipyridyl and bipyidyl-6-one ligands

On the basis of the coordination modes displayed by the 2-aminopyridyl, 2-hydroxypyridyl ligands and the 2-(2-pyridyl)-1,8-naphthyridyl ligands, the likely modes of coordination of the hitherto unreported 6-aminobipyridyl and bipyridyl-6-one ligands can be predicted. These are illustrated below:

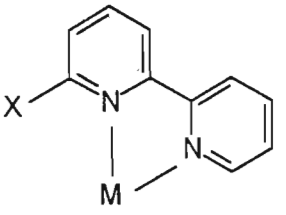

I

$X = NR_2$, OH

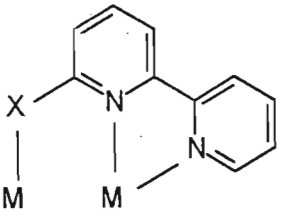

II

$X = NR$, NR_2

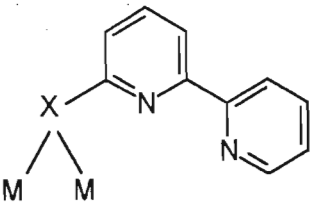

III

$X = NR$, O

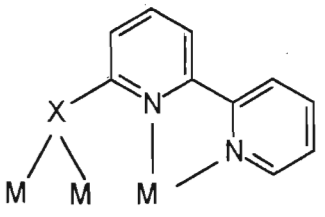

IV

$X = NR$, O

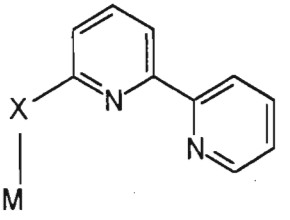

V

$X = NR$, NR_2 , O

Modes **I** and **II**, where $X = NR_2$ have both been reported for the 2-(2-pyridyl)-1,8-naphthyridine ligand, which like the 6-amino bipyridyl and bipyridyl-6-one ligands is tridentate. The bridging in mode **II** can either occur through NCN^-, NCO^-, or NCN chains, all of which have been reported for the analogous pyridyl ligands. The bridging mode **III** has the anionic exocylic nitrogen or oxygen bridging two metals, while the bipyridyl fragment remains pendant. Although this mode is displayed by the analogous pyridyl ligands, the presence of the bipyridyl fragment which has a strong tendency to chelate may render this mode less likely. A more probable mode is the bridging / chelating coordination as in shown in **IV**. The terminal mode displayed in **V** is a possibility, yet

once again, the tendency for the bipyridyl fragment to chelate may confine this mode to intermediate complexes formed *en route* to complexes containing ligands displaying modes **II** or **IV**.

1.4 Objectives of this work

The initial objective of this work was to synthesise and characterise novel 6-aminobipyridyl ligands. Although the synthesis of the bipyridyl-6-one ligand is known, no reports have appeared describing the coordination chemistry of this ligand. Thus the prime objective of this work was to study the coordination chemistry of the bipyridyl-6-one ligand as well as that of the newly synthesised 6-aminobipyridyl ligands. Both the exocyclic nitrogen and oxygen atoms are relatively 'hard' atoms, serving largely as σ donors, and their coordination to higher oxidation state transition metals situated to the left of the periodic table is favoured. The bipyridine ligand is known to stabilise transition metals in their low formal oxidation states and therefore its coordination to low oxidation state metals is expected to be favoured. A study of the coordination of these ligands to both high and low oxidation state transition metals was thus another objective.

The presence of low lying π^* orbitals on the bipyridine ligand has been critical to the function of complexes such as $[Ru(bipy)_2(CO)H](PF_6)$[29] and $[Rh(bipy)_2Cl_2](PF_6)$[30] as effective electrocatalysts for processes such as the reduction of carbon dioxide. This has been one of the driving forces for the study of the coordination of these polypyridyl ligands to transition metals.

Another objective was to synthesise aminobipyridyl and bipyridyl-6-one ligand bridged dinuclear complexes. Because of the presence of two metal centres a dinuclear complex has, in principle, the potential to accommodate small molecules in a manner not possible for mononuclear complexes. One example is that the substrate molecule can adopt a bridging mode of coordination in a dinuclear complex which is clearly not possible for a mononuclear species.

Chapter two

The synthesis and characterisation of 6-anilino-2,2'-bipyridine, 6-N-methylanilino-2,2'-bipyridine and 6-piperidino-2,2'-bipyridine

2.1 Introduction

The nitrogen atom in amine ligands of the type NR_3 is mainly a donor of σ electrons [31]. The donor ability of the nitrogen can however be altered by varying the R groups on the amine: the more electron rich the R group, the better the σ donor ability of the nitrogen. In view of this trend, the exocyclic nitrogen in the 6-aminobipyridyl ligands was substituted by various R groups (within the confines of synthesis) with the aim of maximising the σ donor ability of this group. Amido ligands are better donors of σ electrons and it was therefore of importance to also synthesise an aminobipyridyl ligand containing an acidic amino hydrogen.

The most successful route for the synthesis of amino substituted aromatic heterocyclic amines has involved the nucleophilic substitution of halides by free amines. The only reported synthesis of a 6-aminobipyridine has been by Burstall in 1938, who described the preparation of 6-amino-2,2'-bipyridine from the reaction of 6-bromo-2,2'-bipyridine with aqueous ammonia at high pressure and temperature [32]. This heterocycle has two potential drawbacks with respect to its ability to bridge two metals as a tridentate ligand: firstly, the absence of electron rich R groups on the exocyclic amino group means that in its neutral form the σ donor ability of this group is not optimal and secondly, the presence of two amino protons means the amido form of the ligand is sterically unhindered and therefore capable of forming polymeric complexes via bridging through the amido group.

Work carried out by Halcrow and Kermack on 2-amino substituted derivatives of *o*-phenanthroline has shown that substitution of chloro groups by aniline and piperidine can be facilitated at relatively low temperatures [33]. An extension of this work to the substitution of 6-chloro-2,2'-bipyridine by various amines has been carried out in this thesis (though not with the intention of synthesising new antimalarials).

The substitution of the chloro group in 6-choro-2,2'-bipyridine by aniline, N-methylaniline, and piperidine has resulted in the isolation of three new ligands: 6-anilino-2,2'-bipyridine (Habipy), 6-N-methylanilino-2,2'-bipyridine (mabipy) and 6-piperidyl-2,2'-bipyridine (pipbipy). The Habipy ligand has a relatively acidic proton and therefore has the potential to coordinate as an amido ligand. The presence of the phenyl group on the amine also provides a degree of steric hindrance, thereby reducing the chance of bridging by the amido group. The mabipy ligand has an exocyclic nitrogen which is a better σ donor, while the pipbipy ligand is the best σ donor. The piperidyl group in pipbipy is also less sterically bulky due to its ability to adopt either a chair or boat conformation. In order of increasing donor ability of the exocyclic amines: Habipy < mabipy < pipbipy < abipy.

2.2 Synthesis and characterisation

The reactions of 6-chloro-2,2'-bipyridine with aniline, N-methylaniline and piperidine are shown in Fig. 2.1.

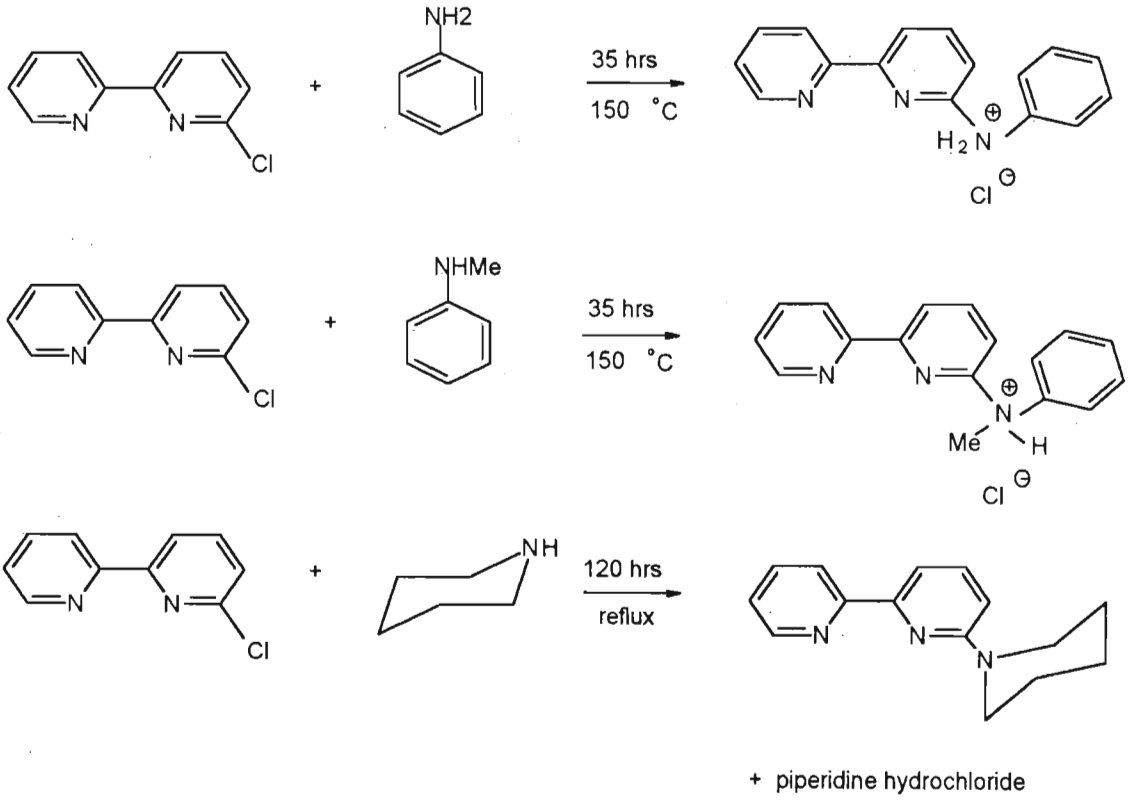

Fig. 2.1: Reactions of 6-chloro-2,2'-bipyridine with aniline, N-methylaniline and piperidine

The 6-chloro-2,2'-bipyridine used in all of the above reactions was synthesised by the literature method [34] with the exception that 1-methyl-2,2'-bipyridin-6-one, normally isolated as a very dark oil, was purified by extraction with boiling ether which yielded a pale yellow crystalline material. Purification at this stage enabled the chlorination step to proceed cleanly so that further treatment with activated charcoal was unnecessary. The overall yield for the synthesis of the 6-chloro-2,2'-bipyridine was 30% which was found to be slightly higher then the reported yield of 22%[34].

The reactions of aniline, N-methylaniline and piperidine with 6-chloro-2,2'-bipyridine were all carried out under a nitrogen atmosphere to prevent excessive oxidation of the amines for the duration of the reaction. For the anilino and N-methlyanilino reactions the temperatures were kept at 150 °C as higher temperatures were found to cause excesssive oxidation of the amines. Hydrochloride salts of Habipy and mabipy were formed due to the higher basicity of these products. Liberation of the amines from their salts was best achieved by bubbling dry ammonia gas through solutions of the amine salts in chloroform. The reaction of piperidine with 6-chloro-2,2'-bipyridine proceeded relatively slowly possibly due to the lower temperature, although piperidine is one of the strongest amine bases and is also a good nucleophile. The yields of Habipy, mabipy and pipbipy from the reaction of the relevant amine with 6-chloro-2,2'-bipyridine were found to be 82, 85 and 72% respectively. All three ligands are soluble in common organic solvents.

Table 2.1 : Spectroscopic data for Habipy, mabipy and pipbipy

	Habipy	Mabipy	Pipbipy
IR[a]	3396(m), 1603(m), 1580(m), 1565(m), 1516(m), 1448(m), 1427(m), 1342(m), 777(m), 762(m), 698(m)	1582(m), 1563(m), 1497(m), 1460(m), 1420(m), 1354(m), 1271(w), 1138(w), 982(w), 768(m), 698(m)	2933(m), 2840(m), 1582(m), 1453(m), 1429(m), 1381(w), 1252(m), 980(w), 949(w), 775(m)
UV-Vis[b]	342, 280, 247	344, 280, 248, 223	347, 268, 250, 228
GC-MS	247 m/z	261 m/z	239 m/z

a = Spectra recorded as KBr discs (pipbipy recorded as thin film on KBr). b = MeCN as solvent.

Table 2.2 : NMR spectroscopic data for Habipy, mabipy and pipbipy

	Habipy	mabipy	pipbipy
	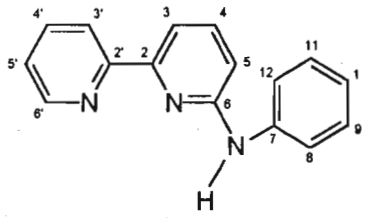	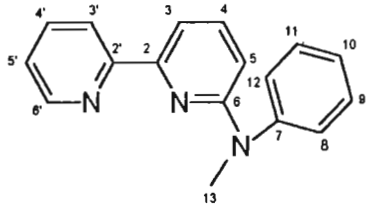	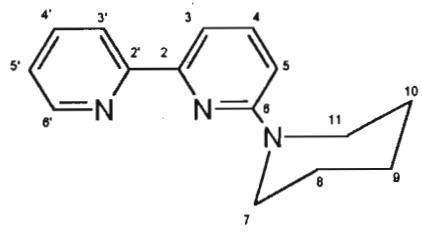
^{1}H nmr[a]	8.67 (1H, dbrm, $H_{6'}$) , 8.33 (1H, d, $H_{3'}$) , 7.85 (1H, d, $H_{4'}$), 7.80(1H, m, H_4) , 7.63(1H, t, H_3) , 7.46-7.25 (5H, m, $H_{5'}$, Ph) , 7.06 (1H, m, Ph) , 6.87 (1H, dbr, H_5) , 6.68 (1H , sbr, NH)	866 (1H, dbrm, $H_{6'}$) , 8.44 (1H, dbrm, $H_{3'}$) , 7.82 (1H , m, $H_{4'}$) , 7.78 (1H, m, H_3) , 7.5 - 7.18 (7H, m, $H_{4,\,5'}$, Ph) , 6.60 (1H, dd, H_5) , 3.61 (3H, s, CH_3)	8.64 (1H, dbrm, $H_{6'}$) , 8.38 (1H, dbrm, $H_{3'}$) , 7.79 (1H, d, H_3) , 7.75 (1H, tbrm, $H_{4'}$) , 7.6 (1H , t, H_4) , 7.21 (1H, m, $H_{5'}$) , 6.65(1H, d, H_5) , 3.6(4H, sbr, $H_{7a+b,\,11a+b}$) , 1.66(6H,sbr, $H_{8a+b,\,9a+b,\,10a+b}$)
^{13}C nmr[a]	156-154 (3C, s, $C_{2,\,2',\,6}$) , 149 (1C, d, $C_{6'}$) , 141 (1C, s, C_7) , 139 (1C, d, C_4) , 137 (1C, d, C_3) , 129 (2C, d, Ph) , 123 (1C, d, $C_{5'}$) , 122 (1C, d, Ph) , 121 (1C, d, $C_{3'}$) , 120 (2C, d, Ph) , 113 (1C, d, $C_{4'}$) , 109 (1C, d, C_5)	159-154 (3C, s, $C_{2,\,2',\,6}$) , 149 (1C, d, $C_{6'}$) ,147 (1C, s, C_7) , 138 (1C, d, C_4) , 137 (1C, d, C_3), 130-126 (4C, d, Ph) , 125 (1C, d, $C_{5'}$) , 123 (1C, d, Ph) , 121 (1C, d, $C_{4'}$) , 110 (1C, d, C_5), 109 (1C, d, C_5) , 38 (1C, q, CH_3)	159-154 (3C, s, $C_{2,\,2',\,6}$) , 149 (1C, d, C_4) , 138 (1C, d, C_4) , 137 (1C, d, C_3) , 123 (1C, d, $C_{5'}$) , 120 (1C, d, $C_{3'}$) , 109 (1C, d, $C_{4'}$) ,107 (1C, d, C_5) , 46 (2C, t, $C_{7,\,11}$) , 26 (2C, t, $C_{8,\,10}$) , 25 (1C, t, C_9)

a = spectra run in $CDCl_3$ at 303K

The spectroscopic data recorded for Habipy, mabipy and pipbipy are presented in Table 2.1. The infrared spectra display aromatic stretches typical of polypyridyl ligands. Of importance from an analytical point of view however is the manifestation of the N-H stretch at 3396 cm^{-1} in the spectrum of Habipy. This peak can be useful in distinguishing the amino from the amido forms of this ligand in transition metal complexes containing this ligand. Peaks in the ^{1}H and ^{13}C NMR spectra were assigned to individual protons and carbon atoms based on evidence obtained from their COSY and HETCOR spectra.

2.3 Crystal structure determination of 6-N-methylanilino-2,2'-bipyridine and 6-piperidino-2,2'-bipyridine

The crystal structures of the free mabipy and pipbipy ligands have been determined, the latter by its unusual inclusion in the crystal structure of $[Cu(pipbipy)_2](SbF_6) \cdot 0.5$ pipbipy, discussed in Chapter 3. Fig. 2.2 and Fig. 2.3 depict ORTEP plots of mabipy and pipbipy respectively. Tables 2.4 and 2.5 list the interatomic distances and angles for mabipy while those for pipbipy are listed later in Tables 3.9 and 3.10.

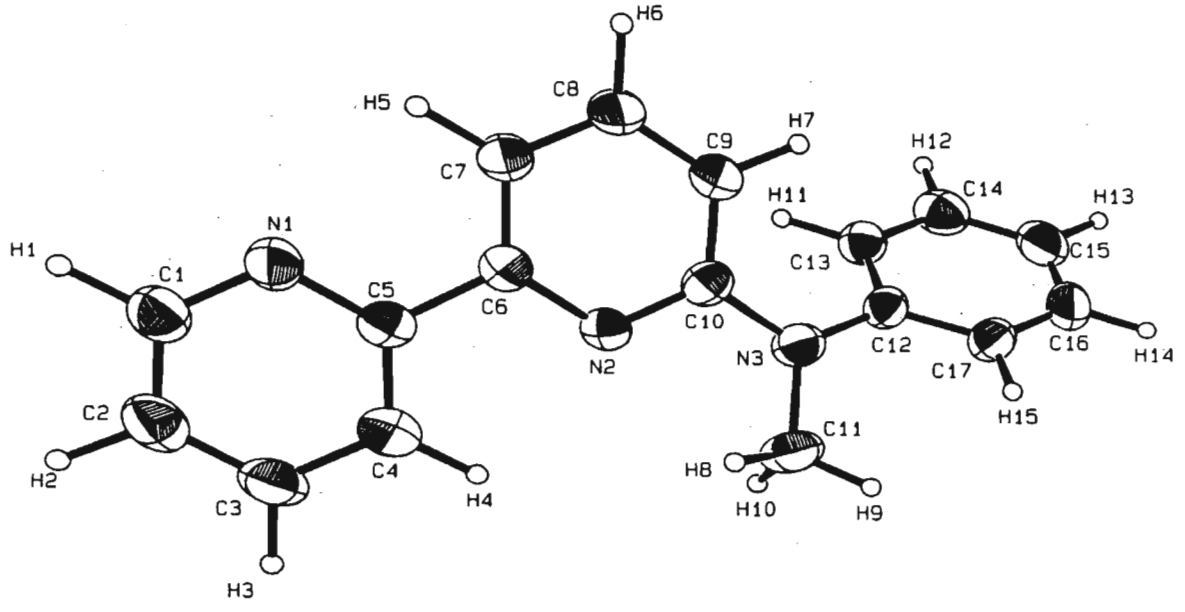

Fig. 2.2 : ORTEP plot of mabipy with thermal elipsoids at 30%

In both structures the uncoordinated ligand molecules exist as discrete entities in the crystals, there being no non-bonded contact distances less than the sum of the van der Waals radii for the atoms concerned.

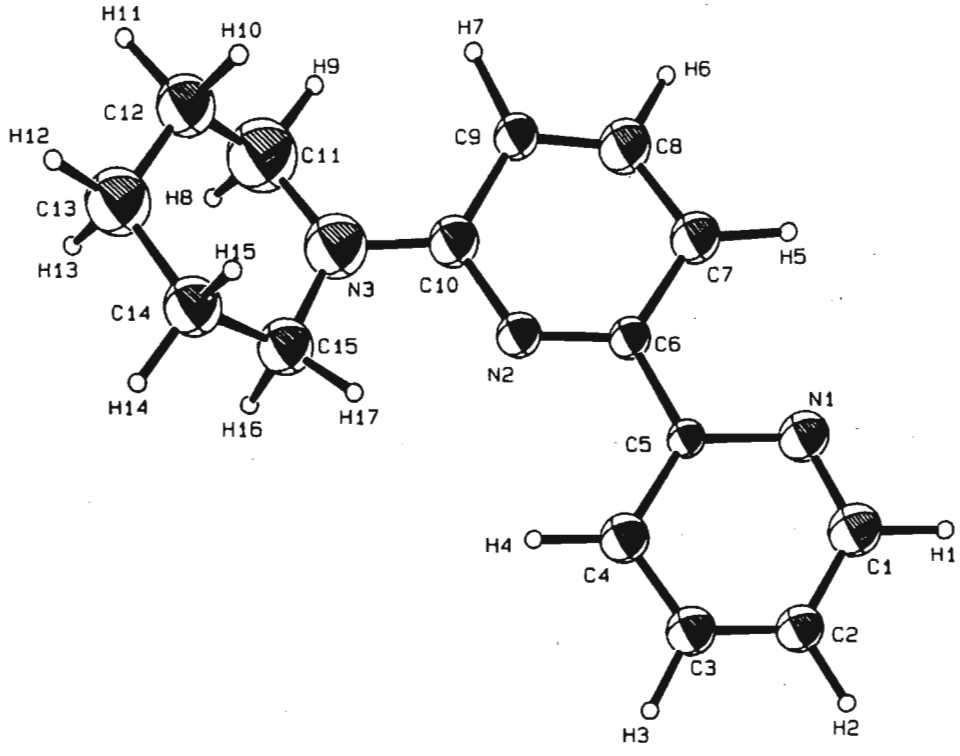

Fig. 2.3 : ORTEP plot of pipbipy with thermal elipsoids at 20 %

The crystal structures of mabipy and pipbipy reveal a near planar transoid conformation of the bipyridyl fragment which is known for uncoordinated bipyridine[36]. The dihedral angle between the two pyridyl planes is 5.0° for mabipy and 3.2° for pipbipy. The geometry about the exocyclic nitrogen in both mabipy and pipbipy is very close to triangular. The angles about N3 range between 117.2 and 122.0° for mabipy and 114.0 and 128.0°for pipbipy. For mabipy the distance of N3 from the plane C10-C11-C12 is 0.079 Å and for pipbipy the distance of N3 from the plane C10-C11-C15 is 0.017 Å. The deviation from planarity is thus very small. The planar geometry about N3 can be attributed to a substantial overlap of the nitrogen lone pair orbital with the π electron system of the pyridyl ring. In both ligands the N3-C10 bond length is significantly shorter than normal nitrogen-carbon single bonds[63]. In mabipy the N3-C10 bond length of 1.386 (4) Å

is 0.075 Å shorter then the N3-C11 bond length which was found to be 1.461(3) Å, a distance typical for N-C single bonds[63]. The N3-C10 bond length in pipbipy was found to be 1.379 (53) Å, whereas the N3-C11 and N3-C15 bond lengths in pipbipy were found to be 1.47(6) Å and 1.42(6) Å respectively, typical of N-C single bonds. In both the free ligands the N3-C10 bond lengths approach the distance normally associated with carbon-nitrogen double bonds[63].

The significant involvement of the nitrogen lone pair in the π electron system of the bipyridine ligand, as suggested by the crystallographic evidence, could be an important factor in the coordination of the exocyclic nitrogen. If a significant energy barrier must be overcome in order for the nitrogen lone pair to break its association with the bipyridyl ring, coordination of the exocyclic nitrogen could be difficult.

2.4 Experimental

All solvents were purified according to the literature methods [35]. 6-Chloro-2,2'-bipyridine was prepared by the literature method [34].

2.4.1 *Synthesis of 6-anilino-2,2'-bipyridine (Habipy)*

6-Chloro-2,2'-bipyridine (1.0g; 5.24 mmol) was heated in freshly distilled aniline (2 ml; 0.022 mol) at 150°C for 35 hrs under a nitrogen atmosphere. The resulting dark oil was steam distilled to remove excess aniline and dissolved in chloroform (40 ml). Dry ammonia was bubbled through the chloroform solution to liberate the 6-anilino-2,2'-bipyridine from its hydrochloride salt. The mixture was filtered to remove insoluble ammonium chloride and the filtrate evaporated to dryness. The solid material was dissolved in a minimum volume of ether and the solution then heated and stirred for 10 min with 1 g of activated charcoal. Filtration through a celite pad, addition of an equal volume of petroleum ether (60-80°C) and subsequent cooling yielded 6-anilino-2,2'-bipyridine (1.06 g ; 82%) as pale yellow needles. [Found: C,77.1; H, 5.74; N, 16.82. Calc. For $C_{16}H_{13}N_3$: C, 77.7; H, 5.30; N, 17.0 %]

2.4.2 *Synthesis of 6-N-methylanilino-2,2'-bipyridine (mabipy)*

6-Chloro-2,2'-bipyridine (1.0 g; 5.24 mmol) was heated in freshly distilled N-methylaniline (3 ml) at 150°C for 35 hrs under a nitrogen atmosphere. The product 6-N-methylanilino-2,2'-bipyridine was worked up by a method analogous to that for Habipy, with the exception that treatment with activated charcoal was unnecessary. Yield: 85%. [Found: C, 78.14; H, 5.93; N, 16.02. Calc. for $C_{17}H_{15}N_3$: C, 78.14; H, 5.79; N, 16.02 %]

2.4.3 *Synthesis of 6-piperidino-2,2'-bipyridine (pipbipy)*

6-Chloro-2,2'-bipyridine (1.0 g; 5.24 mmol) was refluxed in freshly distilled piperidine (10 ml) for 120 hrs. On completion of the reaction, the mixture was filtered to remove the poorly soluble piperidine hydrochloride and the piperidine removed under vacuum to afford a yellow oil. The oil was further purified by passing through a silica gel column using choroform as eluent. The yellow band collected was concentrated under vacuum and distilled at 150°C/0.5 mm Hg to yield the product as a yellow oil (0.95g; 72%). [Found: C, 74.97; H,7.02; N, 16.99. Calc. for $C_{15}H_{17}N_3$: C, 75.3; H,7.16; N, 17.56 %]

Single crystal X-ray diffraction study of 6-n-methylanilino-2,2'-bipyridine (mabipy)

Pale yellow prismatic crystals of mabipy were grown by cooling of a hot, concentrated solution of mabipy in 60-80° petroleum ether. The general approach used for the intensity data collection is described in Appendix A. Details of the crystallographic data are given in Table 2.3, the interatomic distances in Table 2.4, the interatomic angles in Table 2.5, and the fractional coordinates and equivalent isotropic thermal factors in Table 2.6. The observed and calculated structure factors may be found on microfische in an envelope fixed to the inside back cover. All non hydrogens were made anisotropic and the hydrogen atoms were placed in calculated positions. The phenyl rings where defined as rigid groups.

Table 2.3 : Crystal data and details of the crystallographic analysis for 6-N-methylanilino-2,2'-bipyridine.

Formula	$C_{17}H_{15}N_3$
Molecular mass ($g.mol^{-1}$)	291.33
Crystal system	Orthorhombic
Space group	*Pmna*
a (Å)	21.550(4)
b (Å)	7.568(2)
c (Å)	8.6530(3)
V ($Å^3$)	1411.1(6)
Z	4
D_c ($g.cm^{-3}$)	1.23
F (000)	552
λ (Mo - K_α) (Å)	0.71069
Scan mode	ω - 2θ
ω scan angle	0.41 + 0.35tanθ
Horizontal aperture width (mm)	2.7 + 0.1tanθ
Scattering range (°)	$2 \leq \theta \leq 30$
μ (cm^{-1})	0.809
Absorption corrections	Semi empirical
Measured intensities	1662
Unique intensities	1132
Unique intensities [$I > 3\sigma(I)$]	909
Structure solution	Direct methods
Weighting scheme	$1/[(\sigma^2(F) + 0.01F^2)]$
$R = \Sigma(F_o-F_c)/\Sigma F_o$	0.0396
$R_w = \Sigma_w ½(F_o-F_c)/\Sigma_w ½F_o$	0.0448
$(\Delta/\sigma)_{max}$	0.381
$\Delta\rho_{max}(eÅ^{-3})$	0.110
Number of parameters	172

Table 2.4 : Interatomic distances (Å) for 6-N-methylanilino-2,2'-bipyridine

N(1)-C(1)	1.336(3)	N(1)-C(5)	1.343(3)
N(2)-C(6)	1.363(3)	N(2)-C(10)	1.343(3)
N(3)-C(10)	1.386(3)	N(3)-C(11)	1.461(3)
N(3)-C(12)	1.426(3)	C(1)-C(2)	1.369(5)
C(2)-C(3)	1.379(5)	C(3)-C(4)	1.391(4)
C(4)-C(5)	1.399(4)	C(5)-C(6)	1.483(3)
C(6)-C(7)	1.387(3)	C(7)-C(8)	1.385(3)
C(8)-C(9)	1.376(4)	C(9)-C(10)	1.403(4)
C(13)-C(14)	1.395(0)	C(13)-C(12)	1.395(0)
C(14)-C(15)	1.395(0)	C(15)-C(16)	1.395(0)
C(16)-C(17)	1.395(0)	C(17)-C(12)	1.395(0)

Table 2.5 : Interatomic angles (°) for 6-N-methylanilino-2,2'-bipyridine

C(1)-N(1)-C(5)	117.2(3)	C(6)-N(2)-C(10)	117.9(2)
C(10)-N(3)-C(11)	119.9(2)	C(10)-N(3)-C(1)	122.0(2)
C(11)-N(3)-C(12)	117.2(2)	N(1)-C(1)-C(2)	124.0(3)
C(1)-C(2)-C(3)	119.0(3)	C(2)-C(3)-C(4)	118.8(3)
C(3)-C(4)-C(5)	118.1(3)	N(1)-C(5)-C(4)	122.8(2)
N(1)-C(5)-C(6)	116.7(2)	C(4)-C(5)-C(6)	120.5(2)
N(2)-C(6)-C(5)	115.1(2)	N(2)-C(6)-C(7)	123.8(2)
C(5)-C(6)-C(7)	121.2(2)	C(6)-C(7)-C(8)	117.3(3)
C(7)-C(8)-C(9)	120.0(3)	C(8)-C(9)-C(10)	119.7(2)
N(2)-C(10)-N(3)	116.1(2)	N(2)-C(10)-C(9)	121.3(2)
N(3)-C(10)-C(9)	122.6(2)	C(14)-C(13)-C(12)	120.0(0)
C(13)-C(14)-C(15)	120.0(0)	C(14)-C(15)-C(16)	120.0(0)
C(15)-C(16)-C(17)	120.0(0)	C(16)-C(17)-C(12)	120.0(0)
N(3)-C(12)-C(13)	119.5(1)	N(3)-C(12)-C(17)	120.5(1)
C(13)-C(12)-C(17)	120.0(0)		

Table 2.6 : Fractional coordinates ($x10^4$) and equivalent isotropic thermal factors ($Å^2$, $x10^3$) for 6-N- methylanilino-2,2'-bipyridine .

	x/a	y/b	z/c	U_{eq}
N(1)	7079(2)	2383(4)	8814	67(1)
N(2)	6242(2)	552(4)	5296(7)	53(1)
N(3)	5732(2)	-919(4)	3219(8)	69(1)
C(1)	7380(2)	3708(5)	9104(11)	79(1)
H(1)	7601(2)	3869(5)	10357(11)	120(5)*
C(2)	7406(2)	4902(6)	7933(11)	82(1)
H(2)	7668(2)	5934(6)	8226(11)	120(5)*
C(3)	7119(3)	4735(6)	6335(11)	83(1)
H(3)	7129(3)	5668(6)	5398(11)	120(5)*
C(4)	6800(2)	3373(5)	5982(10)	76(1)
H(4)	6569(2)	3203(5)	4746(10)	120(5)*
C(5)	6802(2)	2213(5)	7255(8)	58(1)
C(6)	6504(2)	699(5)	6908(8)	54(1)
C(7)	6509(2)	-469(5)	8149(9)	63(1)
H(5)	6720(2)	-290(5)	9412(9)	120(5)*
C(8)	6235(2)	-1860(5)	7699(9)	67(1)
H(6)	6231(2)	-2806(5)	8620(9)	120(5)*
C(9)	5974(2)	-2043(5)	6071(9)	64(1)
H(7)	5754(2)	-3116(5)	5708(9)	120(5)*
C(10)	5988(2)	-815(5)	4875(9)	57(1)
C(11)	5636(3)	478(5)	2185(10)	88(1)
H(8)	5574(3)	1313(5)	3219(10)	120(5)*
H(9)	5216(3)	402(5)	1422(10)	120(5)*
H(10)	6014(3)	837(5)	1355(10)	120(5)*
C(13)	6137(1)	-3441(3)	2377(7)	64(1)
C(14)	6075(1)	-4837(3)	1484(7)	79(1)
C(15)	5532(1)	-5159(3)	565(7)	95(2)
C(16)	5050(1)	-4083(3)	540(7)	92(2)
C(17)	5111(1)	-2687(3)	1433(7)	75(1)
C(12)	5655(1)	-2365(3)	2352(7)	58(1)
H(11)	6558(1)	-3192(3)	3088(7)	120(5)*

Table 2.6 / Cont.

H(12)	6448(1)	-5670(3)	1504(7)	120(5)*
H(13)	5484(1)	-6240(3)	-127(7)	120(5)*
H(14)	4629(1)	-4332(3)	-172(7)	120(5)*
H(15)	4738(1)	-1854(3)	1413(7)	120(5)*

*** isotropic temperature factor.**

$$\underline{U}_{eq} = 1/3 \, \Sigma_i \Sigma_j \underline{U}_{ij} \underline{a}_i^* \underline{a}_j^* (a_i . a_j)$$

Chapter three

The synthesis and characterisation of homoleptic mononuclear aminobipyridyl complexes of copper(I) and copper(II)

3.1 Introduction

Having designed the 6-aminobipyridyl ligands with the intention of utilising the bridging capacity of these ligands to synthesise dinuclear complexes of transition metals, an initial study of the coordination of these ligands to mononuclear copper(I) and copper(II) precursors was undertaken. Copper(I) was chosen in view of its known propensity to form dinuclear complexes with the 6-diphenylphosphino-2,2'-bipyridyl ligand (Ph_2Pbipy). Such complexes include $[Cu_2(\mu\text{-}Ph_2Pbipy)_2(NCMe)_2](PF_6)_2$ and $[Cu_2(\mu\text{-}Ph_2Pbipy)_2(bipy)](PF_6)_2$ which are known to behave as electrocatalysts towards the reduction of carbon dioxide[37] . The Ph_2Pbipy ligand is similar to the 6-aminobipyridyl ligands, differing only in the donor atom substituted in the 6-position. The phosphorus atom in the phosphine ligand is however both a donor of σ electrons and an acceptor of π electrons, whereas the exocyclic nitrogen in the 6-aminobipyridyl ligands is only a donor of σ electrons. Phosphorus is also a much 'softer' donor atom than nitrogen and for this reason the 'harder' copper(II) system was also studied.

3.2 Reaction of Habipy, mabipy and pipbipy with copper(I)

The slow addition of either one or two equivalents of pipbipy, mabipy or Habipy to a solution of $[Cu(NCMe)_4]^+$ in methanol or acetonitrile was found to afford mononuclear products of stoichiometry $[Cu(\eta^2\text{-}L)_2]^+$, where L= mabipy **1**, pipbipy **2** or Habipy **3**. All three complexes proved to be relatively air stable compounds, best soluble in methanol. They could only be isolated as solid, crystalline materials by the slow evaporation of their methanolic solutions and otherwise were isolated as oils. The microanalytical data presented in Table 3.1 are consistent in each case with the formulation of homoleptic complexes of copper(I).

Table 3.1 : Microanalytical data

	Analysis : Calculated (Found)		
Complex	%C	%H	%N
$[Cu(\eta^2\text{-mabipy})_2](PF_6)$ **1**	55.85 (55.54)	4.11 (4.02)	11.50 (11.49)
$[Cu(\eta^2\text{-pipbipy})_2](PF_6)$ **2**	52.44 (52.23)	4.98 (5.08)	12.23 (11.84)
$[Cu(\eta^2\text{-Habipy})_2](PF_6)$ **3**	54.67 (54.70)	3.73 (4.03)	11.95 (11.69)

The infrared spectra, the data from which are presented in Table 3.2, exhibit the characteristic ligand peaks in the aromatic region and also shows the characteristic P-F stretching modes at approximately 840 cm^{-1}, confirming the presence of the PF_6^- counter ion. It is noteworthy that the infrared spectrum of $[Cu(\eta^2\text{-Habipy})_2]^+$ (**3**) displays the N-H stretch at 3390 cm^{-1} confirming the presence of the amino form of the ligand in the complex.

Table 3.2 Spectroscopic data

Complex	IR[a] (cm^{-1})	UV-Vis[b] (nm)	(δ) ^{1}H NMR[c] (ppm)
1	1591 (m), 1562 (w), 1494 (m), 1450 (m), 1364 (w), 840 (s)	345 280 244 221	8.30-6.30 (24H, m, $H_{6',5',4',3',3,4,5}$, Ph), 3.20 (6H, s, H_{11})
2	2944 (m), 2854 (w), 1593 (m), 1566 (m), 1447 (m), 1251 (m), 840 (s), 775 (w)	346 268 227	8.65-7.0 (14H, vbrm, $H_{6',5',4',3',3,4,5}$), 1.35 (8H, sbr, H_{8a+b}, H_{12a+b}), 1.20 (12H, sbr, H_{9a+b}, $H_{10a+b,11a+b}$)
3	3390 (w), 1593 (m), 1570 (m), 1508 (m), 1474 (s), 1339 (w), 1304 (w), 845, (s), 768 (m), 698 (w)	343 280 245	8.40-6.60 (26H, vbrm, Habipy)

a = recorded as KBr disc , b = recorded in MeCN , c = recorded in CD_3OD at 303K

vbrm = very broad multiplet , sbr = broad singlet

The UV-Vis spectra of all three complexes are very similar to those of the uncoordinated ligands, there being no detectable metal to ligand charge transfer peaks. The ^{1}H NMR spectra for complexes **2** and **3** display ligand peaks which are substantially broadened whereas the spectrum for complex **1** has relatively well resolved ligand peaks. Another unusual feature exhibited by the ^{1}H NMR spectrum of complex **2** is the substantial upfield shift of the α piperidyl protons (H_{8a+b} and H_{12a+b}), which shift from 3.60 ppm for the uncoordinated ligand to 1.35 ppm for complex **2**. No upfield shift is exhibited by any of the ligand protons of complexes **1** or **3**. The uniqueness of the pipbipy ligand in this respect is possibly due to the ability of the sterically unhindered piperidyl group to rotate more easily about its C(py)-N(methylanilino) bond, thereby bringing these protons in close proximity to the metal. Indirect evidence from the X-ray crystal structure study of $[Cu(\eta^2\text{-pipbipy})_2](SbF_6) \cdot 0.5$ pipbipy, discussed later, is supportive of this notion.

Single crystals of complexes **1** and **2** were grown for the purpose of structural determination by X-ray diffraction methods and the structures of the SbF_6^- salts of these complexes were solved. An ORTEP generated representation of the structure of $[Cu(\eta^2\text{-mabipy})_2]^+$ is illustrated in Fig. 3.1. The cations and anions are well separated, there being no contact distances less than the sum of the van der Waals radii for the atoms concerned.

Both mabipy ligands chelate to the copper ion through their bipyridyl fragments, with the N-methylanilino nitrogens remaining uncoordinated. The copper ion adopts a very irregular tetrahedral geometry, with angles subtended at it ranging from 80.9 to 140.0° (see Table 3.5). The interatomic distances for $[Cu(\eta^2\text{-mabipy})_2](SbF_6)$ are reported in Table 3.4. The Cu-N bond lengths are typically of the order of 2.0 Å for N1, N2, N4 and N5. The N3-Cu and N6-Cu distances are 3.234 Å and 3.303 Å respectively, being too long for any significant interaction. The N3-C10 and N6-C27 bond lengths are 1.372(6) and 1.382(6) Å respectively which implies substantial overlap of the nitrogen lone pair orbital with the π electron system of the bipyridyl rings as was the case for the uncoordinated ligand . The N3-C10 and N6-C27 bond lengths in complex **1** are not significantly different from the N3-C10 bond length in the uncoordinated ligand, discussed in Chapter 2, which was found to be 1.386(3) Å . The angles about the exocyclic nitrogens N3 and N6 range from 116.8 to 121.9 ° which is similar to those established for the

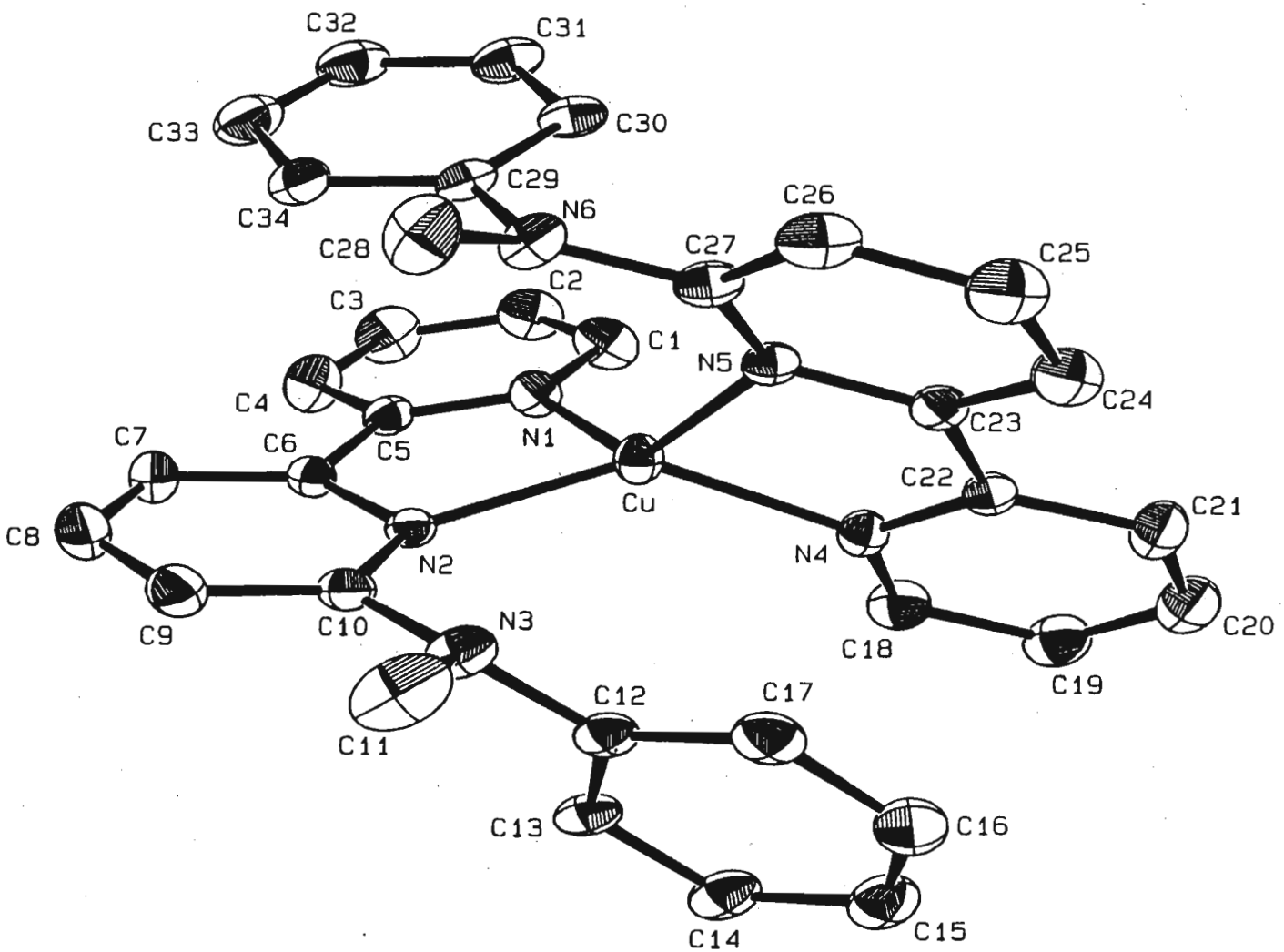

Fig 3.1 : ORTEP representation at 20% probability of $[Cu(\eta^2\text{-mabipy})_2]^+$ 1

uncoordinated mabipy. The distance of N3 from the plane C10, C11, C12 is 0.168 Å and the distance of N6 from the plane C27, C28, C29 is 0.076 Å. Thus the geometries about N3 and N6 are very close to being planar. In complex **1** C11 is *trans* to N2, whereas in the free ligand, discussed in Chapter **2**, C11 is *cis* to N2. This suggests that rotation about the N3-C10 bond is possible and that the overlap of the nitrogen lone pair orbital with the π electron system of the bipyridyl rings is not as rigid as might be assumed from structural evidence.

An ORTEP generated representation of the crystal structure of $[Cu(\eta^2\text{-pipbipy})_2]^+$ is depicted in Fig. 3.2. The crystal structure features the unusual inclusion of uncoordinated ligand in the lattice of the crystal. The cations, anions and uncoordinated ligand molecules exist as separate entities in the crystal, there being no contact distances less then the sum of the van der Waals radii for the atoms concerned. Like complex **1**, complex **2** crystallised in the triclinic space group $P\bar{1}$. There are two cations, two anions and one uncoordinated ligand molecule per asymmetric unit in the $[Cu(\eta^2\text{-pipbipy})_2](SbF_6) \cdot 0.5$ pipbipy crystal.

As found for the mabipy ligand in complex **1**, the two pipbipy ligands are chelated to the copper ion through their bipyridyl fragments, with the piperidyl fragments remaining uncoordinated. The geometry about the copper ion is a very distorted tetrahedron with angles ranging from 80.4 to 141.5°, as listed in Table 3.9. The bond lengths for complex **2** listed in Table 3.8 are very similar to those found for complex **1**. The N3A-Cu1A and N6A-Cu1A distances are 3.262 Å and 3.303 Å respectively, being too long for any significant interaction. The distance of N3A from the plane C10A, C11A, C15A is 0.305 Å and the distance of N6A from the plane C25A, C26A, C30A is 0.275 Å . Thus the geometries about the two exocyclic nitrogens are nearly planar. The N3-C10 bond length in complex **2** is also relatively short, not differing much form the corresponding N3-C10 distance in the uncoordinated ligand.

As mentioned earlier, the upfield shift observed for the α-protons of the piperidyl group in the ^1H NMR spectrum of **2** can be explained by indirect evidence obtained from the crystal structure determination of $[Cu(\eta^2\text{-pipbipy})_2](SbF_6) \cdot 0.5$ pipbipy. Rotation of the piperidyl group about the C10A-N3A bond should be both possible and likely, taking into account the existence of both *cis* and *trans* forms of the N-methyl anilino group in the mabipy ligand, discussed earlier, and

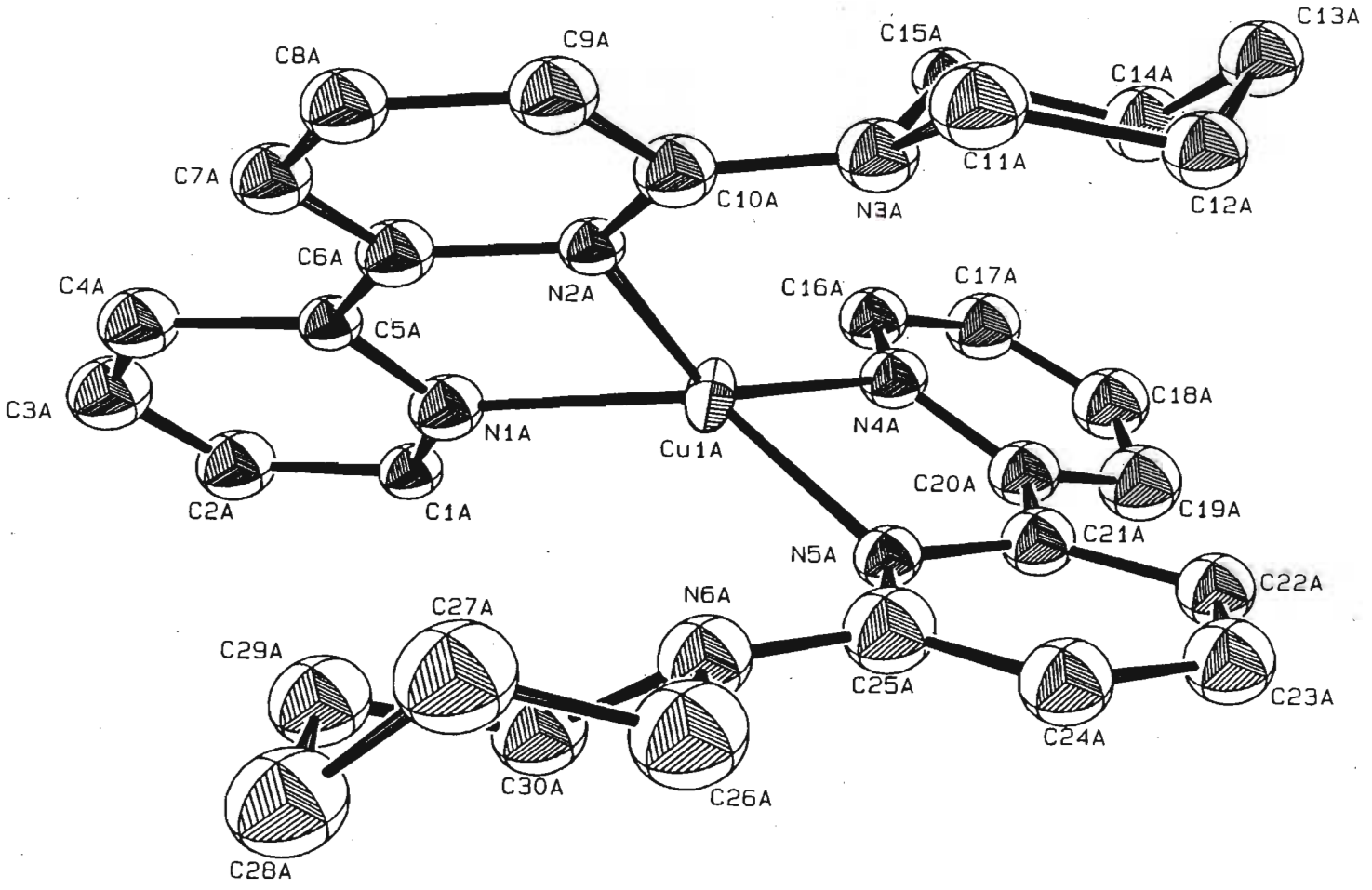

Fig 3.2 : ORTEP representation at 20% probability of $[Cu(\eta^2\text{-pipbipy})_2]^+$ 2

considering the compact nature of the piperidyl group. Calculations presented in Appendix C show that the minimum distance of an α-proton from Cu1A would be approached when H_α, N3A, C10A and Cu1A are all coplanar. In such a case the Cu1A-H_α distance is calculated to be 1.76 Å, which is significantly short to suggest some agostic interaction. Such an interaction would clearly explain the shift for the α-protons from 3.60 ppm to 1.35 ppm. No upfield shift is displayed by the α-protons in complexes **1** and **3** presumably due to restricted rotation about the N3-C10 bonds caused by the bulky phenyl rings.

3.3 Reaction of mabipy with copper(II)

The slow addition of either 1 or 2 equivalents of mabipy to a solution of copper(II) perchlorate hexahydrate in methanol at room temperature was found to afford the mononuclear Cu(II) species $[Cu(\eta^2\text{-mabipy})_2](ClO_4)_2 \cdot 2H_2O$ (**4**), isolated as a microcrystalline green material. The microanalytical data, presented in Table 3.3 are consistent with the formulation of the material as the bis mabipy copper(II) perchlorate dihydrate species.

The infrared spectrum of complex **4** exhibits the typical ligand vibrational bands in the aromatic region as well as the Cl-O stretch at 1094 cm^{-1} confirming the presence of the perchlorate counter ions. The UV-Vis spectrum is identical to the UV-Vis spectra of uncoordinated mabipy and complex **1**.

Table 3.3 : Microanalytical and spectroscopic data for $[Cu(\eta^2\text{-mabipy})_2](ClO_4)_2 \cdot 2H_2O$

Analysis : calculated (found)	%C 49.73 (49.78) %H 4.17 (3.82) %N 10.24 (10.35)
IR[a] (cm^{-1})	1603(m), 1566(w), 1499(m), 1455(m), 1373(w) 1317(w), 1244(w), 1094(s), 779(m), 769(m), 623(m)
UV-Vis[b] (nm)	347, 280, 246, 223

a = measured as KBr disc

b = measured in acetonitrile

Single crystals suitable for an X-ray crystal structure determination were grown from a propionitrile solution. These crystals were anhydrous but contained propionitrile as solvent of crystallisation. Fig. 3.3 depicts an ORTEP generated representation of the cation of complex **4**. The cations anions and solvent molecules are well separated in the crystal, there being no contact distances less then the sum of the van der Waals radii for the atoms concerned.

There are no major differences between the crystal structures of complexes **1** and **4**. The angles about the copper ion vary from 82.2 to 149.5° as presented in Table 3.13. The Cu-N bond lengths are slightly shorter for the copper(II) species, ranging from 1.961(9) to 1.986(8) Å. The N3-Cu and N6-Cu distances are 3.310 Å and 3.211 Å respectively, being too long for any significant interaction. The disance of N3 from the C10, C11, C12 plane is 0.119 Å and the distance of N6 from the C27, C28, C29 plane is 0.149 Å. Thus both N3 and N6 can essentially be regarded as having nearly planar geometry. Other then these minor differences, the structure of the cation of complex **4** is essentially the same as that of complex **1**.

Considering the geometric similarities between complexes **1** and **4** and the stabilities of the two species, their electrochemical relationship was expected to be one of facile reversibility. The CV plot for both species was found to be identical and is depicted in Fig. 3.4. The cyclic voltammogram shows reversible oxidation /reduction of the copper bis mabipy species at $E_{1/2}$ = 0.45V.

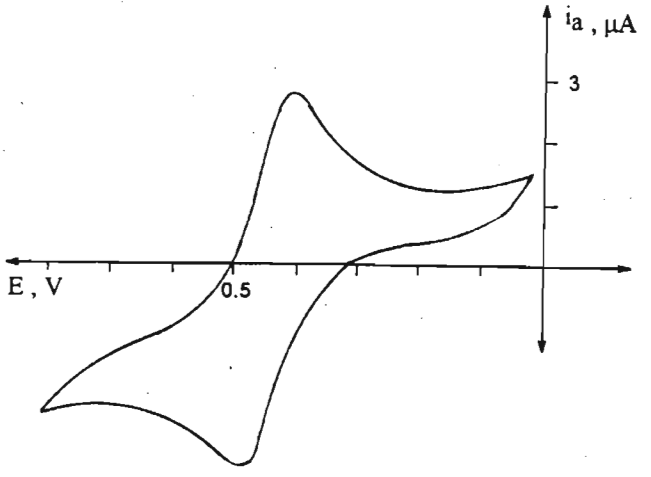

Fig. 3.4 : Cyclic voltammogram of [Cu(η^2-mabipy)$_2$](PF$_6$) in MeCN containing 0.1M TBAP

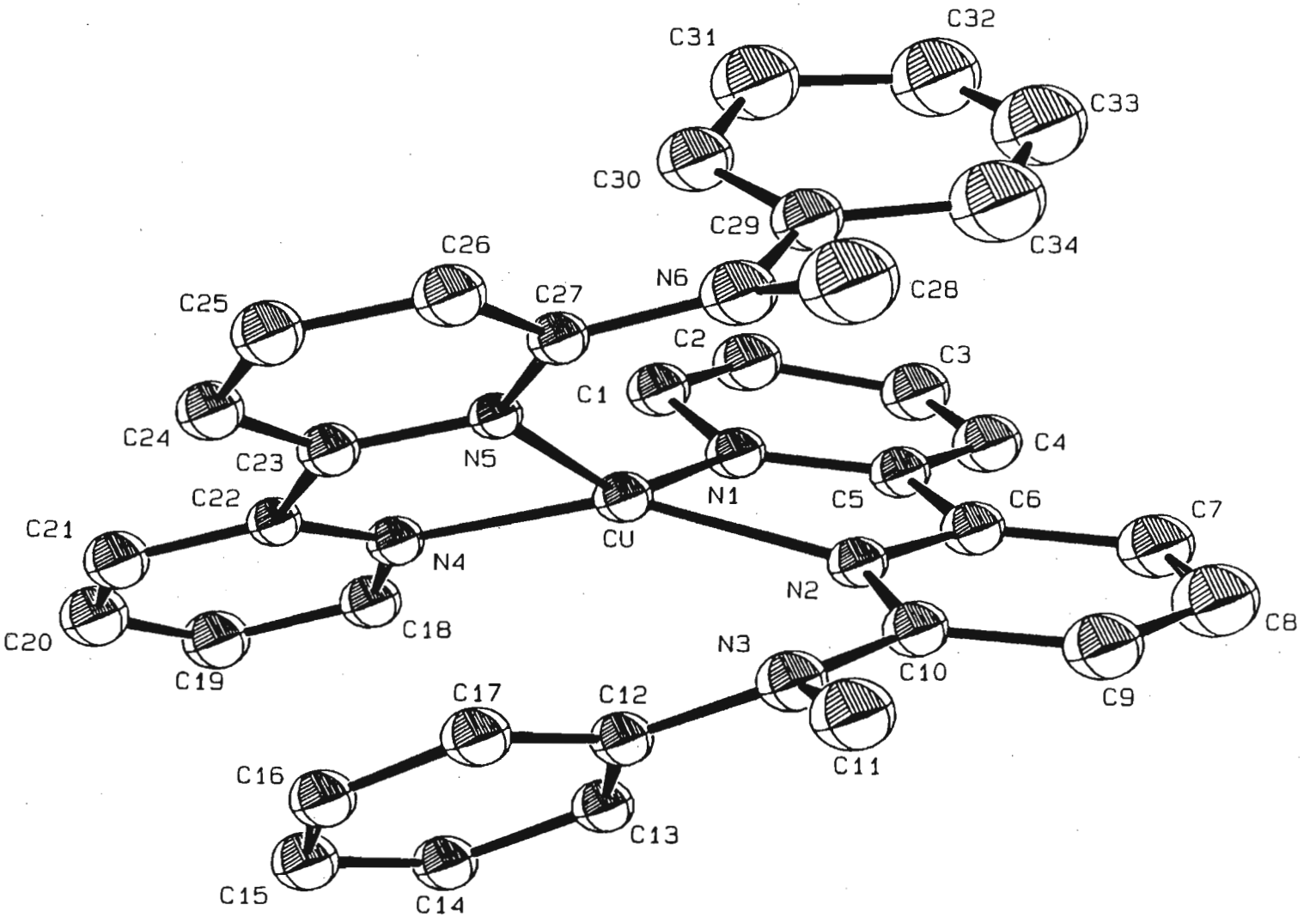

Fig 3.3 : ORTEP representation at 20% probability of $[Cu(\eta^2\text{-mabipy})_2]^{2+}$ 4

3.4 Discussion

The potentially tridentate ligands: mabipy, pipbipy and Habipy all preferentially afford mononuclear species with copper(I) or copper(II) where chelation occurs through the bipyridyl fragments with the exocyclic nitrogens remaining uncoordinated. This differs markedly from the behaviour of the analogous phosphine ligand PPh_2bipy, which preferentially forms dinuclear species with copper(I) via the formation of three membered NCP bridges.

Reasons for the different coordination behaviour of the aminobipyridyl ligands are at this stage somewhat speculative, although evidence obtained from the X-ray crystallographic study of the aminobipyridyl complexes does help in explaining the behaviour of these ligands. Nitrogen is accepted as being a 'harder' base than phosphorous and in this respect is less suited to coordination to the relatively 'soft'copper(I) ion, yet the same coordination behaviour is shown towards the relatively 'harder' copper(II) ion. An explanation based solely on 'hard' and 'soft' acid-base theory is thus inconclusive. Of greater significance is the observed involvement of the nitrogen lone pair orbital in the π electron system of the bipyridyl rings. In complexes **1 - 4** the exocyclic nitrogen has planar geometry typical of sp^2 hybrids, and presumably an energy barrier exists between sp^2 and the sp^3 hybrids, the latter being the required hybridisation for coordination of this nitrogen. Overcoming this energy barrier appears to be difficult and changing the reaction conditions and starting materials had no effect on the products formed. In another attempt to circumvent this problem, the synthesis of a ligand containing a sterically fixed lone pair orbital, depicted in Fig. 3.5 was attempted.

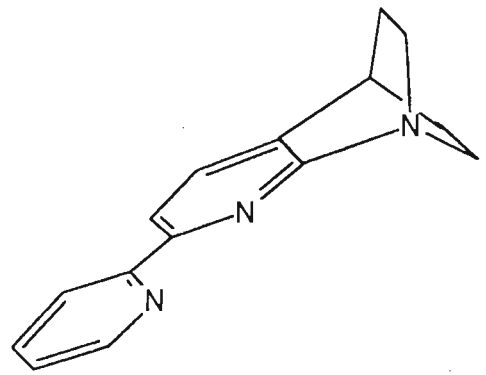

Fig. 3.5 : Hypothetical ligand

In this ligand the exocyclic nitrogen has its lone pair orbital perpendicular to the π electron system of the bipyridyl rings, such that no overlap of the lone pair orbital with the π electron system of the bipyridyl rings can take place . Unfortunately, despite exploring several routes to the synthesis of this ligand, this task proved insurmountable.

3.5 Experimental

All reactions were carried out under a nitrogen atmosphere unless otherwise indicated. All solvents were purified by the literature methods. General experimental methods are outlined in Appendix A.

3.5.1 *Synthesis of* $[Cu(\eta^2\text{-}L)_2](PF_6)$, L= mabipy **1** , pipbipy **2** , Habipy **3**

A solution of mabipy, pipibipy, or Habipy (0.268 mmol) dissolved in methanol (20 ml) was added dropwise to a stirred solution of $[Cu(NCMe)_4](PF_6)$ (50 mg; 0.134 mmol) in methanol (15 ml) at room temperature. After stirring for 10 min, the dark red solution was allowed to evaporate slowly under a nitrogen atmosphere to afford $[Cu(\eta^2\text{-}L)_2](PF_6)$, L= mabipy **1** , pipbipy **2** or Habipy **3**, as dark red crystalline material. Yield **1**= 82% , **2**= 85% , **3**= 83% . $[Cu(\eta^2\text{-}L)_2](SbF_6)$, L= mabipy or pipbipy were synthesised in the same manner from $[Cu(NCMe)_4](SbF_6)$, which was prepared by the reaction of excess $NOSbF_6$ with Cu in acetonitrile.

3.5.2 *Synthesis of* $[Cu(\eta^2\text{-mabipy})_2](ClO_4)_2$ **4**

Mabipy (70.52 mg; 0.2686 mmol) dissolved in methanol (20 ml) was added dropwise to a stirred solution of $Cu(ClO_4)_2 \cdot 6H_2O$ (50mg; 0.1343 mmols) dissolved in methanol (25 ml) at room temperature under an air atmosphere. The green precipitate which formed immediately was filtered and recrystallised from hot methanol to afford $[Cu(\eta^2\text{-mabipy})_2](ClO_4)_2 \cdot 2H_2O$ as a microcrystalline green material. Yield = 99 mg (90%).

Single crystal X-ray diffraction study of $[Cu(\eta^2\text{-mabipy})_2](SbF_6)$

Dark red blocks were grown by slow evaporation of a dilute solution of the complex in methanol under an atmosphere of nitrogen. The general approach used for the intensity data collection is described in Appendix A. Details of the crystallographic data are given in Table 3.4, the interatomic distances in Table 3.5, the interatomic angles in Table 3.6 and the fractional coordinates and equivalent isotropic thermal factors in Table 3.7. The observed and calculated structure factors may be found on micrfiche in an envelope fixed to the inside back cover. All atoms were made anisotropic and the phenyl rings were defined as rigid groups. All hydrogen atoms were placed in calculated positions.

Single crystal X-ray diffraction study of $[Cu(\eta 2\text{-pipbipy})_2](SbF_6) \cdot 0.5$ pipbipy

Dark red rectangular plates were grown by slow evaporation of a dilute solution of the complex in methanol under an atmosphere of nitrogen. The general approach used for the intensity data collection is described in Appendix A. Details of the crystallographic data are given in Table 3.8, the interatomic distances in Table 3.9, the interatomic angles in Table 3.10 and the fractional coordinates and equivalent isotropic thermal factors in Table 3.11. The observed and calculated structure factors may be found on micrfiche in an envelope fixed to the inside back cover. All atoms were made anisotropic and the SbF_6^- counterion was defined as a rigid group. All hydrogen atoms were placed in calculated positions.

Single crystal X-ray diffraction study of $[Cu(\eta^2\text{-mabipy})_2](ClO_4)_2 \cdot NCCH_2CH_3$

Emerald green rectangular crystals were grown by the slow diffusion of ether into a concentrated solution of the complex in propionitrile. The general approach used for the intensity data collection is described in Appendix A. Details of the crystallographic data are given in Table 3.12, the interatomic distances in Table 3.13, the interatomic angles in Table 3.14 and the fractional coordinates and equivalent isotropic thermal factors in Table 3.15. The observed and calculated structure factors may be found on micrfiche in an envelope fixed to the inside back cover. All atoms were made anisotropic and the phenyl rings were defined as rigid groups. All hydrogen atoms were placed in calculated positions.

Table 3.4 : Crystal data and details of the crystallographic analysis for $[Cu(\eta^2\text{-mabipy})_2](SbF_6)$

Formula	$CuC_{34}H_{30}N_6SbF_6$
Molecular mass ($g.mol^{-1}$)	821.94
Crystal system	Triclinic
Space group	$P\bar{1}$
a (Å)	10.379(3)
b (Å)	12.480(2)
c (Å)	13.4061(2)
α (°)	98.83(1)
β (°)	101.47(1)
γ (°)	92.15(2)
V ($Å^3$)	1677.4(6)
Z	2
D_c ($g.cm^{-3}$)	1.627
F (000)	410
λ (Mo - K_α) (Å)	0.71069
Scan mode	ω - 2θ
ω scan angle	0.66 + 0.35tanθ
Horizontal aperture width (mm)	2.7 + 0.1tanθ
Scattering range (°)	$2 \leq \theta \leq 30$
μ (cm^{-1})	16.887
Absorption corrections	Semi empirical
Measured intensities	5379
Unique intensities	4485
Unique intensities [$I > 3\sigma(I)$]	4094
Structure solution	Direct & Fourier
Weighting scheme	$1/[(\sigma^2(F) + 0.0059F^2)]$
$R = \Sigma(F_o\text{-}F_c)/\Sigma F_o$	0.0403
$R_w = \Sigma_w{}^{1/2}(F_o\text{-}F_c)/\Sigma_w{}^{1/2}F_o$	0.0504
$(\Delta/\sigma)_{max}$	0.211
$\Delta\rho_{max}(eÅ^{-3})$	0.659
Number of parameters	416

Table 3.5 : Interatomic distances (Å) for $[Cu(\eta^2\text{-mabipy})_2](SbF_6)$

Cu-N(1)	2.040(3)	Cu-N(2)	2.045(3)
Cu-N(4)	2.034(3)	Cu-N(5)	2.068(3)
N(1)-C(1)	1.328(6)	N(1)-C(5)	1.329(5)
N(2)-C(6)	1.329(5)	N(2)-C(10)	1.360(5)
N(3)-C(10)	1.372(6)	N(3)-C(11)	1.460(6)
N(3)-C(12)	1.420(4)	N(4)-C(18)	1.330(6)
N(4)-C(22)	1.339(5)	N(5)-C(23)	1.343(5)
N(5)-C(27)	1.342(5)	N(6)-C(27)	1.382(6)
N(6)-C(28)	1.473(6)	N(6)-C(29)	1.408(4)
C(1)-C(2)	1.384(7)	C(2)-C(3)	1.354(8)
C(3)-C(4)	1.378(8)	C(4)-C(5)	1.381(6)
C(5)-C(6)	1.497(6)	C(6)-C(7)	1.381(6)
C(7)-C(8)	1.387(7)	C(8)-C(9)	1.375(7)
C(9)-C(10)	1.381(6)	C13)-C(14)	1.395(0)
C(13)-C(12)	1.395(0)	C(14)-C(15)	1.395(0)
C(15)-C(16)	1.395(0)	C(16)-C(17)	1.395(0)
C(17)-C(12)	1.395(0)	C(18)-C(19)	1.368(7)
C(19)-C(20)	1.359(8)	C(20)-C(21)	1.380(7)
C(21)-C(22)	1.385(6)	C(22)-C(23)	1.484(6)
C(23)-C(24)	1.389(6)	C(24)-C(25)	1.390(7)
C(25)-C(26)	1.347(8)	C(26)-C(27)	1.397(6)
C(30)-C(31)	1.395(0)	C(31)-C(32)	1.395(0)
C(32)-C(33)	1.395(0)	C(33)-C(34)	1.395(0)
C(34)-C(29)	1.395(0)	Sb-F(1)	1.870(4)
Sb-F(2)	1.826(4)	Sb-F(3)	1.845(4)
Sb-F(4)	1.811(4)	Sb-F(5)	1.847(4)
Sb-F(6)	1.800(4)		

Table 3.6 : Interatomic angles (°) for $[Cu(\eta^2\text{-mabipy})_2](SbF_6)$

N(1)-Cu-N(2)	80.9(1)	N(1)-Cu-N(4)	109.0(1)
N(2)-Cu-N(4)	141.0(1)	N(1)-Cu-N(5)	136.8(1)
N(2)-Cu-N(5)	118.0(1)	N(4)-Cu-N(5)	81.2(1)
Cu-N(1)-C(1)	128.0(3)	Cu-N(1)-C(5)	113.4(3)
C(1)-N(1)-C(5)	118.6(4)	Cu-N(2)-C(6)	113.2(2)
Cu-N(2)-C(10)	125.5(3)	C(6)-N(2)-C(10)	119.2(3)
C(10)-N(3)-C(11)	118.4(4)	C(10)-N(3)-C(12)	121.1(3)
C(11)-N(3)-C(12)	116.4(4)	Cu-N(4)-C(18)	128.1(3)
Cu-N(4)-C(22)	113.5(3)	C(18)-N(4)-C(22)	118.3(4)
Cu-N(5)-C(23)	112.4(2)	Cu-N(5)-C(27)	127.7(3)
C(23)-N(5)-C(27)	118.7(3)	C(27)-N(6)-C(28)	118.9(4)
C(27)-N(6)-C(29)	121.9(3)	C(28)-N(6)-C(29)	118.4(4)
N1)-C(1)-C(2)	123.5(5)	C(1)-C(2)-C(3)	117.6(5)
C(2)-C(3)-C(4)	119.7(5)	C(3)-C(4)-C(5)	119.5(5)
N(1)-C(5)-C(4)	121.1(4)	N(1)-C(5)-C(6)	116.0(3)
C(4)-C(5)-C(6)	122.9(4)	N(2)-C(6)-C(5)	115.0(3)
N(2)-C(6)-C(7)	122.6(4)	C(5)-C(6)-C(7)	122.4(4)
C(6)-C(7)-C(8)	118.2(4)	C(7)-C(8)-C(9)	119.5(4)
C(8)-C(9)-C(10)	119.4(4)	N(2)-C(10)-N(3)	116.9(4)
N(2)-C(10)-C(9)	121.0(4)	N(3)-C(10)-C(9)	122.1(4)
C(14)-C(13)-C(12)	120.0(0)	C(13)-C(14)-C(15)	120.0(0)
C(14)-C(15)-C(16)	120.0(0)	C(15)-C(16)-C(17)	120.0(0)
C(16)-C(17)-C(12)	120.0(0)	N(3)-C(12)-C(13)	119.8(2)
N(3)-C(12)-C(17)	120.1(2)	C(13)-C(12)-C(17)	120.0(0)
N(4)-C(18)-C(19)	123.2(4)	C(18)-C(19)-C(20)	119.6(5)
C(19)-C(20)-C(21)	117.8(4)	C(20)-C(21)-C(22)	120.3(4)
N(4)-C(22)-C(21)	120.7(4)	N(4)-C(22)-C(23)	116.4(4)
C(21)-C(22)-C(23)	122.8(4)	N(5)-C(23)-C(22)	115.6(3)
N(5)-C(23)-C(24)	122.7(4)	C(22)-C(23)-C(24)	121.7(4)
C(23)-C(24)-H(20)	120.5(3)	C(23)-C(24)-C(25)	117.7(4)
C(24)-C(25)-C(26)	119.8(4)	C(25)-C(26)-C(27)	120.2(5)
N(5)-C(27)-N(6)	118.3(4)	N(5)-C(27)-C(26)	121.0(4)
N(6)-C(27)-C(26)	120.7(4)	C(31)-C(30)-C(29)	120.0(0)
C(30)-C(31)-C(32)	120.0(0)	C(31)-C(32)-C(33)	120.0(0)
C(32)-C(33)-C(34)	120.0(0)	C(33)-C(34)-C(29)	120.0(0)

Table 3.6 / Cont.

N(6)-C(29)-C(30)	120.1(2)	N(6)-C(29)-C(34)	119.8(2)
C(30)-C(29)-C(34)	120.0(0)	F(1)-Sb-F(2)	176.9(2)
F(1)-Sb-F(3)	82.7(3)	F(2)-Sb-F(3)	94.2(3)
F(1)-Sb-F(4)	96.7(3)	F(2)-Sb-F(4)	86.3(3)
F(3)-Sb-F(4)	176.9(2)	F(1)-Sb-F(5)	89.4(2)
F(2)-Sb-F(5)	90.7(2)	F(3)-Sb-F(5)	88.1(3)
F(4)-Sb-F(5)	88.8(3)	F(1)-Sb-F(6)	89.5(3)
F(2)-Sb-F(6)	90.4(3)	F(3)-Sb-F(6)	92.0(4)
F(4)-Sb-F(6)	91.0(4)	F(5)-Sb-F(6)	178.8(3)

Table 3.7 : Fractional coordinates (x 10^3) and equivalent isotropic thermal factors ($Å^2$, x 10^3) for $[Cu(\eta^2\text{-mabipy})_2](SbF_6)$

	x/a	y/b	z/c	U_{eq}
Cu	6265(1)	7846	1829	50
N(1)	4805(3)	6651(3)	1204(3)	53(1)
N(2)	7034(3)	6622(3)	2564(2)	44(1)
N(3)	8993(3)	7615(3)	3412(3)	60(1)
N(4)	6559(3)	8713(3)	717(3)	51(1)
N(5)	6419(3)	9393(2)	2677(2)	46(1)
N(6)	6146(3)	8870(3)	4229(3)	60(1)
C(1)	3763(4)	6676(4)	453(4)	68(1)
H(1)	3626(4)	7421(4)	140(4)	95(3)*
C(2)	2857(5)	5798(4)	47(4)	76(1)
H(2)	2025(5)	5842(4)	-570(4)	95(3)*
C(3)	3035(5)	4880(5)	465(5)	87(1)
H(3)	2348(5)	4178(5)	172(5)	95(3)*
C(4)	4118(5)	4836(4)	1238(4)	76(1)
H(4)	4266(5)	4109(4)	1579(4)	95(3)*
C(5)	4990(4)	5740(3)	1597(3)	48(1)
C(6)	6187(4)	5762(3)	2436(3)	50(1)
C(7)	6362(5)	4975(4)	3062(4)	68(1)
H(5)	5667(5)	4276(4)	2923(4)	95(3)*
C(8)	7452(6)	5108(4)	3869(4)	76(1)
H(6)	7601(6)	4525(4)	4392(4)	95(3)*
C(9)	8351(5)	5980(4)	3993(4)	67(1)
H(7)	9208(5)	6090(4)	4614(4)	95(3)*
C(10)	8136(4)	6725(4)	3325(3)	55(1)
C(11)	9970(6)	7926(7)	4371(4)	97(2)
H(8)	9792(6)	7565(7)	5018(4)	95(3)*
H(9)	10075(6)	8800(7)	4584(4)	95(3)*
H(10)	10863(6)	7641(7)	4158(4)	95(3)*
C(13)	9352(3)	7219(2)	1656(2)	57(1)
C(14)	9714(3)	7565(2)	803(2)	69(1)
C(15)	10016(3)	8666(2)	818(2)	75(1)
C(16)	9955(3)	9423(2)	1686(2)	76(1)

Table 3.7 /Cont.

C(17)	9593(3)	9077(2)	2539(2)	69(1)
C(12)	9291(3)	7975(2)	2524(2)	52(1)
H(11)	9118(3)	6366(2)	1644(2)	95(3)*
H(12)	9761(3)	6979(2)	131(2)	95(3)*
H(13)	10296(3)	8934(2)	157(2)	95(3)*
H(14)	10189(3)	10276(2)	1698(2)	95(3)*
H(15)	9546(3)	9663(2)	3211(2)	95(3)*
C(18)	6568(5)	8345(4)	-266(3)	63(1)
H(16)	6457(5)	7476(4)	-524(3)	95(3)*
C(19)	6683(5)	9012(5)	-968(4)	77(1)
H(17)	6658(5)	8683(5)	-1766(4)	95(3)*
C(20)	6834(5)	10106(5)	-658(4)	74(1)
H(18)	6936(5)	10657(5)	-1190(4)	95(3)*
C(21)	6864(5)	10498(4)	367(4)	66(1)
H(19)	6998(5)	11362(4)	647(4)	95(3)*
C(22)	6704(3)	9789(3)	1041(3)	48(1)
C(23)	6747(3)	10160(3)	2153(3)	47(1)
C(24)	7119(5)	11231(4)	2617(4)	66(1)
H(20)	7365(5)	11827(4)	2167(4)	95(3)*
C(25)	7175(5)	11497(4)	3670(4)	75(1)
H(21)	7482(5)	12318(4)	4054(4)	95(3)*
C(26)	6850(4)	10729(4)	4199(4)	68(1)
H(22)	6876(4)	10937(4)	5016(4)	95(3)*
C(27)	6460(3)	9669(3)	3691(3)	52(1)
C(28)	6873(6)	8891(6)	5294(4)	87(2)
H(23)	7045(6)	8193(6)	5678(4)	95(3)*
H(24)	6443(6)	9500(6)	5765(4)	95(3)*
H(25)	7798(6)	9223(6)	5177(4)	95(3)*
C(30)	3964(2)	8424(2)	3143(2)	55(1)
C(31)	2824(2)	7729(2)	2813(2)	67(1)
C(32)	2737(2)	6758(2)	3197(2)	86(2)
C(33)	3790(2)	6481(2)	3912(2)	83(2)
C(34)	4931(2)	7176(2)	4242(2)	70(1)
C(29)	5018(2)	8148(2)	3858(2)	53(1)
H(26)	4032(2)	9177(2)	2846(2)	95(3)*
H(27)	2008(2)	7944(2)	2260(2)	95(3)*

Table 3.7 /Cont.

H(28)	1854(2)	6219(2)	2941(2)	95(3)*
H(29)	3723(2)	5729(2)	4209(2)	95(3)*
H(30)	5747(2)	6962(2)	4796(2)	95(3)*
Sb	653	3301	2582	62
F(1)	-514(5)	3316(4)	3481(4)	138(2)
F(2)	1827(5)	3220(5)	1728(4)	149(2)
F(3)	1083(6)	2015(4)	3042(5)	173(2)
F(4)	154(7)	4524(4)	2083(6)	182(2)
F(5)	-623(5)	2509(5)	1545(3)	151(2)
F(6)	11872(8)	4080(6)	3607(4)	235(3)

*** isotropic temperature factor.**

$$\underline{U}_{eq} = 1/3\ \Sigma_i \Sigma_j \underline{U}_{ij}\, \underline{a}_i^*\, \underline{a}_j^*\, (a_i \cdot a_j)$$

Table 3.8 : Crystal data and details of the crystallographic analysis for $[Cu(\eta 2\text{-pipbipy})_2](SbF_6) \cdot 0.5$ pipbipy

Formula	$CuC_{35.5}H_{42.5}N_{7.5}SbF_6$
Molecular mass ($g.mol^{-1}$)	873.5629
Crystal system	Triclinic
Space group	$P\bar{1}$
a (A)	12.875(5)
b (A)	14.557(5)
c (A)	23.08(2)
α (°)	81.54(4)
β (°)	86.07(5)
γ (°)	65.16(4)
V (A^3)	3882.6(4)
Z	4
D_c ($g.cm^{-3}$)	1.49
F (000)	908
λ (Mo - K_α) (A)	0.71069
Scan mode	ω - 2θ
ω scan angle	1.00 + 0.35tanθ
Horizontal aperture width (mm)	2.7 + 0.1tanθ
Scattering range (°)	$2 \leq \theta \leq 30$
μ (cm^{-1})	13.39
Absorption corrections	Semi empirical
Measured intensities	9754
Unique intensities	6169
Unique intensities [$I > 3\sigma(I)$]	2497
Structure solution	Direct & Fourier
Weighting scheme	$1/[(\sigma^2(F) + 0.005F^2)]$
$R = \Sigma(F_o\text{-}F_c)/\Sigma F_o$	0.0917
$R_w = \Sigma_w ½(F_o\text{-}F_c)/\Sigma_w ½F_o$	0.0960
$(\Delta/\sigma)_{max}$	0.064
$\Delta\rho_{max}(eA^{-3})$	0.9063
Number of parameters	408

Table 3.9 : Interatomic distances (Å) for $[Cu(\eta 2\text{-pipbipy})_2](SbF_6) \cdot 0.5$ pipbipy

Molecule A

Cu(1A)-N(1A)	2.08(3)	Cu(1A)-N(2A)	2.01(3)
Cu(1A)-N(4A)	2.00(3)	Cu(1A)-N(5A)	2.07(3)
N(1A)-C(1A)	1.33(4)	N(1A)-C(5A)	1.35(4)
N(2A)-C(6A)	1.37(4)	N(2A)-C(10A)	1.42(4)
N(3A)-C(10A)	1.41(4)	N(3A)-C(11A)	1.44(5)
N(3A)-C(15A)	1.45(4)	N(4A)-C(16A)	1.28(4)
N(4A)-C(20A)	1.36(4)	N(5A)-C(21A)	1.36(4)
N(5A)-C(25A)	1.24(5)	N(6A)-C(25A)	1.41(5)
N(6A)-C(26A)	1.54(5)	N(6A)-C(30A)	1.50(5)
C(1A)-C(2A)	1.41(5)	C(2A)-C(3A)	1.34(5)
C(3A)-C(4A)	1.34(5)	C(4A)-C(5A)	1.43(4)
C(5A)-C(6A)	1.41(5)	C(6A)-C(7A)	1.39(5)
C(7A)-C(8A)	1.33(5)	C(8A)-C(9A)	1.33(5)
C(9A)-C(10A)	1.39(5)	C(11A)-C(12A)	1.57(5)
C(12A)-C(13A)	1.47(5)	C(13A)-C(14A)	1.53(5)
C(14A)-C(15A)	1.55(5)	C(16A)-C(17A)	1.45(5)
C(17A)-C(18A)	1.36(5)	C(18A)-C(19A)	1.36(5)
C(19A)-C(20A)	1.45(5)	C(20A)-C(21A)	1.38(5)
C(21A)-C(22A)	1.45(5)	C(22A)-C(23A)	1.38(5)
C(23A)-C(24A)	1.44(5)	C(24A)-C(25A)	1.43(5)
C(26A)-C(27A)	1.48(6)	C(27A)-C(28A)	1.46(5)
C(28A)-C(29A)	1.58(6)	C(29A)-C(30A)	1.52(5)

Molecule B

Cu(1B)-N(1B)	1.99(3)	Cu(1B)-N(2B)	2.10(3)
Cu(1B)-N(4B)	2.03(3)	Cu(1B)-N(5B)	2.02(3)
N(1B)-C(1B)	1.33(4)	N(1B)-C(5B)	1.38(4)
N(2B)-C(6B)	1.37(4)	N(2B)-C(10B)	1.31(4)
N(3B)-C(10B)	1.38(4)	N(3B)-C(11B)	1.39(6)
N(3B)-C(15B)	1.32(5)	N(4B)-C(16B)	1.35(4)
N(4B)-C(20B)	1.33(4)	N(5B)-C(21B)	1.40(4)
N(5B)-C(25B)	1.31(4)	N(6B)-C(25B)	1.47(4)
N(6B)-C(26B)	1.45(5)	N(6B)-C(30B)	1.45(4)

Table 3.9 /Cont.

C(1B)-C(2B)	1.50(6)	C(2B)-C(3B)	1.35(5)
C(3B)-C(4B)	1.30(5)	C(4B)-C(5B)	1.42(5)
C(5B)-C(6B)	1.45(4)	C(6B)-C(7B)	1.45(5)
C(7B)-C(8B)	1.34(5)	C(8B)-C(9B)	1.28(5)
C(9B)-C(10B)	1.47(5)	C(11B)-C(12B)	1.23(7)
C(12B)-C(13B)	1.37(7)	C(13B)-C(14B)	1.78(7)
C(14B)-C(15B)	1.58(7)	C(16B)-C(17B)	1.51(5)
C(17B)-C(18B)	1.31(5)	C(18B)-C(19B)	1.39(5)
C(19B)-C(20B)	1.47(5)	C(20B)-C(21B)	1.44(5)
C(21B)-C(22B)	1.42(5)	C(22B)-C(23B)	1.34(5)
C(23B)-C(24B)	1.39(4)	C(24B)-C(25B)	1.40(4)
C(26B)-C(27B)	1.58(5)	C(27B)-C(28B)	1.44(4)
C(28B)-C(29B)	1.53(5)	C(29B)-C(30B)	1.48(4)
Sb(1A)-F(1A)	1.810(0)	Sb(1A)-F(2A)	1.810(0)
Sb(1A)-F(3A)	1.810(0)	Sb(1A)-F(4A)	1.810(0)
Sb(1A)-F(5A)	1.810(0)	Sb(1A)-F(6A)	1.810(0)
Sb(1B)-F(1B)	1.810(0)	Sb(1B)-F(2B)	1.810(0)
Sb(1B)-F(3B)	1.810(0)	Sb(1B)-F(4B)	1.810(0)
Sb(1B)-F(5B)	1.810(0)	Sb(1B)-F(6B)	1.810(0)

Molecule C

N(1C)-C(1C)	1.30(5)	N(1C)-C(5C)	1.40(4)
N(2C)-C(6C)	1.31(4)	N(2C)-C(10C)	1.38(5)
N(3C)-C(10C)	1.38(5)	N(3C)-C(11C)	1.47(6)
N(3C)-C(15C)	1.42(6)	C(1C)-C(2C)	1.40(6)
C(2C)-C(3C)	1.31(5)	C(3C)-C(4C)	1.39(5)
C(4C)-C(5C)	1.44(5)	C(5C)-C(6C)	1.41(5)
C(6C)-C(7C)	1.43(5)	C(7C)-C(8C)	1.43(5)
C(8C)-C(9C)	1.29(5)	C(9C)-C(10C)	1.45(5)
C(11C)-C(12C)	1.40(6)	C(12C)-C(13C)	1.45(6)
C(13C)-C(14C)	1.52(6)	C(14C)-C(15C)	1.48(6)

Table 3.10 : Interatomic angles (°) for $[Cu(\eta 2\text{-pipbipy})_2](SbF_6) \cdot 0.5$ pipbipy

Molecule A

N(1A)-Cu(1A)-N(2A)	80.4(12)	N(1A)-Cu(1A)-N(4A)	118.7(12)
N(2A)-Cu(1A)-N(4A)	136.8(12)	N(1A)-Cu(1A)-N(5A)	135.8(11)
N(2A)-Cu(1A)-N(5A)	110.8(12)	N(4A)-Cu(1A)-N(5A)	83.0(12)
Cu(1A)-N(1A)-C(1A)	123(3)	Cu(1A)-N(1A)-C(5A)	112(2)
C(1A)-N(1A)-C(5A)	125(3)	Cu(1A)-N(2A)-C(6A)	113(2)
Cu(1A)-N(2A)-C(10A)	128(3)	C(6A)-N(2A)-C(10A)	116(3)
C(10A)-N(3A)-C(11A)	112(3)	C(10A)-N(3A)-C(15A)	120(3)
C(11A)-N(3A)-C(15A)	116(3)	Cu(1A)-N(4A)-C(16A)	127(3)
Cu(1A)-N(4A)-C(20A)	111(3)	C(16A)-N(4A)-C(20A)	121(4)
Cu(1A)-N(5A)-C(21A)	106(2)	Cu(1A)-N(5A)-C(25A)	129(3)
C(21A)-N(5A)-C(25A)	122(4)	C(25A)-N(6A)-C(26A)	122(4)
C(25A)-N(6A)-C(30A)	114(4)	C(26A)-N(6A)-C(30A)	114(3)
N(1A)-C(1A)-C(2A)	117(4)	C(1A)-C(2A)-C(3A)	119(4)
C(2A)-C(3A)-C(4A)	125(4)	C(3A)-C(4A)-C(5A)	116(4)
N(1A)-C(5A)-C(4A)	118(3)	N(1A)-C(5A)-C(6A)	117(3)
C(4A)-C(5A)-C(6A)	125(4)	N(2A)-C(6A)-C(5A)	116(4)
N(2A)-C(6A)-C(7A)	120(4)	C(5A)-C(6A)-C(7A)	125(4)
C(6A)-C(7A)-C(8A)	122(4)	C(7A)-C(8A)-C(9A)	121(4)
C(8A)-C(9A)-C(10A)	120(4)	N(2A)-C(10A)-N(3A)	112(4)
N(2A)-C(10A)-C(9A)	121(4)	N(3A)-C(10A)-C(9A)	126(4)
N(3A)-C(11A)-H(8A)	110(2)	N(3A)-C(11A)-H(9A)	110(2)
N(3A)-C(11A)-C(12A)	109(4)	C(11A)-C(12A)-C(13A)	111(3)
C(12A)-C(13A)-C(14A)	112(3)	C(13A)-C(14A)-C(15A)	106(3)
N(3A)-C(15A)-C(14A)	111(3)	N(4A)-C(16A)-C(17A)	127(4)
C(16A)-C(17A)-C(18A)	112(4)	C(17A)-C(18A)-C(19A)	124(5)
C(18A)-C(19A)-C(20A)	119(5)	N(4A)-C(20A)-C(19A)	117(4)
N(4A)-C(20A)-C(21A)	116(4)	C(19A)-C(20A)-C(21A)	127(4)
N(5A)-C(21A)-C(20A)	121(4)	N(5A)-C(21A)-C(22A)	118(4)
C(20A)-C(21A)-C(22A)	121(4)	C(21A)-C(22A)-C(23A)	118(4)
C(22A)-C(23A)-C(24A)	122(4)	C(23A)-C(24A)-C(25A)	112(4)
N(5A)-C(25A)-N(6A)	119(4)	N(5A)-C(25A)-C(24A)	126(4)
N(6A)-C(25A)-C(24A)	114(4)	N(6A)-C(26A)-C(27A)	109(4)
C(26A)-C(27A)-C(28A)	109(5)	C(27A)-C(28A)-C(29A)	108(4)
C(28A)-C(29A)-C(30A)	110(4)	N(6A)-C(30A)-C(29A)	109(4)

Table 3.10 /Cont.

Molecule B

N(1B)-Cu(1B)-N(2B)	82.4(12)	N(1B)-Cu(1B)-N(4B)	115.6(12)
N(2B)-Cu(1B)-N(4B)	134.1(11)	N(1B)-Cu(1B)-N(5B)	141.5(11)
N(2B)-Cu(1B)-N(5B)	110.5(11)	N(4B)-Cu(1B)-N(5B)	81.9(11)
Cu(1B)-N(1B)-C(1B)	127(3)	Cu(1B)-N(1B)-C(5B)	115(2)
C(1B)-N(1B)-C(5B)	118(3)	Cu(1B)-N(2B)-C(6B)	107(2)
Cu(1B)-N(2B)-C(10B)	131(3)	C(6B)-N(2B)-C(10B)	119(3)
C(10B)-N(3B)-C(11B)	119(5)	C(10B)-N(3B)-C(15B)	117(4)
C(11B)-N(3B)-C(15B)	114(4)	Cu(1B)-N(4B)-C(16B)	124(3)
Cu(1B)-N(4B)-C(20B)	110(2)	C(16B)-N(4B)-C(20B)	126(3)
Cu(1B)-N(5B)-C(21B)	114(2)	Cu(1B)-N(5B)-C(25B)	133(2)
C(21B)-N(5B)-C(25B)	113(3)	C(25B)-N(6B)-C(26B)	116(3)
C(25B)-N(6B)-C(30B)	112(3)	C(26B)-N(6B)-C(30B)	115(3)
N(1B)-C(1B)-C(2B)	125(4)	C(1B)-C(2B)-C(3B)	109(4)
C(2B)-C(3B)-C(4B)	131(5)	C(3B)-C(4B)-C(5B)	117(4)
N(1B)-C(5B)-C(4B)	121(3)	N(1B)-C(5B)-C(6B)	112(3)
C(4B)-C(5B)-C(6B)	127(3)	N(2B)-C(6B)-C(5B)	120(3)
N(2B)-C(6B)-C(7B)	119(3)	C(5B)-C(6B)-C(7B)	121(3)
C(6B)-C(7B)-H(5B)	121(2)	C(6B)-C(7B)-C(8B)	118(4)
C(7B)-C(8B)-C(9B)	125(5)	C(8B)-C(9B)-C(10B)	117(5)
N(2B)-C(10B)-N(3B)	112(4)	N(2B)-C(10B)-C(9B)	121(4)
N(3B)-C(10B)-C(9B)	126(4)	N(3B)-C(11B)-C(12B)	130(7)
C(11B)-C(12B)-C(13B)	119(8)	C(12B)-C(13B)-C(14B)	116(5)
C(13B)-C(14B)-C(15B)	99(4)	N(3B)-C(15B)-C(14B)	121(5)
N(4B)-C(16B)-C(17B)	117(4)	C(16B)-C(17B)-C(18B)	118(4)
C(17B)-C(18B)-C(19B)	124(4)	C(18B)-C(19B)-C(20B)	118(4)
N(4B)-C(20B)-C(19B)	117(3)	N(4B)-C(20B)-C(21B)	123(3)
C(19B)-C(20B)-C(21B)	121(4)	N(5B)-C(21B)-C(20B)	111(3)
N(5B)-C(21B)-C(22B)	125(3)	C(20B)-C(21B)-C(22B)	124(3)
C(21B)-C(22B)-C(23B)	116(4)	C(22B)-C(23B)-C(24B)	121(4)
C(23B)-C(24B)-C(25B)	118(3)	N(5B)-C(25B)-N(6B)	114(3)
N(5B)-C(25B)-C(24B)	126(3)	N(6B)-C(25B)-C(24B)	120(3)
N(6B)-C(26B)-C(27B)	106(3)	C(26B)-C(27B)-C(28B)	111(3)
C(27B)-C(28B)-C(29B)	111(3)	C(28B)-C(29B)-C(30B)	110(3)
N(6B)-C(30B)-C(29B)	110(3)	F(1A)-Sb(1A)-F(2A)	180.0(0)
F(1A)-Sb(1A)-F(3A)	90.0(0)	F(2A)-Sb(1A)-F(3A)	90.0(0)

Table 3.10 /Cont.

F(1A)-Sb(1A)-F(4A)	90.0(0)	F(2A)-Sb(1A)-F(4A)	90.0(0)
F(3A)-Sb(1A)-F(4A)	180.0(0)	F(1A)-Sb(1A)-F(5A)	90.0(0)
F(2A)-Sb(1A)-F(5A)	90.0(0)	F(3A)-Sb(1A)-F(5A)	90.0(0)
F(4A)-Sb(1A)-F(5A)	90.0(0)	F(1A)-Sb(1A)-F(6A)	90.0(0)
F(2A)-Sb(1A)-F(6A)	90.0(0)	F(3A)-Sb(1A)-F(6A)	90.0(0)
F(4A)-Sb(1A)-F(6A)	90.0(0)	F(5A)-Sb(1A)-F(6A)	180.0(0)
F(1B)-Sb(1B)-F(2B)	180.0(0)	F(1B)-Sb(1B)-F(3B)	90.0(0)
F(2B)-Sb(1B)-F(3B)	90.0(0)	F(1B)-Sb(1B)-F(4B)	90.0(0)
F(2B)-Sb(1B)-F(4B)	90.0(0)	F(3B)-Sb(1B)-F(4B)	180.0(0)
F(1B)-Sb(1B)-F(5B)	90.0(0)	F(2B)-Sb(1B)-F(5B)	90.0(0)
F(3B)-Sb(1B)-F(5B)	90.0(0)	F(4B)-Sb(1B)-F(5B)	90.0(0)
F(1B)-Sb(1B)-F(6B)	90.0(0)	F(2B)-Sb(1B)-F(6B)	90.0(0)
F(3B)-Sb(1B)-F(6B)	90.0(0)	F(4B)-Sb(1B)-F(6B)	90.0(0)
F(5B)-Sb(1B)-F(6B)	180.0(0)		

Molecule C

C(1C)-N(1C)-C(5C)	116(4)	C(6C)-N(2C)-C(10C)	123(4)
C(10C)-N(3C)-C(11C)	128(5)	C(10C)-N(3C)-C(15C)	114(5)
C(11C)-N(3C)-C(15C)	119(5)	N(1C)-C(1C)-C(2C)	124(5)
C(1C)-C(2C)-C(3C)	119(5)	C(2C)-C(3C)-C(4C)	125(5)
C(3C)-C(4C)-C(5C)	113(4)	N(1C)-C(5C)-C(4C)	124(4)
N(1C)-C(5C)-C(6C)	116(4)	C(4C)-C(5C)-C(6C)	1 2 1 (4)
N(2C)-C(6C)-C(5C)	119(4)	N(2C)-C(6C)-C(7C)	1 2 2 (4)
C(5C)-C(6C)-C(7C)	119(4)	C(6C)-C(7C)-H(5C)	1 2 4 (3)
C(6C)-C(7C)-C(8C)	112(4)	C(7C)-C(8C)-C(9C)	127(5)
CC(8C)-C(9C)-C(10C)	117(4)	N(2C)-C(10C)-N(3C)	123(4)
N(2C)-C(10C)-C(9C)	117(4)	N(3C)-C(10C)-C(9C)	119(5)
N(3C)-C(11C)-C(12C)	106(6)	C(11C)-C(12C)-C(13C)	111(5)
C(12C)-C(13C)-C(14C)	116(5)	C(13C)-C(14C)-C(15C)	110(5)
N(3C)-C(15C)-C(14C)	111(4)		

Table 3.11 : Fractional coordinates (x 10^4) and equivalent isotropic thermal factors(A^2,x10^3) for [Cu(η2-pipbipy)$_2$](SbF$_6$) · 0.5 pipbipy

	x/a	y/b	z/c	U_{eq}
Molecule A				
Cu(1A)	4932(4)	1119(3)	3750(2)	56(1)
N(1A)	6701(25)	331(22)	3824(14)	60(9)*
N(2A)	5328(24)	788(20)	2925(12)	47(8)*
N(3A)	3478(27)	1704(24)	2545(14)	68(10)*
N(4A)	4140(25)	2376(22)	4141(13)	57(9)*
N(5A)	3527(23)	842(22)	4058(12)	49(8)*
N(6A)	4043(29)	-701(26)	3733(15)	76(11)*
C(1A)	7272(30)	280(25)	4293(16)	50(11)*
H(1A)	6830(30)	639(25)	4669(16)	128(4)*
C(2A)	8475(36)	-236(30)	4266(20)	76(13)*
H(2A)	8987(36)	-308(30)	4635(20)	128(4)*
C(3A)	8965(37)	-656(31)	3782(20)	78(13)*
H(3A)	9887(37)	-1053(31)	3772(20)	128(4)*
C(4A)	8401(33)	-608(28)	3304(19)	66(12)*
H(4A)	8827(33)	-992(28)	2933(19)	128(4)*
C(5A)	7187(28)	-34(24)	3320(15)	40(10)*
C(6A)	6438(34)	95(29)	2865(18)	64(12)*
C(7A)	6765(32)	-397(27)	2367(17)	56(11)*
H(5A)	7657(32)	-890(27)	2309(17)	128(4)*
C(8A)	6021(34)	-277(29)	1961(18)	67(13)*
H(6A)	6291(34)	-733(29)	1604(18)	128(4)*
C(9A)	4938(34)	382(29)	1996(18)	67(12)*
H(7A)	4347(34)	530(29)	1648(18)	128(4)*
C(10A)	4565(33)	917(29)	2474(18)	63(12)*
C(11A)	2646(36)	1683(33)	2165(20)	88(15)*
H(8A)	2760(36)	1996(33)	1724(20)	128(4)*
H(9A)	2756(36)	904(33)	2170(20)	128(4)*
C(12A)	1416(34)	2358(29)	2385(19)	76(13)*
H(10A)	1292(34)	2009(29)	2815(19)	128(4)*
H(11A)	774(34)	2400(29)	2092(19)	128(4)*
C(13A)	1307(33)	3386(30)	2449(19)	72(13)*

Table 3.11 /Cont.

H(12A)	1467(33)	3724(30)	2023(19)	128(4)*
H(13A)	454(33)	3848(30)	2595(19)	128(4)*
C(14A)	2194(34)	3346(31)	2871(19)	82(14)*
H(14A)	2109(34)	4102(31)	2917(19)	128(4)*
H(15A)	2080(34)	2968(31)	3294(19)	128(4)*
C(15A)	3381(28)	2709(25)	2615(16)	49(10)*
H(16A)	4046(28)	2634(25)	2904(16)	128(4)*
H(17A)	3478(28)	3093(25)	2192(16)	128(4)*
C(16A)	4563(33)	2990(28)	4238(17)	65(12)*
H(18A)	5381(33)	2876(28)	4034(17)	128(4)*
C(17A)	4055(39)	3818(32)	4595(19)	87(14)*
H(19A)	4434(39)	4329(32)	4663(19)	128(4)*
C(18A)	3042(39)	3877(35)	4840(20)	91(15)*
H(20A)	2553(39)	4510(35)	5080(20)	128(4)*
C(19A)	2591(41)	3196(35)	4789(21)	98(15)*
H(21A)	1819(41)	3248(35)	5026(21)	128(4)*
C(20A)	3174(35)	2389(30)	4426(18)	69(12)*
C(21A)	2797(33)	1690(29)	4292(17)	62(12)*
C(22A)	1595(33)	1889(31)	4336(17)	69(12)*
H(22A)	978(33)	2564(31)	4506(17)	128(4)*
C(23A)	1266(39)	1195(33)	4149(19)	86(14)*
H(23A)	381(39)	1311(33)	4203(19)	128(4)*
C(24A)	2067(37)	312(31)	3900(19)	79(13)*
H(24A)	1806(37)	-196(31)	3714(19)	128(4)*
C(25A)	3223(39)	187(34)	3938(20)	80(14)*
C(26A)	3699(42)	-1443(36)	3472(22)	105(17)*
H(25A)	2950(42)	-1012(36)	3204(22)	128(4)*
H(26A)	3511(42)	-1937(36)	3819(22)	128(4)*
C(27A)	4668(40)	-2092(36)	3122(22)	103(16)*
H(27A)	4938(40)	-1599(36)	2815(22)	128(4)*
H(28A)	4422(40)	-2557(36)	2886(22)	128(4)*
C(28A)	5629(42)	-2703(36)	3510(22)	104(16)*
H(29A)	5307(42)	-3064(36)	3876(22)	128(4)*
H(30A)	6302(42)	-3281(36)	3291(22)	128(4)*
C(29A)	6059(38)	-1954(33)	3737(20)	91(15)*
H(31A)	6286(38)	-1531(33)	3364(20)	128(4)*
H(32A)	6802(38)	-2391(33)	4009(20)	128(4)*

Table 3.11 /Cont.

C(30A)	5116(34)	-1216(31)	4091(19)	80(13)*
H(33A)	5368(34)	-642(31)	4199(19)	128(4)*
H(34A)	4958(34)	-1632(31)	4489(19)	128(4)*

Molecule B

Cu(1B)	5228(4)	3948(3)	1292(2)	56(1)
N(1B)	6144(24)	2669(21)	950(13)	53(9)*
N(2B)	6635(23)	4277(22)	1010(13)	52(8)*
N(3B)	5948(31)	5871(28)	1231(16)	82(11)*
N(4B)	3533(23)	4617(20)	1095(13)	46(8)*
N(5B)	4623(21)	4465(18)	2067(12)	34(7)*
N(6B)	6349(24)	3742(21)	2564(13)	49(8)*
C(1B)	5810(34)	1945(30)	871(18)	72(13)*
H(1B)	5014(34)	1980(30)	1071(18)	128(4)*
C(2B)	6462(42)	1080(37)	524(21)	102(16)*
H(2B)	6362(42)	447(37)	384(21)	128(4)*
C(3B)	-2527(37)	1101(31)	353(18)	73(13)*
H(3B)	-1731(37)	491(31)	244(18)	128(4)*
C(4B)	7881(33)	1764(28)	407(16)	60(11)*
H(4B)	8716(33)	1543(28)	203(16)	128(4)*
C(5B)	7203(28)	2578(25)	729(15)	42(10)*
C(6B)	7482(31)	3389(27)	858(16)	53(11)*
C(7B)	8663(32)	3243(28)	886(16)	57(11)*
H(5B)	9352(32)	2548(28)	775(16)	128(4)*
C(8B)	8865(37)	3995(32)	1050(18)	73(13)*
H(6B)	9749(37)	3867(32)	1085(18)	128(4)*
C(9B)	8097(37)	4858(34)	1158(19)	84(14)*
H(7B)	8309(37)	5443(34)	1286(19)	128(4)*
C(10B)	6898(34)	5019(30)	1107(17)	61(12)*
C(11B)	6101(59)	6628(53)	1470(32)	166(26)*
H(8B)	6704(59)	6821(53)	1188(32)	128(4)*
H(9B)	6487(59)	6265(53)	1891(32)	128(4)*
C(12B)	5401(61)	7475(54)	1567(33)	177(27)*
H(10B)	5076(61)	7354(54)	2002(33)	128(4)*
H(11B)	5731(61)	8049(54)	1550(33)	128(4)*
C(13B)	4402(50)	7934(42)	1260(26)	133(21)*

Table 3.11 /Cont.

H(12B)	3611(50)	7854(42)	1360(26)	128(4)*
H(13B)	4266(50)	8549(42)	908(26)	128(4)*
C(14B)	-6102(53)	7100(48)	1002(27)	154(24)*
H(14B)	-6272(53)	7754(48)	1223(27)	128(4)*
H(15B)	-5410(53)	7007(48)	692(27)	128(4)*
C(15B)	5086(45)	6219(37)	863(22)	103(16)*
H(16B)	4313(45)	6096(37)	931(22)	128(4)*
H(17B)	4939(45)	6867(37)	531(22)	128(4)*
C(16B)	3103(34)	4521(29)	602(19)	73(13)*
H(18B)	3222(34)	4248(29)	181(19)	128(4)*
C(17B)	-8181(35)	4966(30)	552(20)	76(13)*
H(19B)	-8136(35)	4684(30)	139(20)	128(4)*
C(18B)	-8788(34)	5498(29)	963(18)	60(11)*
H(20B)	-9689(34)	5960(29)	1023(18)	128(4)*
C(19B)	1676(36)	5533(28)	1483(18)	67(12)*
H(21B)	755(36)	5872(28)	1446(18)	128(4)*
C(20B)	-7071(31)	5073(27)	1540(17)	54(11)*
C(21B)	3451(28)	5110(24)	2061(15)	41(10)*
C(22B)	2868(33)	5769(26)	2488(17)	56(11)*
H(22B)	1960(33)	6238(26)	2456(17)	128(4)*
C(23B)	3508(33)	5765(29)	2925(18)	70(13)*
H(23B)	3130(33)	6303(29)	3237(18)	128(4)*
C(24B)	4646(25)	5078(22)	2979(13)	26(8)*
H(24B)	5163(25)	5026(22)	3342(13)	128(4)*
C(25B)	5129(29)	4434(25)	2547(16)	45(10)*
C(26B)	7017(35)	3872(32)	3002(20)	85(14)*
H(25B)	6838(35)	4668(32)	2993(20)	128(4)*
H(26B)	6825(35)	3574(32)	3432(20)	128(4)*
C(27B)	8308(31)	3230(27)	2843(18)	70(12)*
H(27B)	8861(31)	3279(27)	3157(18)	128(4)*
H(28B)	8483(31)	3538(27)	2411(18)	128(4)*
C(28B)	8527(30)	2176(26)	2827(16)	54(11)*
H(29B)	9412(30)	1741(26)	2716(16)	128(4)*
H(30B)	8343(30)	1874(26)	3259(16)	128(4)*
C(29B)	7740(29)	2087(27)	2393(16)	56(11)*
H(31B)	7892(29)	1297(27)	2401(16)	128(4)*
H(32B)	7929(29)	2380(27)	1960(16)	128(4)*

Table 3.11 /Cont.

C(30B)	6534(27)	2698(24)	2541(15)	45(10)*
H(33B)	6324(27)	2380(24)	2962(15)	128(4)*
H(34B)	5987(27)	2688(24)	2210(15)	128(4)*
Sb(1A)	2287(2)	1841(2)	10208(1)	60(1)
F(1A)	3404(2)	2201(2)	10382(1)	128(4)*
F(2A)	1171(2)	1480(2)	10034(1)	128(4)*
F(3A)	1581(2)	3067(2)	9768(1)	128(4)*
F(4A)	2994(2)	614(2)	10649(1)	128(4)*
F(5A)	3096(2)	1315(2)	9572(1)	128(4)*
F(6A)	1478(2)	2366(2)	10844(1)	128(4)*
Sb(1B)	7829(2)	2824(2)	5037(2)	77(1)
F(1B)	6837(2)	4020(2)	4655(2)	201(7)*
F(2B)	8822(2)	1628(2)	5419(2)	201(7)*
F(3B)	8268(2)	2316(2)	4347(2)	201(7)*
F(4B)	7393(2)	3333(2)	5727(2)	201(7)*
F(5B)	8934(2)	3295(2)	4960(2)	201(7)*
F(6B)	6724(2)	2354(2)	5116(2)	201(7)*

Molecule C

N(1C)	1094(28)	4366(25)	6782(16)	80(11)*
N(2C)	73(27)	2566(24)	7535(14)	65(9)*
N(3C)	-577(40)	1471(35)	8209(22)	134(16)*
C(1C)	972(39)	4916(35)	6276(22)	90(15)*
H(1C)	1436(39)	5392(35)	6189(22)	128(4)*
C(2C)	279(35)	4930(31)	5829(20)	75(13)*
H(2C)	207(35)	5410(31)	5416(20)	128(4)*
C(3C)	-285(35)	4357(31)	5925(20)	79(14)*
H(3C)	-866(35)	4425(31)	5588(20)	128(4)*
C(4C)	-186(35)	3666(32)	6425(20)	80(14)*
H(4C)	-595(35)	3146(32)	6475(20)	128(4)*
C(5C)	506(30)	3736(26)	6868(17)	51(11)*
C(6C)	608(32)	3165(29)	7429(18)	61(12)*
C(7C)	1359(35)	3201(31)	7845(20)	80(14)*
H(5C)	1885(35)	3621(31)	7757(20)	128(4)*
C(8C)	1312(38)	2638(34)	8399(22)	95(16)*
H(6C)	1729(38)	2740(34)	8759(22)	128(4)*

Table 3.11 /Cont.

C(9C)	845(32)	2005(29)	8513(18)	62(12)*
H(7C)	1013(32)	1494(29)	8920(18)	128(4)*
C(10C)	98(37)	1999(33)	8070(21)	79(14)*
C(11C)	-705(59)	935(48)	8783(31)	165(25)*
H(8C)	-1585(59)	1229(48)	8931(31)	128(4)*
H(9C)	-181(59)	1021(48)	9099(31)	128(4)*
C(12C)	-276(43)	-96(37)	8708(23)	105(17)*
H(10C)	615(43)	-367(37)	8580(23)	128(4)*
H(11C)	-360(43)	-536(37)	9113(23)	128(4)*
C(13C)	-894(49)	-250(43)	8257(25)	134(21)*
H(12C)	-521(49)	-1053(43)	8210(25)	128(4)*
H(13C)	-1774(49)	-21(43)	8399(25)	128(4)*
C(14C)	-914(42)	360(35)	7659(22)	103(16)*
H(14C)	-1546(42)	340(35)	7382(22)	128(4)*
H(15C)	-76(42)	16(35)	7462(22)	128(4)*
C(15C)	-1170(43)	1432(36)	7722(22)	105(17)*
H(16C)	-2080(43)	1841(36)	7786(22)	128(4)*
H(17C)	-904(43)	1783(36)	7330(22)	128(4)*

*** isotropic temperature factor.**

$$\underline{U}_{eq} = 1/3 \, \Sigma_i \Sigma_j \underline{U}_{ij} \underline{a}_i^* \underline{a}_j^* (a_i . a_j)$$

Table 3.12 : Crystal data and details of the crystallographic analysis for $[Cu(\eta^2\text{-mabipy})_2](ClO_4)_2 \cdot NCCH_2CH_3$

Formula	$CuC_{37}H_{35}N_7Cl_2O_8$
Molecular mass ($g.mol^{-1}$)	840.180
Crystal system	Monoclinic
Space group	$P2_1/c$
a (Å)	8.149(4)
b (Å)	14.422(3)
c (Å)	31.58(1)
α (°)	90
β (°)	91.74(2)
γ (°)	90
V ($Å^3$)	3710(2)
Z	4
D_c ($g.cm^{-3}$)	1.504
F (000)	1732
λ (Mo - K_α) (Å)	0.71069
Scan mode	ω - 2θ
ω scan angle	0.53 + 0.35tanθ
Horizontal aperture width (mm)	2.7 + 0.1tanθ
Scattering range (°)	$2 \leq \theta \leq 30$
μ (cm^{-1})	7.450
Absorption corrections	Semi empirical
Measured intensities	6213
Unique intensities	4003
Unique intensities [$I > 3\sigma(I)$]	2434
Structure solution	Direct & Fourier
Weighting scheme	$1/[(\sigma^2(F) + 0.00068F^2)]$
$R = \Sigma(F_o-F_c)/\Sigma F_o$	0.0650
$R_w = \Sigma_w ½(F_o-F_c)/\Sigma_w ½F_o$	0.0668
$(\Delta/\sigma)_{max}$	0.402
$\Delta\rho_{max}(eÅ^{-3})$	0.573
Number of parameters	482

Table 3.13 : Interatomic distances (Å) for $[Cu(\eta^2\text{-mabipy})_2](ClO_4)_2 \cdot NCCH_2CH_3$

Cu-N(5)	1.986(8)	Cu-N(2)	1.983(9)
Cu-N(1)	1.961(9)	Cu-N(4)	1.973(9)
Cl(1)-O(1)	1.430(9)	Cl(1)-O(2)	1.366(10)
Cl(1)-O(3)	1.399(10)	Cl(1)-O(4)	1.416(10)
Cl(2)-O(5)	1.29(2)	Cl(2)-O(6)	1.394(12)
Cl(2)-O(7)	1.23(2)	Cl(2)-O(8)	1.366(13)
N(5)-C(23)	1.333(13)	N(5)-C(27)	1.321(13)
N(2)-C(6)	1.358(14)	N(2)-C(10)	1.364(14)
N(1)-C(1)	1.341(14)	N(1)-C(5)	1.332(13)
N(4)-C(18)	1.315(13)	N(4)-C(22)	1.326(13)
N(3)-C(10)	1.350(14)	N(3)-C(11)	1.459(14)
N(3)-C(12)	1.435(13)	N(6)-C(27)	1.412(14)
N(6)-C(28)	1.47(2)	N(6)-C(29)	1.40(2)
C(1)-C(2)	1.38(2)	C(2)-C(3)	1.41(2)
C(3)-C(4)	1.33(2)	C(4)-C(5)	1.38(2)
C(5)-C(6)	1.49(2)	C(6)-C(7)	1.37(2)
C(7)-C(8)	1.39(2)	C(8)-C(9)	1.34(2)
C(9)-C(10)	1.40(2)	C(13)-C(14)	1.395(0)
C(13)-C(12)	1.395(0)	C(14)-C(15)	1.395(0)
C(15)-C(16)	1.395(0)	C(16)-C(17)	1.395(0)
C(17)-C(12)	1.395(0)	C(18)-C(19)	1.40(2)
C(19)-C(20)	1.36(2)	C(20)-C(21)	1.41(2)
C(21)-C(22)	1.36(2)	C(22)-C(23)	1.48(2)
C(23)-C(24)	1.40(2)	C(24)-C(25)	1.39(2)
C(25)-C(26)	1.39(2)	C(26)-C(27)	1.40(2)
C(30)-C(31)	1.395(0)	C(30)-C(29)	1.395(0)
C(31)-C(32)	1.395(0)	C(32)-C(33)	1.395(0)
C(33)-C(34)	1.395(0)	C(34)-C(29)	1.395(0)
N(1S)-C(1S)	1.14(2)	C(1S)-C(2S)	1.48(2)
C(2S)-C(3S)	1.52(2)		

Table 3.14 : Interatomic angles (Å) for $[Cu(\eta^2\text{-mabipy})_2](ClO_4)_2 \cdot NCCH_2CH_3$

N(5)-Cu-N(2)	112.2(4)	N(5)-Cu-N(1)	145.0(4)
N(2)-Cu-N(1)	83.6(4)	N(5)-Cu-N(4)	82.2(4)
N(2)-Cu-N(4)	149.5(4)	N(1)-Cu-N(4)	99.8(4)
O(1)-Cl(1)-O(2)	110.4(7)	O(1)-Cl(1)-O(3)	110.4(6)
O(2)-Cl(1)-O(3)	107.9(7)	O(1)-Cl(1)-O(4)	106.5(6)
O(2)-Cl(1)-O(4)	111.0(7)	O(3)-Cl(1)-O(4)	110.7(7)
O(5)-Cl(2)-O(6)	109.5(13)	O(5)-Cl(2)-O(7)	105(2)
O(6)-Cl(2)-O(7)	104.6(11)	O(5)-Cl(2)-O(8)	107.4(10)
O(6)-Cl(2)-O(8)	113.2(8)	O(7)-Cl(2)-O(8)	116.4(14)
Cu-N(5)-C(23)	112.2(8)	Cu-N(5)-C(27)	127.1(8)
C(23)-N(5)-C(27)	120.7(10)	Cu-N(2)-C(6)	112.5(8)
Cu-N(2)-C(10)	129.6(8)	C(6)-N(2)-C(10)	117.8(10)
Cu-N(1)-C(1)	125.3(9)	Cu-N(1)-C(5)	113.5(8)
C(1)-N(1)-C(5)	120.6(11)	Cu-N(4)-C(18)	124.2(8)
Cu-N(4)-C(22)	114.4(8)	C(18)-N(4)-C(22)	120.7(10)
C(10)-N(3)-C(11)	118.7(11)	C(10)-N(3)-C(12)	123.1(9)
C(11)-N(3)-C(12)	116.0(10)	C(27)-N(6)-C(28)	117.4(12)
C(27)-N(6)-C(29)	120.8(9)	C(28)-N(6)-C(29)	118.6(11)
N(1)-C(1)-C(2)	121.1(12)	C(1)-C(2)-C(3)	118.5(13)
C(2)-C(3)-C(4)	118.0(13)	C(3)-C(4)-C(5)	122.4(13)
N(1)-C(5)-C(4)	118.9(12)	N(1)-C(5)-C(6)	115.7(11)
C(4)-C(5)-C(6)	125.2(12)	N(2)-C(6)-C(5)	114.4(11)
N(2)-C(6)-C(7)	123.8(13)	C(5)-C(6)-C(7)	121.6(13)
C(6)-C(7)-C(8)	117.0(14)	C(7)-C(8)-C(9)	120.5(13)
C(8)-C(9)-C(10)	120.8(13)	N(2)-C(10)-N(3)	119.0(11)
N(2)-C(10)-C(9)	119.6(12)	N(3)-C(10)-C(9)	121.4(13)
C(14)-C(13)-C(12)	120.0(0)	C(13)-C(14)-C(15)	120.0(0)
C(14)-C(15)-C(16)	120.0(0)	C(15)-C(16)-C(17)	120.0(0)
C(16)-C(17)-C(12)	120.0(0)	N(3)-C(12)-C(13)	120.1(5)
N(3)-C(12)-C(17)	119.8(5)	C(13)-C(12)-C(17)	120.0(0)
N(4)-C(18)-H(16)	119.1(7)	N(4)-C(18)-C(19)	121.7(12)
C(18)-C(19)-C(20)	117.6(13)	C(19)-C(20)-C(21)	120.2(12)
C(20)-C(21)-C(22)	118.0(12)	N(4)-C(22)-C(21)	121.7(11)
N(4)-C(22)-C(23)	113.7(11)	C(21)-C(22)-C(23)	124.5(12)

Table 3.14 /Cont.

N(5)-C(23)-C(22)	116.4(10)	N(5)-C(23)-C(24)	121.9(11)
C(22)-C(23)-C(24)	121.6(11)	C(23)-C(24)-C(25)	117.7(12)
C(24)-C(25)-C(26)	119.8(12)	C(25)-C(26)-C(27)	118.5(12)
N(5)-C(27)-N(6)	118.1(10)	N(5)-C(27)-C(26)	121.4(12)
N(6)-C(27)-C(26)	120.4(12)	C(31)-C(30)-C(29)	120.0(0)
C(30)-C(31)-C(32)	120.0(0)	C(31)-C(32)-C(33)	120.0(0)
C(32)-C(33)-C(34)	120.0(0)	C(33)-C(34)-C(29)	120.0(0)
N(6)-C(29)-C(30)	120.5(6)	N(6)-C(29)-C(34)	119.4(6)
C(30)-C(29)-C(34)	120.0(0)	N(1S)-C(1S)-C(2S)	173(2)
C(1S)-C(2S)-C(3S)	109(2)		

Table 3.15 : Fractional coordinates ($x10^4$) and equivalent isotropic thermal factors ($Å^2, x10^3$) for $[Cu(\eta^2\text{-mabipy})_2](ClO_4)_2 \cdot NCCH_2CH_3$

	x/a	y/b	z/c	U_{eq}
Cu	3000(2)	2587(1)	8482	51
Cl(1)	8061(4)	3186(3)	7648(1)	65(1)
Cl(2)	6437(4)	7473(3)	9188(1)	81(1)
O(1)	-1228(11)	2579(7)	7961(3)	105(3)
O(2)	-3060(14)	3760(8)	7826(4)	138(4)
O(3)	-2752(12)	2674(8)	7329(3)	115(3)
O(4)	-627(14)	3700(7)	7480(3)	115(4)
O(5)	7383(19)	-3239(11)	9153(9)	303(12)
O(6)	5472(20)	-2426(9)	8819(4)	171(5)
O(7)	5465(21)	-2740(23)	9460(5)	340(13)
O(8)	7416(19)	-1778(10)	9275(4)	176(5)
N(5)	1421(9)	1578(6)	8602(3)	41(2)
N(2)	4556(10)	2816(7)	8965(3)	44(2)
N(1)	3248(12)	3923(7)	8386(3)	52(3)
N(4)	2592(11)	2170(7)	7893(3)	47(2)
N(3)	5077(12)	1287(8)	9176(3)	57(3)
N(6)	1068(12)	1997(9)	9311(3)	67(3)
C(1)	2425(14)	4417(9)	8090(4)	59(4)
H(1)	1567(14)	4066(9)	7878(4)	118(8)*
C(2)	2643(17)	5363(10)	8057(4)	67(4)
H(2)	2029(17)	5751(10)	7806(4)	118(8)*
C(3)	3711(17)	5805(10)	8350(5)	73(4)
H(3)	3942(17)	6541(10)	8332(5)	118(8)*
C(4)	4407(15)	5291(10)	8657(5)	67(4)
H(4)	5223(15)	5616(10)	8889(5)	118(8)*
C(5)	4153(14)	4346(9)	8687(4)	52(3)
C(6)	4898(14)	3731(9)	9019(4)	52(3)
C(7)	5732(16)	4085(11)	9368(5)	73(4)
H(5)	5933(16)	4822(11)	9403(5)	118(8)*
C(8)	6316(21)	3456(13)	9667(5)	97(5)
H(6)	6935(21)	3701(13)	9953(5)	118(8)*

Table 3.15 /Cont.

C(9)	6083(17)	2541(12)	9610(4)	80(4)
H(7)	6620(17)	2217(12)	9890(4)	118(8)*
C(10)	-4761(14)	2206(10)	9249(4)	54(3)
C(11)	5361(18)	645(10)	9527(4)	84(4)
H(8)	4956(18)	1001(10)	9806(4)	118(8)*
H(9)	6590(18)	384(10)	9585(4)	118(8)*
H(10)	4542(18)	73(10)	9455(4)	118(8)*
C(13)	5906(9)	1333(4)	8436(3)	51(3)
C(14)	5977(9)	922(4)	8037(3)	64(4)
C(15)	5220(9)	68(4)	7962(3)	66(4)
C(16)	4392(9)	-375(4)	8285(3)	58(3)
C(17)	4321(9)	36(4)	8684(3)	63(4)
C(12)	5078(9)	890(4)	8759(3)	50(3)
H(11)	6491(9)	1994(4)	8495(3)	118(8)*
H(12)	6617(9)	1265(4)	7787(3)	118(8)*
H(13)	5275(9)	-251(4)	7653(3)	118(8)*
H(14)	3807(9)	-1037(4)	8226(3)	118(8)*
H(15)	3681(9)	-307(4)	8934(3)	118(8)*
C(18)	3289(14)	2536(10)	7562(3)	60(3)
H(16)	4008(14)	3161(10)	7603(3)	118(8)*
C(19)	3093(16)	2149(10)	7157(4)	64(4)
H(17)	3618(16)	2471(10)	6884(4)	118(8)*
C(20)	2210(19)	1354(11)	7119(4)	79(5)
H(18)	2072(19)	1026(11)	6812(4)	118(8)*
C(21)	1513(16)	951(9)	7478(4)	67(4)
H(19)	792(16)	323(9)	7456(4)	118(8)*
C(22)	1740(13)	1389(8)	7857(4)	46(3)
C(23)	1077(14)	1061(8)	8261(4)	47(3)
C(24)	55(15)	282(9)	8278(4)	58(4)
H(20)	-226(15)	-120(9)	7997(4)	118(8)*
C(25)	-571(15)	48(9)	8668(6)	74(4)
H(21)	-1352(15)	-553(9)	8695(6)	118(8)*
C(26)	-198(16)	594(10)	9022(5)	70(4)
H(22)	-644(16)	411(10)	9329(5)	118(8)*
C(27)	783(13)	1377(9)	8970(4)	48(3)
C(28)	1143(24)	1605(13)	9739(5)	127(7)

Table 3.15 / Cont.

H(23)	1748(24)	2107(13)	9944(5)	118(8)*
H(24)	2043(24)	1132(13)	9618(5)	118(8)*
H(25)	254(24)	1223(13)	9916(5)	118(8)*
C(30)	-227(11)	3266(8)	8925(3)	69(4)
C(31)	-570(11)	4211(8)	8887(3)	103(6)
C(32)	67(11)	4832(8)	9188(3)	124(7)
C(33)	1047(11)	4509(8)	9526(3)	141(8)
C(34)	1391(11)	3565(8)	9564(3)	103(5)
C(29)	753(11)	2943(8)	9263(3)	71(4)
H(26)	-720(11)	2785(8)	8692(3)	118(8)*
H(27)	-1329(11)	4461(8)	8625(3)	118(8)*
H(28)	-199(11)	5564(8)	9159(3)	118(8)*
H(29)	1540(11)	4991(8)	9759(3)	118(8)*
H(30)	2150(11)	3315(8)	9826(3)	118(8)*
N(1S)	8087(19)	1027(10)	433(5)	102(5)
C(1S)	8333(21)	1666(14)	635(6)	87(5)
C(2S)	8675(19)	2565(14)	850(5)	109(6)
H(1S)	9752(19)	2879(14)	720(5)	118(8)*
H(2S)	7642(19)	3029(14)	809(5)	118(8)*
C(3S)	9015(22)	2386(14)	1319(6)	129(6)
H(3S)	9142(22)	3077(14)	1448(6)	118(8)*
H(4S)	10010(22)	1957(14)	1440(6)	118(8)*
H(5S)	7859(22)	2093(14)	1412(6)	118(8)*

*** isotropic temperature factor.**

$$\underline{U}_{eq} = 1/3 \, \Sigma_i \Sigma_j \underline{U}_{ij} \, \underline{a}_i^* \, \underline{a}_j^* \, (a_i \, . \, a_j)$$

Chapter four

The synthesis and characterisation of dinuclear complexes of ruthenium, molybdenum and rhodium containing bridging anionic 6-anilinobipyridyl or bipyridyl-6-one ligands

Introduction

The aim of this study was to synthesise and characterise complexes in which the anionic ligands 6-anilino-2,2'-bipyridine (abipy) and 2,2'-bipyridin-6-one (obipy) bridge two metal centres via either NCN^- or NCO^- chains. The abipy and obipy ligands are formed by deprotonation of Habipy and and Hobipy respectively, and like the amidopyridyl and oxypyridinate ligands should be effective in bridging two metal centres. The reaction of abipy and obipy with precursors containing the 'hard acid' Ru_2^{5+}, Mo_2^{4+}, Rh_2^{4+} cores, and the relatively 'softer' Ru_2^{2+} core were studied with a view to achieving this end.

4.1 Ligand bridged complexes of ruthenium(I)

4.1.1 Introduction

A number of complexes of ruthenium(I) have been synthesised in which a dinuclear framework is maintained by either OCO^-, NCO^- or NCN^- chain bridges[38-41]. Such examples include $[Ru_2(O_2CCH_3)_2(CO)_4(L)_2]$ where L= MeCN, CO, py, PPh_3 or $AsPh_3$[38], $[Ru_2(hp)_2(CO)_4(L)_2]$ where L= Hhp, PPh_3, MeCN, CO, $P(OPh)_3$[41], and $[Ru_2(bmanapy)_2(CO)_4]$ (bmanapy=2-benzylamido-7-methyl-1,8-naphthyridine)[40]. In the case of the acetate and hydroxypyridyl bridged dimers, represented by the general formula $[Ru_2(XY)_2(CO)_4(L)_2]$, shown in Fig 4.1, the axial positions occupied by ligand L may easily be substituted by a variety of donor ligands as indicated.

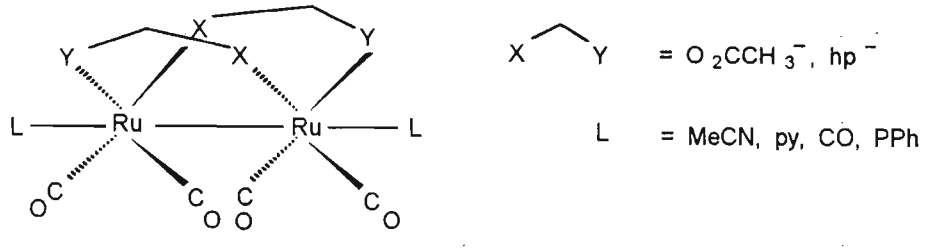

Fig. 4.1 : Structure of $[Ru_2(XY)_2(CO)_4(L)_2]$

These axial positions may also be occupied by the oxygen atoms of the acetate groups on adjacent ruthenium dimers to form polymeric compounds such as $[\{Ru_2(O_2CCH_3)_2(CO)_4\}_n]$[38] and $[\{Ru_2(hp)_2(CO)_4\}_n]$[41]. These polymers are however easily broken down in donor solvents to afford the dimeric solvento species.

Thus far the synthetic routes to these ruthenium(I) dimers have in general been either via reaction of the free ligand with $[Ru_3(CO)_{12}]$[40] as in eqn. **1**, or via ligand metathesis involving the reaction of $[Ru_2(O_2CCH_3)_2(CO)_4(L)_2]$ species with the sodium salt of the ligand[39] as in eqn. **2**. However the polymeric species $[\{Ru_2(O_2CCH_3)_2(CO)_4\}_n]$ and $[\{Ru_2(hp)_2(CO)_4\}_n]$ have also been used successfully as starting materials for the synthesis of these dimers[41].

$$[Ru_3(CO)_{12}] + Hbmanapy \rightarrow [Ru_2(bmanapy)_2(CO)_4] \qquad \mathbf{1}$$

$$[Ru_2(O_2CCH_3)_2(CO)_4(MeCN)_2] + 2Na\ hp \rightarrow [Ru_2(hp)_2(CO)_4(MeCN)_2] + NaO_2CCH_3 \qquad \mathbf{2}$$

The recently synthesised $[Ru_2(bmanapy)_2(CO)_4]$ complex (where bmanapy = 2-benzylamido-7-methyl-1,8-naphthyridine), shown in Fig. 4.2 appears to be the only example of a dinuclear ruthenium(I) species in which the ruthenium atoms are bridged by a NCN^- chain. This complex is also unique in that it represents the first dinuclear ruthenium(I) species to be characterised without additional axial ligands. The the naphthyridyl portion of the bmanapy ligand, in the $[Ru_2(bmanapy)_2(CO)_4]$ complex, displays uncharacteristic chelating behaviour in occupying the axial sites of the Ru atoms. The bipyridyl fragment in general shows a higher preference toward chelating then does the naphthyridyl fragment and thus the abipy and obipy ligands seem ideally suited to this system.

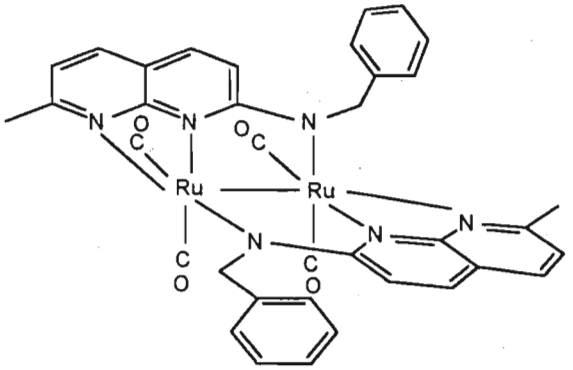

Fig. 4.2 : Structure of $[Ru_2(bmanapy)_2(CO)_4]$

4.1.2 Synthesis and characterisation of $[Ru_2(\mu\text{-}L)_2(CO)_4]$, L = abipy (5) or obipy (6)

The reaction of three equivalents of Habipy with $[Ru_3(CO)_{12}]$ in toluene was found to lead to a product, characterised as dinuclear $[Ru_2(\mu\text{-abipy})_2(CO)_4]$ **(5)** in 25% yield. Other products from the reaction, some being largely insoluble and presumably polymeric materials, have as yet not been identified. The reaction is temperature dependent, the formation of insoluble polymeric products being minimised by maintaining the reaction temperature below 50°C for a period of 9 days.

Complex **5** is obtained almost quantitatively from the reaction of two equivalents of Habipy with $[\{Ru_2(O_2CCH_3)_2(CO)_4\}_n]$ in refluxing toluene. The corresponding reaction of two equivalents of Hobipy with $[\{Ru_2(O_2CCH_3)_2(CO)_4\}_n]$ in refluxing toluene affords $[Ru_2(\mu\text{-obipy})_2(CO)_4]$ **(6)** in 80% yield. Table 4.1 lists the microanalytical data for complexes **5** and **6**, which are consistent with their formulation as $[Ru_2(\mu\text{-abipy})_2(CO)_4]$ and $[Ru_2(\mu\text{-abipy})_2(CO)_4]$ respectively.

Table 4.1 : Microanalytical data for complexes $[Ru_2(\mu\text{-abipy})_2(CO)_4]$ (5) and $[Ru_2(\mu\text{-obipy})_2(CO)_4]$ (6)

	analysis: calculated (found)		
Complex	**%C**	**%H**	**%N**
$[Ru_2(\mu\text{-abipy})_2(CO)_4]$	53.60 (53.56)	3.00 (3.28)	10.41 (10.38)
$[Ru_2(\mu\text{-obipy})_2(CO)_4]$	43.91 (43.45)	2.15 (2.33)	8.53 (8.14)

The infrared spectra of **5** and **6** exhibit four carbonyl stretches, though the shoulder at 1889 cm^{-1} in the spectrum of **5** is weak and is sometimes obscured by the more intense peak at 1923 cm^{-1}. The infrared spectra of $[Ru_2(hp)_2(CO)_4(L)_2]$ when L=MeCN, PPh_3, $P(OPh)_3$, or Hhp all show four carbonyl peaks which range from 1911 cm^{-1} to 2044 cm^{-1} [41]. The pattern of intensities of the four carbonyl peaks in these spectra are similar to those assigned for complexes **5** and **6**.

Table 4.2 : Spectroscopic data for $[Ru_2(\mu\text{-abipy})_2(CO)_4]$ (5)and $[Ru_2(\mu\text{-obipy})_2(CO)_4]$(6)

	$[Ru_2(\mu\text{-abipy})_2(CO)_4]$ (5)	$[Ru_2(\mu\text{-obipy})_2(CO)_4]$ (6)
IR[a] (cm^{-1})	2002(s), 1950(m), 1923(s), 1889(wsh), 1612(m), 1589(m), 1539(m), 1497(m), 1470(m)	2012(s), 1961(m), 1933(s), 1897(wsh), 1609(m), 1598(m), 1544(m), 1497(m), 1468(m), 770(w)
UV-vis[b] (nm)	462, 279	369, 265
δ NMR[c] (ppm)	5.8-8.10 (12H, m, abipy protons)	9.07 (1H, dbr, $H_{6'}$), 8.0 (2H, m, $H_{4'}$, $H_{3'}$), 7.5 (1H, m, $H_{5'}$), 7.25 (1H, m, H_4), 7.1 (1H, m, H_3), 6.25 (1H, d, H_5)

a= measured as KBr disc, b= measured in MeCN, c= complex **5** measured in $CDCl_3$ and complex **6** measured in CD_2Cl_2. s= strong, m= medium, w= weak, wsh= weak shoulder in the context of IR spectroscopy.

Single crystals of **5** and **6** were obtained for the purpose of structural characterisation and the structures of **5** and **6** where determined by X-ray diffraction methods. Figs. 4.3 and 4.4 depict the ORTEP representations of complexes **5** and **6** respectively. The crystal structures of **5** and **6** consist of well separated dimers, there being no contact distances between atoms of adjacent dimers less then the sum of the van der Waals radii for the atoms concerned. The molecules in the crystals of **5** posses a crystallographically imposed two-fold rotation axis situated midway between the two ruthenium atoms. The crystallographic asymmetric unit comprises two half-dimers unrelated by the symmetry operations of the space group P2/n. Both dimers in **5** are very similar and in describing the crystal structure in detail bond distances and angles are quoted as averages for the two dimers.

As shown in Fig. 4.3 complex **5** has two ruthenium centres bridged in a head-to-tail fashion by the two abipy ligands. Each ruthenium has an irregular octahedral geometry in which the axial sites opposite the Ru-Ru bond are occupied by nitrogen atoms of the bipyridyl fragment of the abipy ligands. The equatorial sites on each metal are occupied by the nitrogen atoms of the two abipy ligands, which are mutually *cis*, and by two carbonlys which are also *cis* to one another.

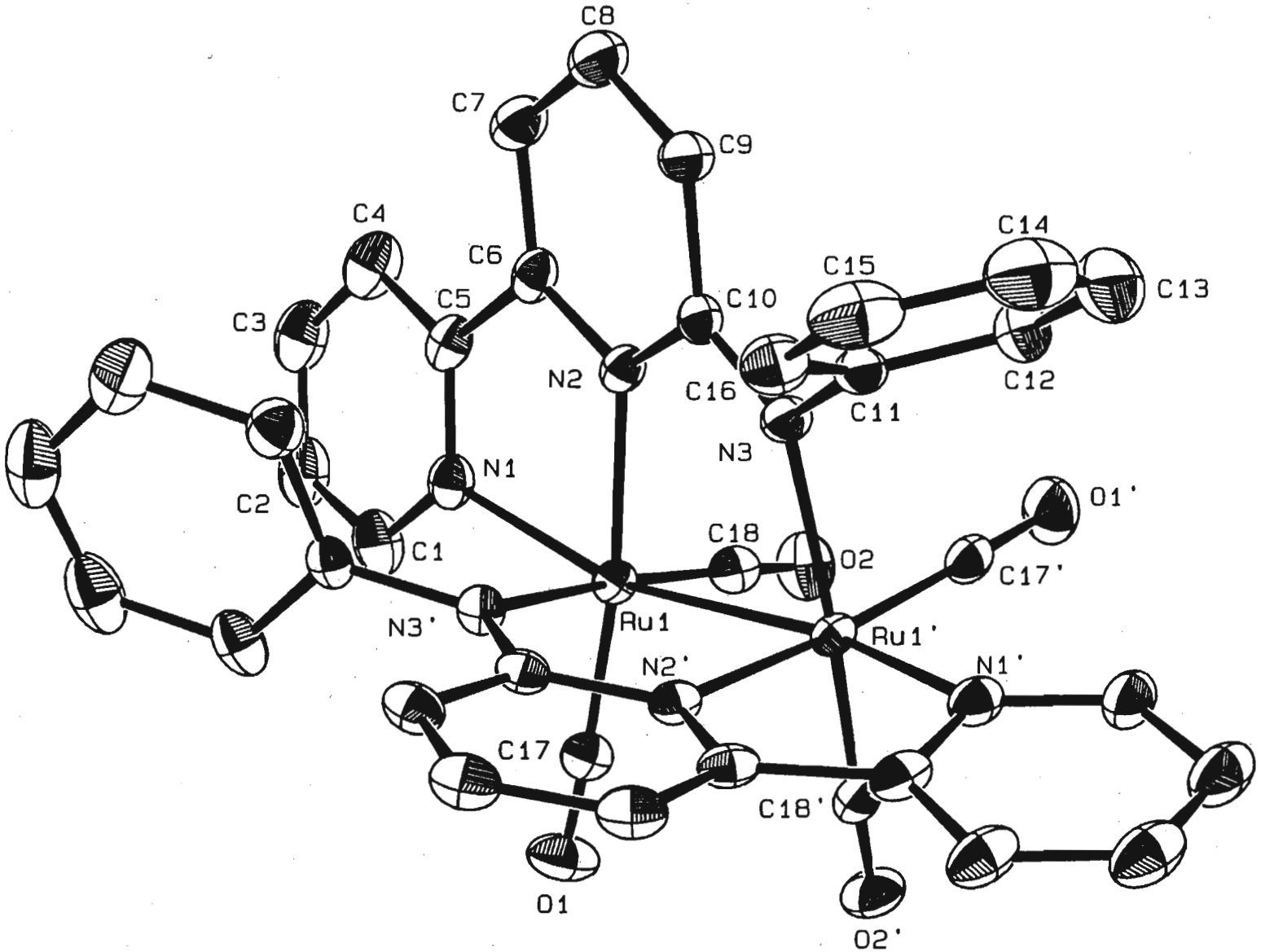

Fig 4.3 : ORTEP representation at 20% probability of $[Ru_2(\mu\text{-abipy})_2(CO)_4]$ 5

The Ru-Ru separation in complex **5** is 2.668(1) Å.This separation is normal for a Ru-Ru single bond and can be compared to values ranging from 2.639(1) to 2.759(4) Å in analogous ruthenium(I) dimers [46-49]. The Ru-N_{ax} distance in **5** is found to be 2.17(4) Å, which is shorter than those in $[Ru_2(hp)_2(CO)_4(Hhp)_2]$ which are 2.291(3) and 2.316(2) Å. The Ru-N_{eq} distances in **5** are only slightly shorter than the Ru-N_{ax} distances, ranging from 2.123(3) to 2.150(3) Å. The Ru-C distances are all typically of the order of 1.85 Å and no *trans* influence is observed by carbon atoms *trans* to the anionic anilino nitrogens. The C10-N3 length is 1.331(4) Å which does not appear unusually short for these ligands, as discussed in Chapters 2 and 3, and does indicate some multiple bond character.

The angles about each Ru atom range from 75.9 to 102.5°. Distortions from the idealized value of 90° result from the geometric constraints imposed by the bridging ligands, which in **5** have a N2-N3 bite distance of ca. 2.36 Å that is significantly shorter than the Ru-Ru separation distance of 2.668(1) Å. The bipyridyl fragment also induces strain which is evident from the small angle of 75.9° which it subtends at the Ru atmoms. These same forces are probably responsible for the deviation of the groups about the ruthenium atoms from adopting a perfectly eclipsed conformation. The torsion angles for N2-Ru1-Ru1′-N3 and C18-Ru1-Ru1′-C17′ are 12.7 and 7.7° respectively. The two Ru equatiorial planes N2, N3′, C17, C18, Ru1 and N2′, N3, C17′, C18′, Ru1′ are inclined to each another by 11.4°, which is somewhat smaller then the equivalent dihedral angles in $[Ru_2(CO)_4(hp)_2(PPh_3)_2]$[39] and $[Ru_2(bmanapy)_2(CO)_4]$[40] which are 16.2 and 17.6° respectively.

The crystal structure of **6** depicted in Fig. 4.4 shows two ruthenium atoms bridged in a head to tail fashion by the two obipy ligands. The structure of **6** is similar to that of **5**, there being minor differences in the bond lengths and angles, which are listed in Tables 4.12 and 4.13 respectively. The angles about the Ru atoms range from 76.2 to 103°. The torsion angles N2-Ru1-Ru2-O1, O2-Ru1-Ru2-N4, C21-Ru1-Ru2-C22 and C24-Ru1-Ru2-C23 are 8.5, 7.9, 5.6, and 3.3° respectively. The two Ru equatorial planes N2, O2, C21, C24, Ru1 and O1, N4, C22, C23, Ru2 have a dihedral angle of 15.1°, which is similar to those in $[Ru_2(CO)_4(hp)_2(PPh_3)_2]$[39] and $[Ru_2(bmanapy)_2(CO)_4]$[40]. The Ru-Ru bond length in **6** is 2.671(1) Å, which is statistically the same as that in complex **5**. The Ru-N_{ax} and Ru-N_{eq} distances are also very similar to those in **5**.

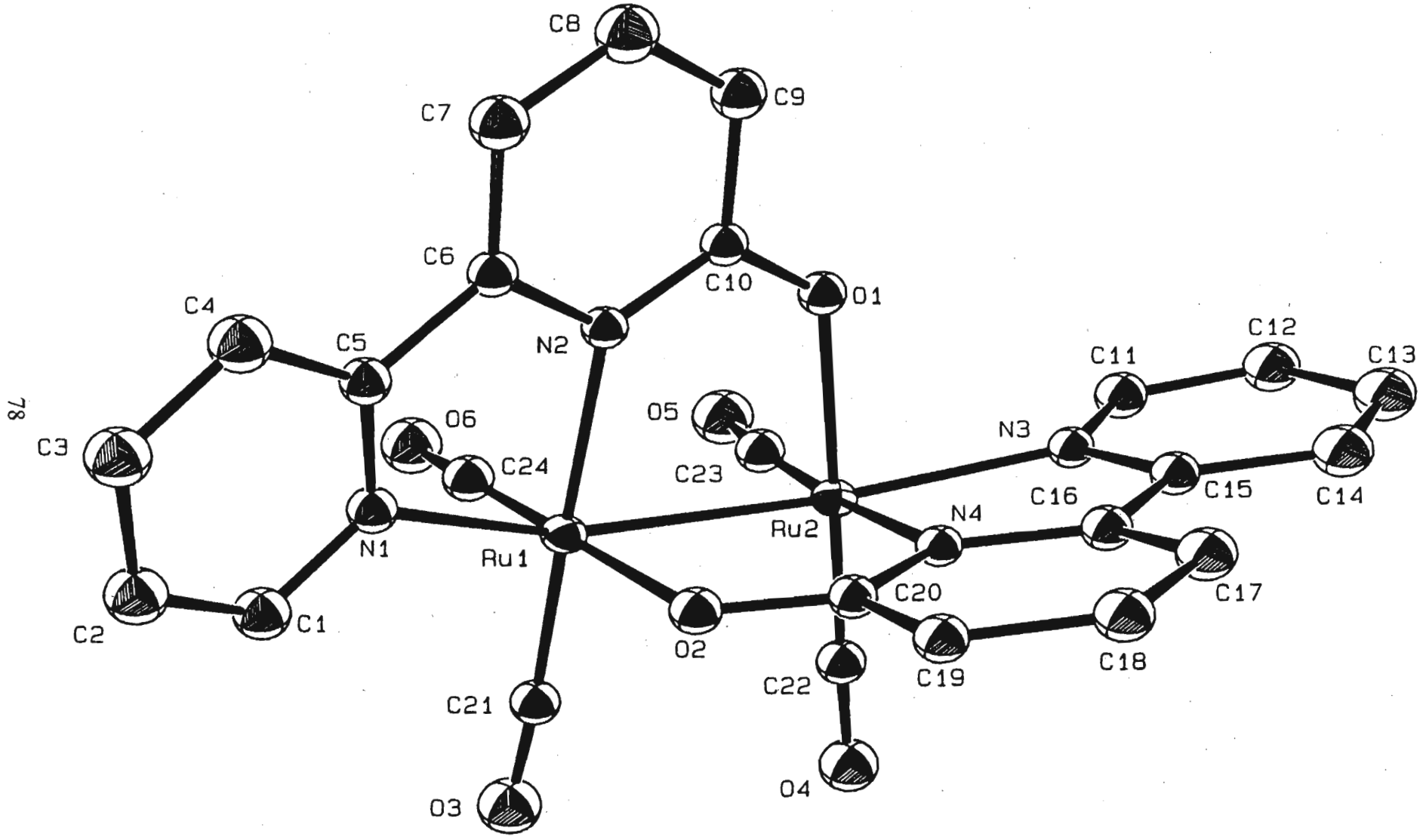

Fig 4.4 : ORTEP representation at 20% probability of $[Ru_2(\mu\text{-obipy})_2(CO)_4]$ 6

The C10-O1 and C20-O2 distances are 1.272(8) and 1.276(8) Å respectively which are short compared to C-O single bonds which are normally[63] of the order of 1.4 Å. This suggests some multiple bond character which is also found in analogous hp complexes. The N-O bite distance of the obipy ligand in complex **6** is 2.29 Å.

4.2 Abipy ligand bridged complexes of ruthenium (II,III)

4.2.1 Introduction

The number of complexes containing the Ru_2^{5+} core has increased substantially over the last three decades[1], since the first reported characterisation of $[Ru_2(O_2CCH_3)_4Cl]_n$ in 1966[42]. This multiply bonded mixed valence species is an air stable polymer, the dimeric units of which are held together by bridging chloro groups. The increasing number of reports of Ru_2^{5+} complexes is largly due to the success of the Ru_2^{5+} acetate polymer as a suitable starting material for other Ru_2^{5+} complexes. Work done to date has included substitution of the acetate groups by 2-substituted naphthyridyl ligands[43,44], the hydroxypyridinate ligands[11,45] and amidopyridyl ligands[11,12,22].

Synthetic methods have included the reaction of the sodium or lithium salts of the ligands with the acetate polymer in THF[43], the reaction of the free ligand with the acetate polymer in methanol[22], or the reaction of the free ligand with the acetate polymer as a melt[11,12]. Yields vary from very good to very poor, the reasons for which are not always obvious. Although the metathesis reaction using the sodium or lithium salt has been used to effect[43], it has been regarded as being inferior due to the tendency of the alkali metal ions to form chloride salts, thus breaking down the polymer to yield intractable mixtures.

4.2.2 Synthesis and characterisation of $[Ru_2(\mu\text{-abipy})(O_2CCH_3)_3Cl]$ (7)

The reaction of Habipy with $[Ru_2(O_2CCH_3)_4Cl]_n$ was found to produce a variety of products which proved difficult to isolate. Thus reaction of one equivalent of Habipy with

$[Ru_2(O_2CCH_3)_4Cl]_n$ in either methanol or acetonitrile at various temperatures was shown to afford a mixture from which $[Ru_2(\mu\text{-abipy})(O_2CCH_3)_3Cl]$ (7) was isolated in very poor yields of < 10%. A variety of products (including 7) were also formed by carrying out the reaction in a melt under an argon atmosphere. In all cases complex 7 was best purified by preparative column chromatography using silica gel and acetone-glacial acetic acid mixtures, as eluants.

Although difficulty was experienced in obtaining accurate microanalytical data, single crystals could be isolated and an X-ray crystal structure determination confirmed the formulation of the material as $[Ru_2(\mu\text{-abipy})(O_2CCH_3)_3Cl]$. The infrared specrtrum, the data from which are presented in Table 4.3, shows the characteristic ligand peaks as well as a symmetric $\nu(CO_2)$ band at 1439 cm^{-1} due to the bridging acetates. The absence of a N-H stretch at 3390 cm^{-1} confirms the amido form of the ligand. The UV-vis spectrum of 7 shows intense abipy π-π^* bands in the UV region and (MLCT) $d\pi(Ru) \rightarrow \pi^*$(abipy) bands in the visible region as listed in Table 4.3. Due to the poor solubility of 7 in organic solvents no ^1H NMR spectrum could be recorded.

Table 4.3 : Spectroscopic data for complex $[Ru_2(\mu\text{-abipy})(O_2CCH_3)_3Cl]$ (7)

IR[a] (cm^{-1})	1595(w), 1479(w), 1439(s), 775(w), 690(m)
UV-vis[b] (nm)	654, 514, 382, 339, 260, 230

a= recorded as KBr disc

b= recorded in MeCN.

An ORTEP generated representation of the molecular structure of 7 is depicted in Fig. 4.5. The $[Ru_2(\mu\text{-abipy})(O_2CCH_3)_3Cl]$ molecules exist as isolated molecules in the crystal, there being no contact distances between the molecules less then the sum of the van der Waals radii for the atoms concerned. A single abipy ligand bridges two Ru metals by a NCN^- chain and forms a chelate with one ruthenium atom (Ru1) via its bipyridyl fragment. The remaining equatorial sites of each Ru atom are taken up by the oxygen atoms of the three bridging acetate groups, while the axial site on Ru2 is occupied by a terminally bound chloro group. Excluding the axially bound Cl and N atoms, each ruthenium atom has a nearly perfect square pyramidyl geometry; however introduction of the axial ligands gives each ruthenium a distorted octahedral geometry, with N1-Ru1-N2 and N3-Ru2-Cl angles being 75.9 and 101.8° respectively. The equatorial bonds adopt

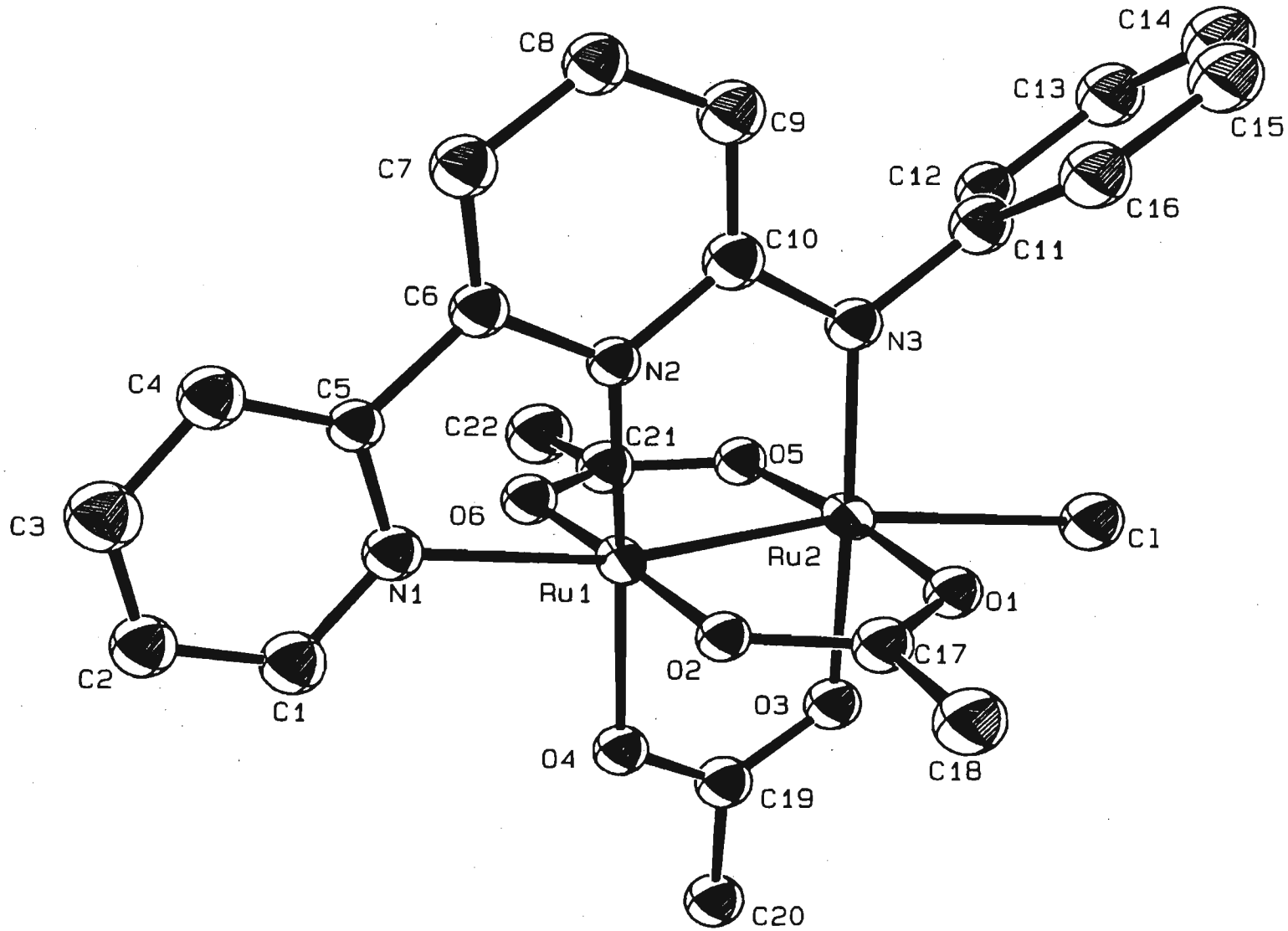

Fig 4.5 : ORTEP representation at 30% probability of $[Ru_2(\mu\text{-abipy})(O_2CCH_3)_3Cl]$ 7

a near perfect eclipsed conformation when viewed down the Ru1-Ru2 axis with the average torsion angles formed by the bridging ligands being 4.47°. The Ru1-Ru2 distance of 2.294(2) Å is typical of Ru_2^{5+} compounds and may be compared with others which range from 2.24 to 2.32 Å. This bond length suggests some multiple bonding character and indeed bond order calculations for the Ru_2^{5+} core, which has the ground state electronic configuration $(\sigma)^2(\pi)^4(\delta)^2(\pi^*\delta^*)^3$, indicate a bond order of 2.5. The Ru-N_{ax} distance of 2.15(2) Å is only 0.16 Å longer then the equatorial N2-Ru1 distance which is 1.99(2) Å. This Ru-N_{ax} distance is short when compared to the Ru-N_{ax} distance in $[Ru_2(O_2CCH_3)_2(ap)_2(Hap)Cl]$ which is 2.457(6) Å [22]. Ru-N_{ax} bonds are typically long in compounds containing the Ru_2^{5+} core due to the *trans* effect produced by the electron density in the metal-metal bond. The Ru-O bond lengths in 7 range from 2.01(2) Å to 2.05(1) Å which is typical of these species [12]. The Ru-Cl distance of 2.535(5) Å is in agreement with that reported for other Ru_2Cl^{4+} species [22].

4.3 Abipy ligand bridged complexes of molybdenum(II)

4.3.1 Introduction

The ability of ligands containing NCN^-, NCS^- or NCO^- chains to bridge quadruply bonded molybdenum(II) atoms is well known and such complexes have been well characterised [1-3]. Those compounds containing anionic aminopyridyl or anionic hydroxpyridyl ligands are important in that they contain the shortest Mo-Mo bond lengths as discussed in Chapter 1.

The majority of complexes that contain a Mo_2^{4+} core are synthesised either by the reaction of the sodium or lithium salt of the ligands with molybdenum acetate in THF [2] or by reaction of the free ligand with $[Mo_2(O_2CCH_3)_4]$ in methanol [51]. In some cases $[Mo(CO)_6]$ is reacted with the free ligand at high temperatures to yield species $[Mo_2(L)_4]$ where L= an anionic bridging ligand [56]. Whereas the former method has lead to species of the type $[Mo_2(O_2CCH_3)_x(L)_{4-x}]$ where x ranges from 0 to 3, the latter method produces tetrasubstituted dinuclear species exclusively.

Recently the reaction of the bis(pyridylimino) isoindoline (BAII) ligand, shown in Fig. 4.6, with $[Mo_2(O_2CCH_3)_4]$ was found to produce $[Mo_2(BAII)(O_2CCH_3)_3]$ in which the BAII ligand bridges

the Mo atoms via a NCN^- chain whilst one of the pyridyl groups coordinates in an axial position to complete a chelate[51].The $[Mo_2(BAII)(O_2CCH_3)_3]$ complex is the only example of a derivative of molybdenum acetate in which only one acetate group has been substituted by a bridging ligand. Considering the mode of coordination of the BAII ligand in the $[Mo_2(BAII)(O_2CCH_3)_3]$ complex it seems likely that the abipy ligand will coordinate in a similar manner.

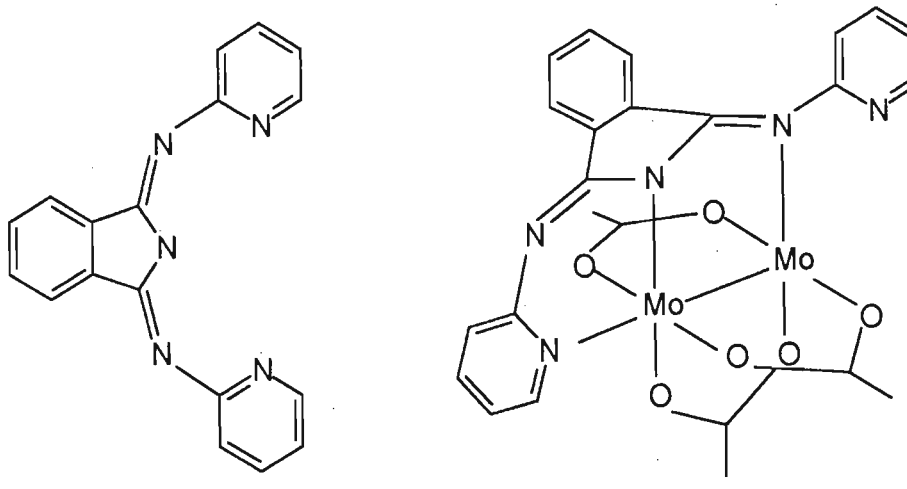

BAII **$[Mo_2(BAII)(O_2CCH_3)_3]$**

Fig 4.6 Structures of BAII and $[Mo_2(BAII)(O_2CCH_3)_3]$

4.3.2 Synthesis and characterisation of $[Mo_2(\mu\text{-abipy})(O_2CCH_3)_3]$ (8)

The reaction of 1 or 2 equivalents of Habipy with $[Mo_2(O_2CCH_3)_4]$ in refluxing methanol was found to afford $[Mo_2(\mu\text{-abipy})(O_2CCH_3)_3]$ (**8**) in good yield. This complex is a microcrystalline green material which is oxidised in air over a period of weeks. It is moderately soluble in polar organic solvents, but insoluble in nonpolar solvents such as ether. Solutions of **8** are highly air sensitive and are oxidised in seconds.

The microanalytical data presented in Table 4.4 are consistent with the formulation of **8** as $[Mo_2(\mu\text{-abipy})(O_2CCH_3)_3]$. The infrared spectrum of **8** shows the typical ligand peaks in the aromatic region and the absence of the N-H stretch at 3990 cm^{-1} confirms the presence of the amido form of the ligand. The ^1H NMR spectrum shows that the abipy ligand protons resonate

in the 7 to 8 ppm range. The methyl protons on the acetate *trans* to the abipy ligand are shifted further downfield than those *cis* to the abipy ligand. This phenomenon is also observed in the ^1H NMR spectrum of $[Mo_2(BAII)(O_2CCH_3)_3]$ [51].

Table 4.4 : Microanalytical and spectroscopic data for $[Mo_2(\mu\text{-abipy})(O_2CCH_3)_3]$ (8)

Analysis : calculated (found)	%C 42.94 (42.62) %H 3.44 (3.41) %N 6.83 (6.74)
IR[a] (cm^{-1})	1591(m), 1521(w), 1485(w), 1452(s), 1375(w), 1022(m), 765(m), 669(m)
UV-vis[b] (nm)	607, 451, 397, 340, 288, 264, 233
δ ^1H NMR[c] (ppm)	6.96-8.05 (12H, m, abipy protons) 2.8 (3H, s, acetate) 2.5 (6H, s, acetates)

a= recorded as KBr disc b= recoreded in MeCN c= recorded in $CDCl_3$. In the context of the IR spectrum m, w, and s refer to intensity whereas in the context of the NMR spectrum m and s refer to multiplicity.

Single crystals of complex **8** were isolated and the X-ray crystal structure of **8** was determined. Fig. 4.7 shows an ORTEP generated representation of complex **8**. The dimers exist as separate entities in the crystal, there being no contact distances less then the sum of the van der Waals radii for the atoms concerned.

The two molybdenum atoms are bridged by three acetate groups and one abipy ligand. The abipy ligand chelates via its bipyridyl fragment thus occupying one of the axial sites on one molybdenum atom. The other molybdenum atom has one unoccupied axial site. Thus one molybdenum atom (Mo1) has a distorted octahedral geometry whilst the other (Mo2) has a slightly distorted square pyramidal geometry. The angles about Mo2 range from 88.7 to 94.4°, whereas those about Mo1 range from 69.8 to 106.1°, the distortion in the geometry about Mo1 only really arising from the axially coordinated nitrogen which makes an angle of 18.2° with the Mo-Mo axis. The Mo1-Mo2 bond length of 2.094(2) Å in **8** is statistically indistinguishable from the Mo-Mo bond length reported for the parent acetate[1].Table 4.5 presents some structural information of some Mo_2^{4+} complexes containing axially coordinating ligands.

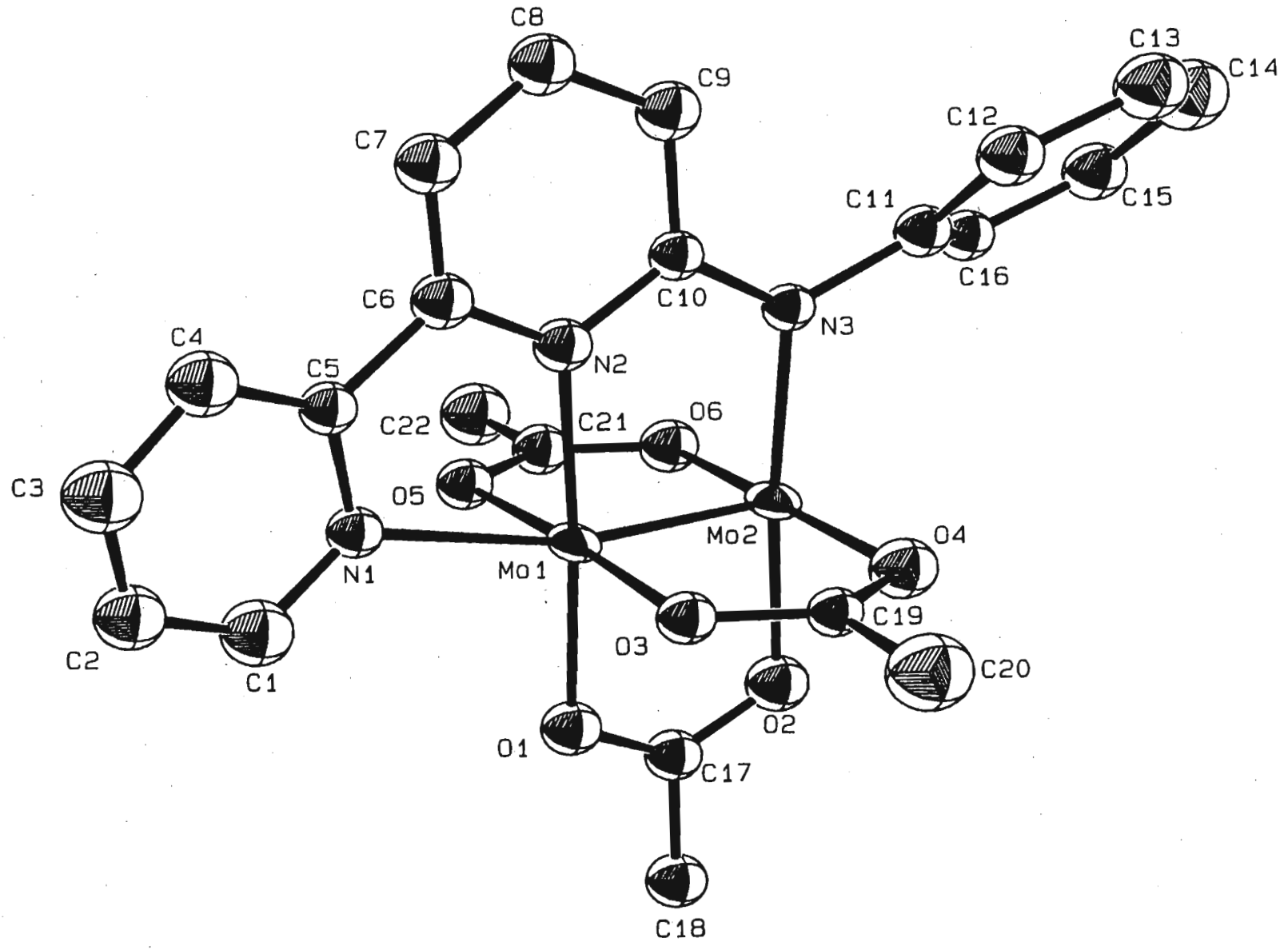

Fig 4.7 : ORTEP representation at 30% probability of $[Mo_2(\mu\text{-abipy})(O_2CCH_3)_3]$ 8

Table 4.5 : Structural data of some Mo_2^{4+} complexes containing axially coordinating ligands

Complex	Mo-Mo (Å)	Mo-N_{ax} (Å)	Mo-Mo-N_{ax} (°)	ref.
$[Mo_2(O_2CCF_3)_4(py)_2]$	2.129(2)	2.548(8)	171.0	53
$[Mo_2(tbp)_2(O_2CCH_3)_2]$	2.147(3)	2.45	170.1	52
$[Mo_2(BAII)(O_2CCH_3)_3]$	2.106(1)	2.466(7)	169.0	51
$[Mo_2(\mu\text{-abipy})(O_2CCH_3)_3]$	2.094(2)	2.39(1)	161.8	this work

It is accepted that axial ligation causes lengthening of the metal-metal bonds by occupation of orbitals which have some antibonding character. In $[Mo_2(O_2CCH_3)_4]$ there is weak axial coordination in each molecule by oxygen atoms of neighbouring molecules. In complex **8** axial coordination by oxygen atoms on adjacent dimers is not possible as Mo1 is already axially coordinated to one of the nitrogens of the bipyridyl fragment while Mo2 has a bulky phenyl group from the abipy ligand blocking the approach of large molecules. The Mo-N_{ax} bond length in **8** is 2.39(1) Å which is relatively short when compared with Mo-N_{ax} distances in the other complexes presented in Table 4.5. Of the complexes in Table 4.5, **8** has the shortest Mo-Mo bond length. This observation is not easily explained, since contrary to expectation, of the complexes in Table 4.5 the species containing the shortest Mo-Mo distance also has the shortest Mo-N_{ax} distance. What might be of significance however is the relatively large deviation of 18.2° of N_{ax} from the Mo-Mo axis in complex **8**. The N1-Mo1-Mo2 angle in **8** of 161.8° is slightly less then the N_{ax}-Mo-Mo angles in $[Mo_2(BAII)(O_2CCH_3)_3]$ and $[Mo_2(tpb)_2(O_2CCH_3)_2]$ which are 169.0 and 170.1° respectively[51,52]. Even in the $[Mo_2(O_2CCF_3)_4(py)_2]$ complex[53], in which the axially bound pyridyl ligands are under no geometric strain, the Mo-Mo-N_{az} angles are 171.0°. It is possible that the *trans* influence which the electron density in the Mo-Mo bond exerts on the axially coordinated nitrogen is lessened by a greater the deviation of N_{ax} from the Mo-Mo axis.

The average torsion angle formed by the bridging ligands with the Mo-Mo axis is 0.66°.

4.4 Abipy ligand bridged complexes of rhodium(II)

4.4.1 Introduction

Dirhodium(II,II) compounds are well known and reviews covering dirhodium(II) chemistry are numerous [55-57]. The Rh_2^{4+} unit appears to be energetically favourable and mononuclear Rh(II) species are comparatively rare [54]. In addition to rhodium carboxylates, there are many Rh_2^{4+} species containing other bridging ligands. Anionic ligands containing either NCN^-, OCN^- or NCS^- chains are known to bridge the Rh_2^{4+} core [9,10,58-60]. Neutral ligands containing NCN chains are also known to bridge the Rh_2^{4+} core as in $[Rh_2(bpnp)(O_2CCH_3)_3](PF_6)$ (where bpnp = bis 2-(2-pyridyl)-1,8-naphthyridine) and $[Rh_2(pynp)_2(O_2CCH_3)_2](PF_6)$ [28]. In the latter complex, depicted in Fig. 4.8, the structure proposed has the pynp ligand coordinating in a mode analogous to that of abipy in complexes 7 and **8**.

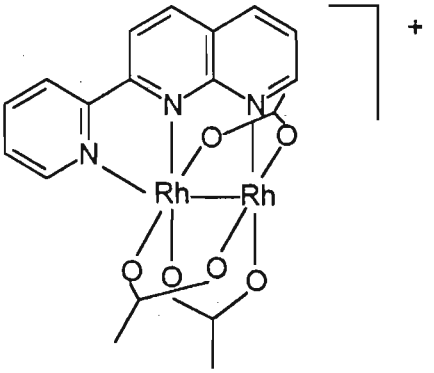

Fig. 4.8 : Proposed structure of $[Rh_2(pynp)(O_2CCH_3)_3]^+$

Synthetic routes to bridged Rh_2^{4+} compounds have been via the reaction of the ligands with rhodium(II) carboxylates [10] or reaction of the ligands with $RhCl_3 \cdot 3H_2O$ under reducing conditions[61].The former method has proved more sucessful.

4.4.2 Synthesis and characterisation of $[Rh_2(\mu\text{-abipy})(O_2CCH_3)_3(L)]$ L= H_2O, NCPh

The reaction of one equivalent of Habipy with $[Rh_2(O_2CCH_3)_4]$ in refluxing methanol was found to afford $[Rh_2(\mu\text{-abipy})(O_2CCH_3)_3(H_2O)]$ (**9**) in good yield. The reaction proceeds relatively

slowly, presumably due to the competition between solvent and ligand molecules for the axial sites on the rhodium dimers. The microanalytical data presented in Table 4.6 are consistent with the formulation of **9** as $[Rh_2(\mu\text{-abipy})(O_2CCH_3)_3(H_2O)]$. The infrared spectrum of **9** shows typical abipy peaks as well as a ν_{sym} (CO_2) band at 1452 cm^{-1}. The ^1H NMR spectrum exhibits peaks due to the abipy protons and the acetate protons. The acetate protons *cis* to the abipy ligand appear slightly upfield from those *trans* to the abipy ligand, as was the case in complex **8**.

Table 4.6 : Microanalytical and spectroscopic data for $[Rh_2(\mu\text{-abipy})(O_2CCH_3)_3(H_2O)]$ (9)

Analysis : calculated (found)	%C 40.81 (40.01) %H 3.58 (4.01) %N 6.52 (6.06)
IR[a] (cm^{-1})	1610(m), 1575(s), 1490(m), 1463(m), 1425(s), 1344(w), 765(m), 698(m)
UV-vis[b] (nm)	520, 305, 235
δ ^1H NMR[c] (ppm)	6.05-9.6 (12H, m, abipy protons) 2.15 (3H, s, acetate) 1.78 (6H, s, acetates)

a= recorded as KBr disc, b= recoreded in MeCN, c= recorded in $CDCl_3$

Single crystals of $[Rh_2(\mu\text{-abipy})(O_2CCH_3)_3(NCPh)]$ were grown by the slow diffusion of petroleum ether 40-60°C into a solution of **9** in acetone/benzonitrile. The X-ray structure of $[Rh_2(\mu\text{-abipy})(O_2CCH_3)_3(NCPh)]$ was determined and an ORTEP representation of the structure is depicted in Fig. 4.8. The rhodium dimers exist as separate entities in the crystal, there being no contact distances less then the sum of the van der Waals radii for the atoms in adjacent dimers concerned.

The Rh_2^{4+} unit is bridged by three acetate molecules and one abipy ligand and contains one terminally bound benzonitrile molecule. The bipyridyl fragment of the abipy ligand chelates to Rh1, and in doing so one of the bipyridyl nitrogens occupies an axial position opposite the Rh-Rh bond. The anionic anilino nitrogen is coordinated to Rh2 in an equatorial position, while the axial position on Rh2 is occupied by a benzonitrile molecule. Each rhodium has a slightly irregular

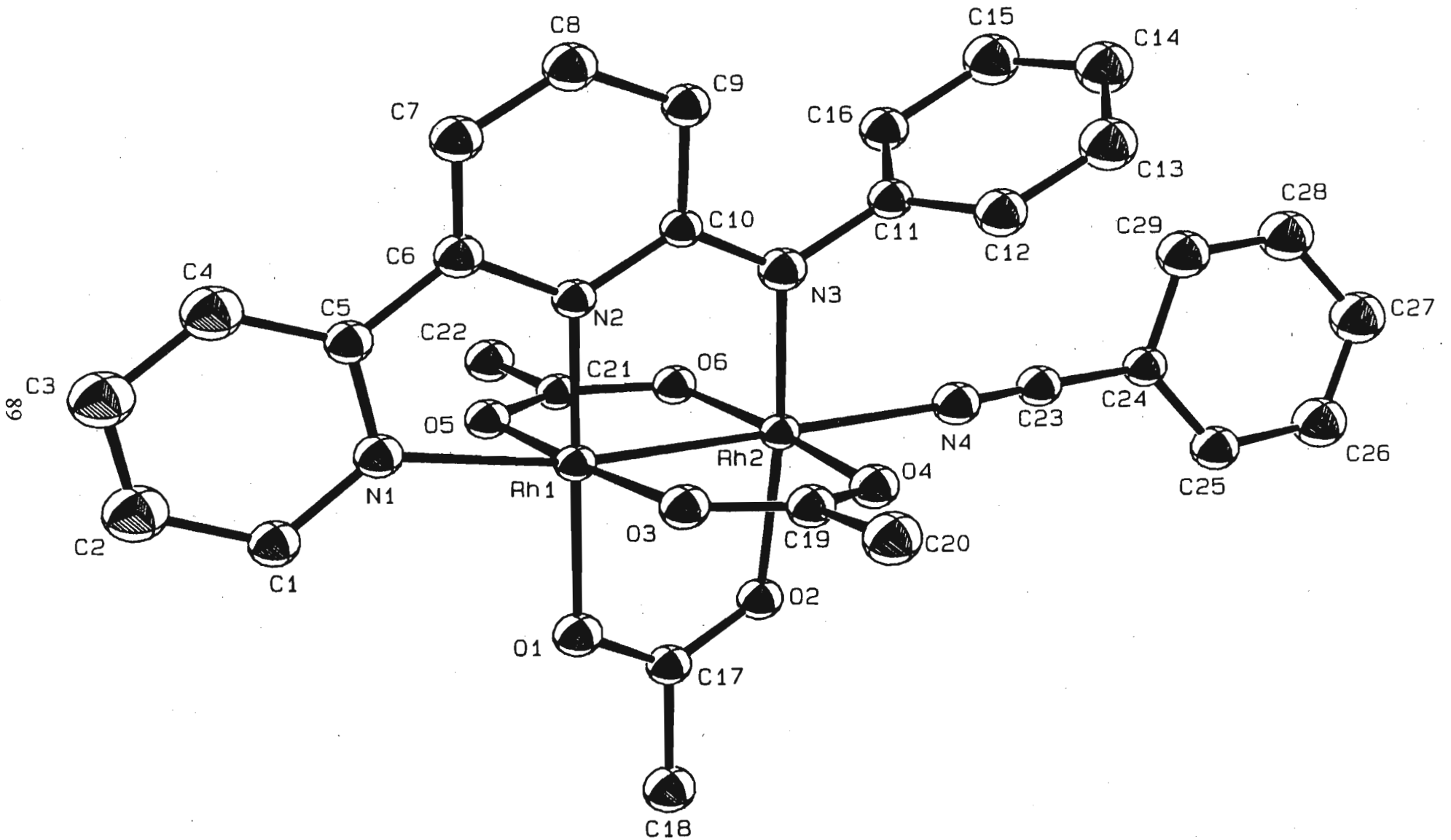

Fig 4.9 : ORTEP representation at 20% probability of $[Rh_2(\mu\text{-abipy})(O_2CCH_3)_3(NCPh)]$

octahedral geometry. The angles about Rh1 range from 78.5 to 102.1°, while those about Rh2 range from 86.4 to 95.1°. The Rh1-Rh2 distance of 2.399(1) Å is typical for the Rh-Rh distance in other Rh_2^{4+} compounds which generally range from 2.35-2.45 Å[1]. These Rh-Rh bonds, though short, are accepted as being single bonds[1]. The Rh1-N1 and Rh2-N4 bond lengths are 2.19(1) and 2.25(1) Å respectively, which are similar to the Rh-N_{ax} bond lengths in $[Rh_2(bpnp)(O_2CCH_3)_3](PF_6)$[28]. The Rh-$N_{eq}$ and Rh-O_{eq} bond lengths in **9** are slightly shorter then the Rh-N_{ax} distsances, all being typically of the order of 2.0 Å as in $[Rh_2(bpnp)(O_2CCH_3)_3](PF_6)$[28].

4.5 Discussion

Complexes **5** - **9**, all of which were characterised by X-ray crystallography, show the abipy or obipy ligands bridging the metals via NCN^- or NCO^- chains with the bipyridyl fragment chelating to one metal atom. In complexes **5** and **6** the abipy and obipy ligands bridge relatively 'soft' Ru(I) atoms whereas in complexes **7**, **8** and **9** the abipy ligand bridges the relatively 'hard' Ru_2^{5+}, Mo_2^{4+} and Rh_2^{4+} cores. With the exception of the molybdenum complex **8**, the geometry about the metal atoms is that of an irregular octahedron. In the case of complex **8**, one molybdenum atom has octahedral geometry while the other has square pyramidal. It does appear that in order for the abipy and obipy ligands to adopt a bridging mode, the metal centres must favour octahedral coordination. Certainly, attempts to form ligand bridged complexes of tetrahedral Cu(I) were unsuccessful; here mononuclear Cu(I) species are formed where the bipyridyl fragment chelates to the copper atom with the exocyclic nitrogen atom remaining uncoordinated (see Chapter 3).

Both Ru(I) compexes **5** and **6** have two bridging abipy ligands, whereas the acetate derived species of Ru_2^{5+}, Mo_2^{4+} and Rh_2^{4+} all only have one bridging abipy ligand. Although substitution of the relatively 'hard' acetate groups by ligands containing both hard and soft donor groups is expected to be easier in the 'softer' Ru(I) species, it is nonetheless not entirely clear as to why difficulty is experienced in obtaining disubstituted species of the harder metals. Examples of complexes resulting from substitution of more than one acetate group for Ru_2^{5+}, Mo_2^{4+} and Rh_2^{4+} are known. For instance $[Ru_2(O_2CCH_3)_2(ap)_2(Hap)Cl]$[22], *trans*-$[Mo_2(O_2CCH_3)_2(mphamnp)_2]$[50] (where mphamnp = the anion of 2-acetamido-7-methyl-1,8-naphthyridine) and $[Rh_2(bpnp)_2(O_2CCH_3)_2]$[28] all form as a result of the substitution of two acetate groups. These

complexes contain both 'hard' (ap and mphamnp) and 'soft' (bpnp) ligands, thus explanation based soley on 'hard' and 'soft' acid-base theory is not conclusive. The methods used for the synthesis of these disubstituted species also vary substantially and have included the reaction of the free ligand with $[M(O_2CCH_3)_4]$ in methanol, reaction of the lithium salt of the ligand with $[M(O_2CCH_3)_4]$ in THF, and also the reaction of the ligand with $[M(O_2CCH_3)_4]$ under mildly acidic conditions. It is thus clear that disubstitution of the acetate groups by these ligands in these species may depend on both the 'hardness' of the ligand relative to that of the acetate ligand, as well as the method of synthesis.

The most successful route to complexes **5 - 9** has involved reaction of the free ligand with the metal precursor. In certain cases the reaction of suitable metal containing precursors with the Li salt of the abipy ligand was attempted; however reaction was always slow and in all cases isolation of the products was difficult. Nontheless, it may be possible by suitable manipulation of reaction conditions, to effect the substitution of two acetate groups by the abipy ligand.

4.6 Experimental

4.6.1 *Synthesis of* $[Ru_2(\mu\text{-abipy})_2(CO)_4]$ (5)

Method A: Habipy (57.4 mg; 0.2325 mmols) was added to a stirred solution containing $Ru_3(CO)_{12}$ (50.0 mg; 0.0779 mmols) in toluene (40 ml). The reaction was heated to 50 °C for a period of 9 days, being frequently monitored by infrared measurements. After completion of the reaction, the orange-red solution was filtered and evaporated to dryness to yield solid orange-red material. The best purification method proved to be the recrystallisation of **5** from an acetone/methanol solution. Yield = 23 mg (25%).

Method B: Habipy (100.0 mg; 0.405 mmols) was added to a stirred suspension containing of $[Ru(CO)_2(O_2CCH_3)]_n$ (87.4 mg ; 0.405 mmols) in toluene (60 ml). Upon refluxing for 3.5 hrs the reaction was complete, affording an orange-red solution. The solution was evaporated to dryness and the resulting orange-red material recrystallised from acetone/methanol at 0°C. Yield =149 mg (91%).

4.6.2 *Synthesis of* $[Ru_2(\mu\text{-obipy})_2(CO)_4]$ (**6**)

Hobipy (100.0 mg; 0.581mmols) was added to a stirred suspension containing of $[Ru(CO)_2(O_2CCH_3)]_n$ (125.4 mg; 0.581 mmols) in toluene (60 ml). After heating under reflux for 4 hrs the reaction was complete, affording a yellow solution. The solution was evaporated to dryness and the residue extracted in 20 ml of acetone. The acetone solution was left overnight at 0°C to afford yellow-orange crystals of **6**. Yield = 153 mg (80%).

4.6.3 *Synthesis of* $[Ru_2(\mu\text{-abipy})(O_2CCH_3)_3Cl]$ (**7**)

Habipy (43.3 mg; 0.175 mmols) was added to a solution containing of $[Ru_2(O_2CCH_3)_4Cl]_n$ (83.0 mg; 0.175 mmols) in methanol (50ml). The methanolic solution was brought to reflux for 2 hrs after which no further reaction took place. The dark solution was concentrated to 10 ml and passed through a short silica gel column using a 1:6 acetone:glacial acetic acid mixture. The dark fraction (having an R_f value of 0.25 on tlc plates using this mixture) was evaporated to dryness. Recrystallisation from an acetone-pet ether mixture at 0°C over a period of days proved the most successfull method of work-up. Yield = 6 mg (9%).

4.6.4 *Synthesis of* $[Mo_2(\mu\text{-abipy})(O_2CCH_3)_3]$ (**8**)

Habipy (50 mg; 0.202 mmols) added to a degassed suspension containing of $[Mo_2(O_2CCH_3)_4]$ (86 mg; 0.202 mmols) in methanol (40 ml), under an argon atmosphere. After heating under reflux for a period of 2 hrs, the solution was cooled and the resulting emerald green precipitate was separated by filtration to afford 102 mg (82%) of complex **8**.

4.6.5 *Synthesis of* $[Rh_2(\mu\text{-abipy})(O_2CCH_3)_3(NCPh)]$ (**9**)

Habipy (30 mg; 0.121 mmols) was added to a stirred suspension of of $[Rh_2(O_2CCH_3)_4]$ (54 mg; 0.121 mmols) in methanol(50 ml). Upon heating under reflux for a period of 4 hrs the resulting red solution was cooled to 0°C to afford dark red crystals which were filtered and washed with cold acetone. Yield = 56 mg (72%).

Single crystal X-ray diffraction study of $[Ru_2(\mu\text{-abipy})_2(CO)_4]$

Orange-red blocks of $[Ru_2(\mu\text{-abipy})_2(CO)_4]$ were grown by cooling of a solution of the compound in a mixture of acetone and methanol. The general approach used for the intensity data collection is described in Appendix A. Details of the crystallographic data are given in Table 4.7, the interatomic distances in Table 4.8, the interatomic angles in Table 4.9, and the fractional coordinates and equivalent isotropic thermal factors in Table 4.10. The observed and calculated structure factors may be found on microfiche in an envelope fixed to the inside back cover. All non hydrogens were made anisotropic and the phenyl rings were defined as rigid groups. All hydrogen atoms were placed in calculated positions.

Single crystal X-ray diffraction study of $[Ru_2(\mu\text{-obipy})_2(CO)_4] \cdot C_3H_4O$

Yellow-orange rectangular plates of $[Ru_2(\mu\text{-obipy})_2(CO)_4] \cdot C_3H_4O$ were grown by cooling of a hot solution of the compound in xylene. The general approach used for the intensity data collection is described in Appendix A. Details of the crystallographic data are given in Table 4.11, the interatomic distances in Table 4.12, the interatomic angles in Table 4.13, and the fractional coordinates and equivalent isotropic thermal factors in Table 4.14. The observed and calculated structure factors may be found on microfiche in an envelope fixed to the inside back cover. All non hydrogens were made anisotropic and the phenyl rings were defined as rigid groups. All hydrogen atoms were placed in calculated positions. The solvent molecle C_3H_4O is disordered and is proposed to be a molecule of acrolein which is a known impurity in xylene.

Single crystal X-ray diffraction study of $[Ru_2(\mu\text{-abipy})(O_2CCH_3)_3Cl]$

Dark brown blocks of $[Ru_2(\mu\text{-abipy})(O_2CCH_3)_3Cl]$ were grown by the slow diffusion of petroleum ether 40-60°C into a solution of **7** in acetone. The general approach used for the intensity data collection is described in Appendix A. Details of the crystallographic data are given in Table 4.15, the interatomic distances in Table 4.16, the interatomic angles in Table 4.17, and the fractional coordinates and equivalent isotropic thermal factors in Table 4.18. The observed and calculated structure factors may be found on microfiche in an envelope fixed to the inside back cover. All

non hydrogens were made anisotropic and the phenyl rings were defined as rigid groups. All hydrogen atoms were placed in calculated positions.

Single crystal X-ray diffraction study of $[Mo_2(\mu\text{-abipy})(O_2CCH_3)_3] \cdot C_3H_6O$

Emerald green plates of $[Mo_2(\mu\text{-abipy})(O_2CCH_3)_3] \cdot C_3H_6O$ were grown by the slow diffusion of petroleum ether 40-60°C into a solution of **8** in acetone. The general approach used for the intensity data collection is described in Appendix A. Details of the crystallographic data are given in Table 4.19, the interatomic distances in Table 4.20, the interatomic angles in Table 4.21, and the fractional coordinates and equivalent isotropic thermal factors in Table 4.22. The observed and calculated structure factors may be found on microfiche in an envelope fixed to the inside back cover. Only the Mo atoms were made anisotropic and the phenyl rings were defined as rigid groups. All hydrogen atoms were placed in calculated positions.

Single crystal X-ray diffraction study of $[Rh_2(\mu\text{-abipy})(O_2CCH_3)_3(NCPh)]$

Dark brown blocks of $[Rh_2(\mu\text{-abipy})(O_2CCH_3)_3(NCPh)]$ were grown by the slow diffusion of petroleum ether 40-60°C into a solution of **9** in a mixture of acetone and benzonitrile. The general approach used for the intensity data collection is described in Appendix A. Details of the crystallographic data are given in Table 4.23, the interatomic distances in Table 4.24, the interatomic angles in Table 4.25, and the fractional coordinates and equivalent isotropic thermal factors in Table 4.26. The observed and calculated structure factors may be found on microfiche in an envelope fixed to the inside back cover. All non hydrogens were made anisotropic and the phenyl rings were defined as rigid groups. All hydrogen atoms were placed in calculated positions. Examination of the final electron density difference map indicated the presence of a disordered solvent molecule in the lattice. However, the disorder is so severe that it was not possible to establish the nature of the solvent molecule, though the temperature factors did fit best a model containing 5 carbon atoms . Eventually it was decided to simply exclude the solvent atoms from the refinement as this should only have a very small effect on the accuracy of the remaining structural parameters.

Table 4.7 : Crystal data and details of the crystallographic analysis for $[Ru_2(\mu\text{-abipy})_2(CO)_4]$

Formula	$Ru_2C_{36}H_{24}N_6O_4$
Molecular mass ($g.mol^{-1}$)	806.763
Crystal system	Monoclinic
Space group	P 2/n
a (Å)	19.769(3)
b (Å)	6.559(2)
c (Å)	19.802(7)
α (°)	90
β (°)	110.01(2)
γ (°)	90
V ($Å^3$)	3148(1)
Z	4
D_c ($g.cm^{-3}$)	1.70
F (000)	1608
λ (Mo - K_α) (Å)	0.71069
Scan mode	ω - 2θ
ω scan angle	0.40 + 0.35tanθ
Horizontal aperture width (mm)	2.7 + 0.1tanθ
Scattering range (°)	$2 \leq \theta \leq 30$
μ (cm^{-1})	9.915
Absorption corrections	Semi empirical
Measured intensities	5962
Unique intensities	4138
Unique intensities [$I > 3\sigma(I)$]	3715
Structure solution	Direct and Fourier methods
Weighting scheme	$1/[(\sigma^2(F) + 0.002F^2)]$
$R = \Sigma(F_o\text{-}F_c)/\Sigma F_o$	0.0235
$R_w = \Sigma_w{}^{1/2}(F_o\text{-}F_c)/\Sigma_w{}^{1/2}F_o$	0.0295
$(\Delta/\sigma)_{max}$	0.083
$\Delta\rho_{max}$ ($eÅ^{-3}$)	0.272
Number of parameters	410

Table 4.8 : Interatomic distances (Å) for $[Ru_2(\mu\text{-abipy})_2(CO)_4]$

Molecule A

Ru(1A)-N(1A)	2.182(3)	Ru(1A)-N(2A)	2.123(3)
Ru(1A)-C(1A)	1.856(4)	Ru(1A)-C(2A)	1.854(4)
Ru(1A)-Ru(1A')	2.665(1)	Ru(1A')- N(3A)	2.150(4)
N(3A)-C(11A)	1.412(3)	N(3A)-C(10A)	1.328(4)
N(1A)-C(1A)	1.353(5)	N(1A)-C(5A)	1.339(4)
N(2A)-C(6A)	1.358(4)	N(2A)-C(10A)	1.370(4)
O(1A)-C(2A)	1.144(4)	O(2A)-C(1A)	1.139(4)
C(12A)-C(13A)	1.395(0)	C(12A)-C(11A)	1.395(0)
C(13A)-C(14A)	1.395(0	C(14A)-C(15A)	1.395(0)
C(15A)-C(16A)	1.395(0)	C(16A)-C(11A)	1.395(0)
C(1A)-C(2A)	1.383(5)	C(2A)-C(3A)	1.380(7)
C(3A)-C(4A)	1.374(6)	C(4A)-C(5A)	1.397(5)
C(5A)-C(6A)	1.478(5)	C(6A)-C(7A)	1.376(5)
C(7A)-C(8A)	1.401(5)	C(8A)-C(9A)	1.363(5)
C(9A)-C(10A)	1.429(5)		

Molecule B

Ru(1B)-N(1B)	2.175(3)	Ru(1B)-N(2B)	2.129(3)
Ru(1B')-N(3B)	2.145(3)	Ru(1B)-C(1A)	1.855(4)
Ru(1B)-C(2A)	1.847(4)	Ru(1B)-Ru(1B')	2.671(0)
N(1B)-C(1B)	1.328(5)	N(1B)-C(5B)	1.341(5)
N(2B)-C(6B)	1.371(4)	N(2B)-C(10)	1.364(4)
N(3B)-C(10)	1.333(4)	N(3B)-C(11B)	1.414(4)
O(3B)-C(1A)	1.139(4)	O(4B)-C(2A)	1.140(4)
C(1B)-C(2B)	1.371(6)	C(2B)-C(3B)	1.357(7)
C(3B)-C(4B)	1.361(7)	C(4B)-C(5B)	1.401(5)
C(5B)-C(6B)	1.471(5)	C(6B)-C(7B)	1.365(5)
C(7B)-C(8B)	1.402(6)	C(8B)-C(9B)	1.363(5)
C(9B)-C(10)	1.426(5)	C(12B)-C(13B)	1.395(0)
C(12B)-C(11B)	1.395(0)	C(13B)-C(14B)	1.395(0)
C(14B)-C(15B)	1.395(0)	C(15B)-C(16B)	1.395(0)
C(16B)-C(11B)	1.395(0)		

Table 4.9 : Interatomic angles (Å) for $[Ru_2(\mu\text{-abipy})_2(CO)_4]$

Molecule A

N(1A)-Ru(1A)-N(2A)	76.3(1)	N(1A)-Ru(1A)-C(1A)	91.3(1)
N(2A)-Ru(1A)-C(1A)	97.1(1)	N(1A)-Ru(1A)-C(2A)	101.4(1)
N(2A)-Ru(1A)-C(2A)	172.4(1)	C(1A)-Ru(1A)-C(2A)	90.1(1)
C(11A)-N(3A)-C(10A)	117.8(3)	Ru(1A)-N(1A)-C(1A)	125.3(3)
Ru(1A)-N(1A)-C(5A)	114.2(2)	C(1A)-N(1A)-C(5A)	119.5(3)
Ru(1A)-N(2A)-C(6A)	116.5(2)	Ru(1A)-N(2A)-C(10A)	122.5(2)
C(6A)-N(2A)-C(10A)	120.5(3)	C(12A)-C(12A)-C(11A)	120.0(0)
C(12A)-C(12A)-C(14A)	120.0(0)	C(12A)-C(14A)-C(15A)	120.0(0)
C(14A)-C(15A)-C(16A)	120.0(0)	C(15A)-C(16A)-C(11A)	120.0(0)
N(3A)-C(11A)-C(12A)	120.6(1)	N(3A)-C(11A)-C(16A)	119.4(1)
C(12A)-C(11A)-C(16A)	120.0(0)	N(1A)-C(1A)-C(2A)	122.1(4)
C(1A)-C(2A)-C(3A)	118.1(4)	C(2A)-C(3A)-C(4A)	120.3(4)
C(3A)-C(4A)-C(5A)	119.0(4)	N(1A)-C(5A)-C(4A)	121.0(3)
N(1A)-C(5A)-C(6A)	116.2(3)	C(4A)-C(5A)-C(6A)	122.8(3)
N(2A)-C(6A)-C(5A)	115.4(3)	N(2A)-C(6A)-C(7A)	122.7(3)
C(5A)-C(6A)-C(7A)	121.8(3)	C(6A)-C(7A)-C(8A)	118.0(3)
C(7A)-C(8A)-C(9A)	120.0(3)	C(8A)-C(9A)-C(10A)	120.8(3)
N(3A)-C(10A)-N(2A)	118.6(3)	N(3A)-C(10A)-C(9A)	123.5(3)
N(2A)-C(10A)-C(9A)	117.8(3)	Ru(1A)-C(1A)-O(2A)	177.9(3)
Ru(1A)-C(2A)-O(1A)	176.4(3)		

Molecule B

N(1B)-Ru(1B)-N(2B)	76.5(1)	N(1B)-Ru(1B)-C(17B)	101.5(1)
N(2B)-Ru(1B)-C(17B)	172.6(1)	N(1B)-Ru(1B)-C(18B)	93.1(1)
N(2B)-Ru(1B)-C(18B)	97.7(1)	C(1A)-Ru(1B)-C(18B)	89.5(1)
Ru(1B)-N(1B)-C(1B)	125.8(3)	Ru(1B)-N(1B)-C(5B)	114.4(2)
C(1B)-N(1B)-C(5B)	119.2(3)	Ru(1B)-N(2B)-C(6B)	116.3(2)
Ru(1B)-N(2B)-C(10)	123.2(2)	C(6B)-N(2B)-C(10)	119.8(3)
C(10)-N(3B)-C(11B)	117.8(3)	N(1B)-C(1B)-C(2B)	122.9(5)
C(1B)-C(2B)-C(3B)	118.6(5)	C(2B)-C(3B)-C(4B)	119.7(4)
C(3B)-C(4B)-C(5B)	119.7(5)	N(1B)-C(5B)-C(4B)	119.9(4)
N(1B)-C(5B)-C(6B)	117.0(3)	C(4B)-C(5B)-C(6B)	123.0(4)
N(2B)-C(6B)-C(5B)	115.0(3)	N(2B)-C(6B)-C(7B)	122.3(4)

Table 4.9/ Cont.

C(5B)-C(6B)-C(7B)	122.5(3)	C(6B)-C(7B)-C(8B)	118.4(4)
C(7B)-C(8B)-C(9B)	120.2(4)	C(8B)-C(9B)-C(10)	120.0(4)
N(2B)-C(10)-N(3B)	118.4(3)	N(2B)-C(10)-C(9B)	119.0(3)
N(3B)-C(10)-C(9B)	122.6(3)	C(13B)-C(12B)-C(11B)	120.0(0)
C(12B)-C(13B)-C(14B)	120.0(0)	C(13B)-C(14B)-C(15B)	120.0(0)
C(14B)-C(15B)-C(16B)	120.0(0)	C(15B)-C(16B)-C(11B)	120.0(0)
N(3B)-C(11B)-C(12B)	120.6(1)	N(3B)-C(11B)-C(16B)	119.4(1)
C(12B)-C(11B)-C(16B)	120.0(0)	Ru(1B)-C(1A)-O(3B)	175.5(3)
Ru(1B)-C(2A)-O(4B)	176.3(3)		

Table 4.10 : Fractional coordinates ($x10^4$) and equivalent isotropic thermal factors ($Å^2,10^3$) for $[Ru_2(\mu\text{-abipy})_2(CO)_4]$

	x/a	y/b	z/c	U_{eq}
Molecule A				
Ru(1A)	1804	1483	7099	30
Ru(1A')	8196	8517	2901	32
N(3A)	3225(1)	3480(3)	7253(2)	34(1)
N(1A)	778(1)	1960(3)	6253(2)	41(1)
N(2A)	2074(1)	3133(3)	6431(1)	32(1)
O(1A)	1301(2)	-443(4)	8100(2)	68(1)
O(2A)	2015(2)	-1421(3)	6351(2)	63(1)
C(12A)	3842(1)	5816(3)	7866(1)	48(1)
C(13A)	4469(1)	6707(3)	8133(1)	67(1)
C(14A)	5103(1)	6194(3)	8044(1)	77(1)
C(15A)	5111(1)	4791(3)	7688(1)	75(1)
C(16A)	4484(1)	3901(3)	7421(1)	53(1)
C(11A)	3850(1)	4413(3)	7510(1)	36(1)
H(8A)	3352(1)	6213(3)	7935(1)	77(3)*
H(9A)	4463(1)	7793(3)	8408(1)	77(3)*
H(10A)	5588(1)	6884(3)	8250(1)	77(3)*
H(11A)	5602(1)	4395(3)	7619(1)	77(3)*
H(12A)	4490(1)	2815(3)	7145(1)	77(3)*
C(1A)	142(2)	1283(5)	6195(2)	52(1)
H(1A)	102(2)	630(5)	6646(2)	77(3)*
C(2A)	-454(2)	1393(6)	5575(3)	64(1)
H(2A)	-957(2)	843(6)	5540(3)	77(3)*
C(3A)	-387(2)	2223(6)	5004(3)	69(1)
H(3A)	-845(2)	2325(6)	4514(3)	77(3)*
C(4A)	253(2)	2932(5)	5060(2)	56(1)
H(4A)	306(2)	3584(5)	4614(2)	77(3)*
C(5A)	834(2)	2796(4)	5702(2)	38(1)
C(6A)	1537(2)	3553(4)	5819(2)	37(1)
C(7A)	1622(2)	4687(4)	5363(2)	46(1)
H(5A)	1195(2)	4956(4)	4865(2)	77(3)*
C(8A)	2284(2)	5468(5)	5557(2)	49(1)

Table 4.10/ Cont.

H(6A)	2374(2)	6349(5)	5206(2)	77(3)*
C(9A)	2813(2)	5125(4)	6191(2)	42(1)
H(7A)	3309(2)	5785(4)	6355(2)	77(3)*
C(26A)	2722(2)	3895(4)	6640(2)	32(1)
C(1A)	1938(2)	-300(5)	6626(2)	42(1)
C(34A)	1512(2)	261(4)	7722(2)	41(1)

Molecule B

Ru(1B)	2895	3966	3198	31
N(1B)	3719(2)	3441(4)	4227(2)	43(1)
N(2B)	3563(1)	2303(3)	2930(1)	34(1)
N(3B)	2757(1)	1981(3)	1772(1)	37(1)
O(3B)	1893(2)	5898(3)	3693(2)	61(1)
O(4B)	3622(2)	6893(3)	2992(2)	61(1)
C(1B)	3768(2)	4063(5)	4856(2)	62(1)
H(1B)	3326(2)	4776(5)	4889(2)	77(3)*
C(2B)	4350(3)	3837(6)	5469(3)	78(1)
H(2B)	4373(3)	4365(6)	5972(3)	77(3)*
C(3B)	4897(3)	2923(7)	5434(3)	83(1)
H(3B)	5358(3)	2721(7)	5912(3)	77(3)*
C(4B)	4866(2)	2285(6)	4794(3)	72(1)
H(4B)	5304(2)	1575(6)	4759(3)	77(3)*
C(5B)	4262(2)	2556(5)	4181(2)	48(1)
C(6B)	4167(2)	1836(4)	3479(2)	43(1)
C(7B)	4619(2)	711(5)	3391(2)	56(1)
H(5B)	5107(2)	411(5)	3824(2)	77(3)*
C(8B)	4426(2)	-73(5)	2730(2)	57(1)
H(6B)	4774(2)	-966(5)	2645(2)	77(3)*
C(9B)	3810(2)	319(4)	2187(2)	45(1)
H(7B)	3657(2)	-301(4)	1682(2)	77(3)*
C(10)	3363(2)	1541(4)	2286(2)	37(1)
C(12B)	2608(2)	1552(3)	511(1)	60(1)
C(13B)	2326(2)	675(3)	-117(1)	80(1)
C(14B)	1944(2)	-694(3)	-114(1)	78(1)
C(15B)	1844(2)	-1186(3)	517(1)	63(1)

Table 4.10/ Cont.

C(16B)	2126(2)	-310(3)	1145(1)	47(1)
C(11B)	2508(2)	1060(3)	1142(1)	40(1)
H(8B)	2904(2)	2612(3)	509(1)	77(3)*
H(9B)	2404(2)	1057(3)	-605(1)	77(3)*
H(10B)	1726(2)	-1372(3)	-600(1)	77(3)*
H(11B)	1549(2)	-2246(3)	519(1)	77(3)*
H(12B)	2049(2)	-691(3)	1633(1)	77(3)*
C(1A)	2267(2)	5200(4)	3480(2)	39(1)
C(2A)	3362(2)	5747(4)	3065(2)	39(1)

*** isotropic temperature factor.**

$$\underline{U}_{eq} = 1/3 \, \Sigma_i \Sigma_j \underline{U}_{ij} \, \underline{a}_i^* \underline{a}_j^* \, (a_i \, . \, a_j)$$

Table 4.11 : Crystal data and details of the crystallographic analysis for $[Ru_2(\mu\text{-obipy})_2(CO)_4] \cdot C_3H_4O$

Formula	$Ru_2C_{27}H_{18}N_4O_7$
Molecular mass ($g.mol^{-1}$)	712.602
Crystal system	Monoclinic
Space group	$P\ 2_1/c$
a (Å)	12.614(3)
b (Å)	10.038(3)
c (Å)	21.745(5)
α (°)	90
β (°)	105.74(2)
γ (°)	90
V ($Å^3$)	2630(1)
Z	4
D_c ($g.cm^{-3}$)	1.80
F (000)	1408
λ (Mo - K_α) (Å)	0.71069
Scan mode	$\omega - 2\theta$
ω scan angle	$0.52 + 0.35\tan\theta$
Horizontal aperture width (mm)	$2.7 + 0.1\tan\theta$
Scattering range (°)	$2 \leq \theta \leq 30$
μ (cm^{-1})	11.807
Absorption corrections	Semi empirical
Measured intensities	4816
Unique intensities	3208
Unique intensities [$I > 3\sigma(I)$]	2527
Structure solution	Direct and Fourier methods
Weighting scheme	$1/[(\sigma^2(F) + 0.0004F^2)]$
$R = \Sigma(F_o-F_c)/\Sigma F_o$	0.0356
$R_w = \Sigma_w{}^{1/2}(F_o-F_c)/\Sigma_w{}^{1/2}F_o$	0.0362
$(\Delta/\sigma)_{max}$	1.132
$\Delta\rho_{max}(eÅ^{-3})$	0.2358
Number of parameters	352

Table 4.12 : Interatomic distances (Å) for $[Ru_2(\mu\text{-obipy})_2(CO)_4] \cdot C_3H_4O$

Ru(1)-Ru(2)	2.671(1)	Ru(1)-N(1)	2.176(6)
Ru(1)-N(2)	2.136(5)	Ru(1)-O(2)	2.118(4)
Ru(1)-C(21)	1.842(8)	Ru(1)-C(24)	1.813(8)
Ru(2)-N(3)	2.156(6)	Ru(2)-N(4)	2.121(5)
Ru(2)-O(1)	2.124(4)	Ru(2)-C(22)	1.819(8)
Ru(2)-C(23)	1.848(8)	N(1)-C(1)	1.327(10)
N(1)-C(5)	1.353(9)	N(2)-C (6)	1.372(9)
N(2)-C(10)	1.351(9)	N(3)-C(11)	1.332(9)
N(3)-C(15)	1.346(8)	N(4)-C(16)	1.380(8)
N(4)-C(20)	1.349(9)	O(1)-C(10)	1.272(8)
O(2)-C(20)	1.276(8)	O(3)-C(21)	1.148(8)
O(4)-C(22)	1.147(8)	O(5)-C(23)	1.146(8)
O(6)-C(24)	1.167(8)	C(1)-C(2)	1.419(12)
C(2)-C(3)	1.358(12)	C(3)-C(4)	1.454(12)
C(4)-C(5)	1.354(10)	C(5)-C(6)	1.479(11)

Table 4.13 : Interatomic angles (°) for $[Ru_2(\mu\text{-obipy})_2(CO)_4] \cdot C_3H_4O$

Ru(2)-Ru(1)-N(1)	157.1(2)	Ru(2)-Ru(1)-N(2)	84.0(2)
N(1)-Ru(1)-N(2)	76.2(2)	Ru(2)-Ru(1)-O(2)	84.8(1)
N(1)-Ru(1)-O(2)	82.6(2)	N(2)-Ru(1)-O(2)	86.1(2)
Ru(2)-Ru(1)-C(21)	96.3(2)	N(1)-Ru(1)-C(21)	103.1(3)
N(2)-Ru(1)-C(21)	177.7(3)	O(2)-Ru(1)-C(21)	91.6(3)
Ru(2)-Ru(1)-C(24)	93.6(3)	N(1)-Ru(1)-C(24)	99.2(3)
N(2)-Ru(1)-C(24)	94.5(3)	O(2)-Ru(1)-C(24)	178.2(3)
C(21)-Ru(1)-C(24)	87.8(3)	Ru(1)-Ru(2)-N(3)	158.0(2)
Ru(1)-Ru(2)-N(4)	84.4(2)	N(3)-Ru(2)-N(4)	76.3(2)
Ru(1)-Ru(2)-O(1)	85.0(1)	N(3)-Ru(2)-O(1)	83.3(2)
N(4)-Ru(2)-O(1)	86.7(2)	Ru(1)-Ru(2)-C(2)	94.5(2)
N(3)-Ru(2)-C(22)	97.4(3)	N(4)-Ru(2)-C(22)	93.7(3)
O(1)-Ru(2)-C(22)	179.3(3)	Ru(1)-Ru(2)-C(23)	97.2(2)
N(3)-Ru(2)-C(23)	101.3(3)	N(4)-Ru(2)-C(23)	175.9(3)
O(1)-Ru(2)-C(23)	89.7(3)	C(22)-Ru(2)-C(23)	89.9(3)
Ru(1)-N(1)-C(1)	125.7(5)	Ru(1)-N(1)-C(5)	116.3(5)
C(1)-N(1)-C(5)	117.8(7)	Ru(1)-N(2)-C(6)	116.2(5)
Ru(1)-N(2)-C(10)	123.6(5)	C(6)-N(2)-C(10)	120.2(6)
Ru(2)-N(3)-C(11)	126.0(5)	Ru(2)-N(3)-C(15)	116.1(5)
C(11)-N(3)-C(15)	118.0(6)	Ru(2)-N(4)-C(16)	116.8(4)
Ru(2)-N(4)-C(20)	123.3(5)	C(16)-N(4)-C(20)	119.9(6)
Ru(2)-O(1)-C(10)	124.8(4)	Ru(1)-O(2)-C(20)	124.6(4)
N(1)-C(1)-C(2)	124.2(8)	C(1)-C(2)-C(3)	117.7(9)
C(2)-C(3)-C(4)	118.3(8)	C(3)-C(4)-C(5)	119.0(8)
N(1)-C(5)-C(4)	123.0(8)	N(1)-C(5)-C(6)	115.0(7)
C(4)-C(5)-C(6)	122.0(7)		

Table 4.14:Fractional coordinates ($x10^4$) and equivalent isotropic thermal factors ($Å^2$, $x10^3$) for $[Ru_2(\mu\text{-obipy})_2(CO)_4] \cdot C_3H_4O$

	x/a	y/b	z/c	U_{eq}
Ru(1)	1458	2200(1)	1280	39
Ru(2)	2312	4549(1)	1088	37
N(1)	1201(4)	446(6)	1809(3)	47(2)
N(2)	1721(4)	2909(6)	2236(3)	39(1)
N(3)	3462(5)	6186(6)	1257(3)	41(1)
N(4)	3844(4)	3636(6)	1535(3)	38(1)
O(1)	2206(4)	5015(5)	2022(2)	44(1)
O(2)	3118(3)	1555(5)	1571(2)	46(1)
O(3)	1152(5)	1113(7)	-37(3)	85(2)
O(4)	2449(5)	3900(7)	-219(3)	79(2)
O(5)	197(5)	6022(7)	560(3)	91(2)
O(6)	-860(5)	3160(8)	835(3)	92(2)
C(1)	1018(7)	-780(9)	1576(4)	62(2)
H(1)	855(7)	-1636(9)	1264(4)	154(12)*
C(2)	951(7)	8079(10)	1949(5)	70(3)
H(2)	599(7)	8713(10)	1544(5)	154(12)*
C(3)	1035(7)	8266(9)	2579(5)	69(3)
H(3)	886(7)	8866(9)	2960(5)	154(12)*
C(4)	1243(6)	-394(9)	2838(4)	66(2)
H(4)	1215(6)	-1010(9)	3241(4)	154(12)*
C(5)	1324(5)	618(8)	2442(4)	48(2)
C(6)	1572(5)	1998(8)	2675(3)	44(2)
C(7)	1661(6)	2349(9)	3304(4)	59(2)
H(5)	1547(6)	1617(9)	3645(4)	154(12)*
C(8)	1908(7)	3670(10)	3486(4)	67(3)
H(6)	1961(7)	3978(10)	3969(4)	154(12)*
C(9)	2078(6)	4565(9)	3057(3)	52(2)
H(7)	2268(6)	5587(9)	3201(3)	154(12)*
C(10)	2008(5)	4176(8)	2415(3)	40(2)
C(11)	3210(7)	7464(8)	1131(4)	55(2)
H(8)	2351(7)	7714(8)	935(4)	154(12)*
C(12)	3980(8)	8481(9)	1244(4)	66(2)

Table 4.14/ Cont.

H(9)	3730(8)	9506(9)	1148(4)	154(12)*
C(13)	5052(8)	8143(9)	1474(5)	72(3)
H(10)	5677(8)	8909(9)	1554(5)	154(12)*
C(14)	5348(7)	6835(9)	1604(4)	63(2)
H(11)	6203(7)	6555(9)	1778(4)	154(12)*
C(15)	4527(6)	5867(8)	1509(3)	44(2)
C(16)	4761(6)	4449(8)	1675(3)	45(2)
C(17)	5785(6)	3965(9)	1976(4)	57(2)
H(12)	6478(6)	4637(9)	2105(4)	154(12)*
C(18)	5917(6)	2636(9)	2115(4)	55(2)
H(13)	6726(6)	2242(9)	2340(4)	154(12)*
C(19)	5026(6)	1806(8)	1968(3)	47(2)
H(14)	5132(6)	751(8)	2064(3)	154(12)*
C(20)	3952(6)	2327(8)	1679(3)	39(2)
C(21)	1286(6)	1552(8)	466(4)	51(2)
C(22)	2385(6)	4141(8)	286(4)	49(2)
C(23)	993(6)	5424(8)	749(3)	51(2)
C(24)	49(6)	2793(9)	1016(3)	56(2)
O(1S)	131(33)	751(37)	9961(14)	343(16)
C(2S)	3810(47)	-492(50)	9796(17)	375(23)
C(3S)	4686(19)	-1298(19)	9814(8)	140(5)*
C(4S)	4305(15)	-2754(21)	9668(9)	193(7)*

*** isotropic temperature factor.**

$$\underline{U}_{eq} = 1/3\ \Sigma_i \Sigma_j \underline{U}_{ij}\, \underline{a}_i^*\, \underline{a}_j^*\, (a_i \cdot a_j)$$

Table 4.15 : Crystal data and details of the crystallographic analysis for $[Ru_2(\mu\text{-abipy})(O_2CCH_3)_3Cl]$

Formula	$Ru_2C_{22}ClH_{21}N_3O_6$
Molecular mass ($g.mol^{-1}$)	661.017
Crystal system	Monoclinic
Space group	Cc
a (Å)	21.556(4)
b (Å)	12.851(3)
c (Å)	20.555(6)
α (°)	90
β (°)	102.53(2)
γ (°)	90
V ($Å^3$)	5558(2)
Z	8
D_c ($g.cm^{-3}$)	1.58
F (000)	2616
λ (Mo - K_α) (Å)	0.71069
Scan mode	ω - 2θ
ω scan angle	0.96 + 0.35tanθ
Horizontal aperture width (mm)	2.7 + 0.1tanθ
Scattering range (°)	$2 \leq \theta \leq 30$
μ (cm^{-1})	11.454
Absorption corrections	Semi empirical
Measured intensities	4908
Unique intensities	3844
Unique intensities [$I > 3\sigma(I)$]	2818
Structure solution	Direct and Fourier methods
Weighting scheme	$1/[(\sigma^2(F) + 0.03F^2)]$
$R = \Sigma(F_o-F_c)/\Sigma F_o$	0.1160
$R_w = \Sigma_w½(F_o-F_c)/\Sigma_w½F_o$	0.1134
$(\Delta/\sigma)_{max}$	1.446
$\Delta\rho_{max}(eÅ^{-3})$	4.519
Number of parameters	305

Table 4.16 : Interatomic distances (Å) for $[Ru_2(\mu\text{-abipy})(O_2CCH_3)_3Cl]$

Ru(1)-Ru(2)	2.294(2)	Ru(1)-N(1)	2.15(2)
Ru(1)-N(2)	2.00(2)	Ru(1)-O(2)	2.043(13)
Ru(1)-O(4)	2.047(14)	Ru(1)-O(6)	2.049(14)
Ru(2)-Cl	2.535(5)	Ru(2)-N(3)	1.96(2)
Ru(2)-O(1)	2.01(2)	Ru(2)-O(3)	2.029(13)
Ru(2)-O(5)	2.02(2)	N(1)-C(1)	1.41(3)
N(1)-C(5)	1.32(2)	N(2)-C(6)	1.43(2)
N(2)-C(10)	1.39(3)	N(3)-C(10)	1.35(2)
N(3)-C(11)	1.46(2)	C(1)-C(2)	1.41(3)
C(2)-C(3)	1.33(4)	C(3)-C(4)	1.43(4)
C(4)-C(5)	1.31(3)	C(5)-C(6)	1.47(3)
C(6)-C(7)	1.34(3)	C(7)-C(8)	1.42(3)
C(8)-C(9)	1.45(3)	C(9)-C(10)	1.41(3)
C(12)-C(13)	1.395(0)	C(12)-C(11)	1.395(0)
C(13)-C(14)	1.395(0)	C(14)-C(15)	1.395(0)
C(15)-C(16)	1.395(0)	C(6)-C(11)	1.395(0)
C(17)-C(18)	1.46(3)	C(17)-O(1)	1.28(2)
C(17)-O(2)	1.23(2)	C(19)-C(20)	1.48(3)
C(19)-O(3)	1.24(3)	C(19)-O(4)	1.33(3)
C(21)-C(22)	1.49(3)	C(21)-O(5)	1.26(3)
C(21)-O(6)	1.27(3)		

Table 4.17 : Interatomic angles (Å) for $[Ru_2(\mu\text{-abipy})(O_2CCH_3)_3Cl]$

Ru(2)-Ru(1)-N(1)	165.8(5)	Ru(2)-Ru(1)-N(2)	89.9(4)
N(1)-Ru(1)-N(2)	75.9(6)	Ru(2)-Ru(1)-O(2)	89.4(3)
N(1)-Ru(1)-O(2)	90.5(5)	N(2)-Ru(1)-O(2)	92.5(6)
Ru(2)-Ru(1)-O(4)	91.3(4)	N(1)-Ru(1)-O(4)	102.8(6)
N(2)-Ru(1)-O(4)	178.5(6)	O(2)-Ru(1)-O(4)	88.2(6)
Ru(2)-Ru(1)-O(6)	89.1(4)	N(1)-Ru(1)-O(6)	91.5(6)
N(2)-Ru(1)-O(6)	90.2(6)	O(2)-Ru(1)-O(6)	176.9(5)
O(4)-Ru(1)-O(6)	89.1(6)	Ru(1)-Ru(2)-Cl	168.0(2)
Ru(1)-Ru(2)-N(3)	89.6(5)	Cl-Ru(2)-N(3)	101.8(5)
Ru(1)-Ru(2)-O(1)	87.6(4)	Cl-Ru(2)-O(1)	88.3(4)
N(3)-Ru(2)-O(1)	91.9(7)	Ru(1)-Ru(2)-O(3)	87.0(3)
Cl-Ru(2)-O(3)	81.6(4)	N(3)-Ru(2)-O(3)	176.5(6)
O(1)-Ru(2)-O(3)	88.8(6)	Ru(1)-Ru(2)-O(5)	88.9(4)
Cl-Ru(2)-O(5)	94.4(4)	N(3)-Ru(2)-O(5)	91.9(7)
O(1)-Ru(2)-O(5)	174.8(6)	O(3)-Ru(2)-O(5)	87.2(6)
Ru(1)-N(1)-C(1)	124(2)	Ru(1)-N(1)-C(5)	117.6(13)
C(1)-N(1)-C(5)	118(2)	Ru(1)-N(2)-C(6)	119.5(14)
Ru(1)-N(2)-C(10)	122.3(12)	C(6)-N(2)-C(10)	118(2)
Ru(2)-N(3)-C(10)	125(2)	Ru(2)-N(3)-C(11)	121.0(11)
C(10)-N(3)-C(11)	113(2)	N(1)-C(1)-C(2)	121(2)
C(1)-C(2)-C(3)	115(2)	C(2)-C(3)-C(4)	125(2)
C(3)-C(4)-H(4)	122(2)	C(3)-C(4)-C(5)	115(2)
N(1)-C(5)-C(4)	126(2)	N(1)-C(5)-C(6)	114(2)
C(4)-C(5)-C(6)	120(2)	N(2)-C(6)-C(5)	112(2)
N(2)-C(6)-C(7)	121(2)	C(5)-C(6)-C(7)	126(2)
C(6)-C(7)-C(8)	121(2)	C(7)-C(8)-C(9)	119(2)
C(8)-C(9)-C(10)	117(2)	N(2)-C(10)-N(3)	113(2)
N(2)-C(10)-C(9)	123(2)	N(3)-C(10)-C(9)	124(2)
C(13)-C(12)-C(11)	120.0(0)	C(12)-C(13)-C(14)	120.0(0)
C(13)-C(14)-C(15)	120.0(0)	C(14)-C(15)-C(16)	120.0(0)
C(15)-C(16)-C(11)	120.0(0)	N(3)-C(11)-C(12)	120.6(9)
N(3)-C(11)-C(16)	119.4(9)	C(12)-C(11)-C(16)	120.0(0)
C(18)-C(17)-O(1)	119(2)	C(18)-C(17)-O(2)	119(2)
O(1)-C(17)-O(2)	122(2)	C(20)-C(19)-O(3)	125(2)
C(20)-C(19)-O(4)	113(2)	O(3)-C(19)-O(4)	121(2))

Table 4.17/ Cont.

C(22)-C(21)-O(5)	122(2)	C(22)-C(21)-O(6)	115(2)
O(5)-C(21)-O(6)	124(2)	Ru(2)-O(1)-C(17)	121.7(13)

Table 4.18 : Fractional coordinates ($x10^4$) and equivalent isotropic thermal factors ($Å^2$, $x10^3$) for $[Ru_2(\mu\text{-abipy})(O_2CCH_3)_3Cl]$

	x/a	y/b	z/c	U_{eq}
Ru(1)	3217(1)	2645(1)	2547(1)	36
Ru(2)	3395(1)	3456(1)	3565(1)	39
Cl	3428(3)	4071(5)	4744(3)	62(1)
N(1)	3147(8)	2236(13)	1519(8)	44(4)
N(2)	3598(7)	3860(14)	2169(7)	38(4)
N(3)	3737(8)	4666(14)	3178(8)	46(4)
O(1)	2502(7)	4011(12)	3305(6)	51(4)
O(2)	2327(6)	3280(12)	2320(6)	41(3)
O(3)	3046(7)	2154(10)	3915(6)	46(3)
O(4)	2836(7)	1377(12)	2918(7)	52(4)
O(5)	4258(7)	2771(13)	3798(6)	49(3)
O(6)	4097(7)	1968(14)	2817(6)	50(4)
C(1)	2901(10)	1287(19)	1237(13)	58(6)
H(1)	2636(10)	788(19)	1500(13)	125(27)*
C(2)	2907(13)	1039(21)	570(10)	65(7)
H(2)	2735(13)	300(21)	351(10)	125(27)*
C(3)	3179(18)	1752(30)	252(13)	105(11)
H(3)	3196(18)	1580(30)	-258(13)	125(27)*
C(4)	3446(13)	2715(22)	531(12)	69(7)
H(4)	3660(13	3263(22)	247(12)	125(27)*
C(5)	3402(10)	2876(15)	1150(9)	37(4)
C(6)	3682(10)	3816(17)	1499(10)	44(5)
C(7)	3941(9)	4605(21)	1230(9)	51(6)
H(5)	3959(9)	4582(21)	709(9)	125(27)*
C(8)	4191(10)	5490(18)	1615(10)	47(5)
H(6)	4424(10)	6105(18)	1401(10)	125(27)*
C(9)	4109(11)	5579(20)	2293(13)	61(6)
H(7)	4272(11)	6263(20)	2585(13)	125(27)*
C(10)	3832(10)	4720(17)	2550(10)	41(5)
C(12)	4548(6)	5460(10)	4087(7)	54(6)
C(13)	4779(6)	6310(10)	4489(7)	60(6)

Table 4.18/ Cont.

C(14)	4458(6)	7259(10)	4396(7)	92(9)
C(15)	3905(6)	7358(10)	3901(7)	78(8)
C(16)	3674(6)	6509(10)	3498(7)	57(6)
C(11)	3995(6)	5560(10)	3591(7)	46(5)
H(8)	4796(6)	4725(10)	4159(7)	125(27)*
H(9)	5206(6)	6233(10)	4873(7)	125(27)*
H(10)	4637(6)	7916(10)	4708(7)	125(27)*
H(11)	3657(6)	8093(10)	3828(7)	125(27)*
H(12)	3246(6)	6586(10)	3114(7)	125(27)*
C(17)	2139(11)	3799(16)	2738(10)	44(5)
C(18)	1478(11)	4143(24)	2605(12)	65(6)
H(13)	1188(11)	4567(24)	2881(12)	125(27)*
H(14)	1352(11)	3328(24)	2591(12)	125(27)*
H(15)	1399(11)	4442(24)	2103(12)	125(27)*
C(19)	2846(11)	1389(17)	3565(10)	51(6)
C(20)	2640(15)	391(20)	3813(12)	75(7)
H(16)	2538(15)	787(20)	4241(12)	125(27)*
H(17)	3148(15)	8(20)	3864(12)	125(27)*
H(18)	2439(15)	-382(20)	3781(12)	125(27)*
C(21)	4427(10)	2154(17)	3396(11)	45(5)
C(22)	5063(11)	1653(28)	3545(12)	80(8)
H(19)	5485(11)	2046(28)	3812(12)	125(27)*
H(20)	5067(11)	1624(28)	3021(12)	125(27)*
H(21)	5053(11)	871(28)	3735(12)	125(27)*

*** isotropic temperature factor.**

$$\underline{U}_{eq} = 1/3 \, \Sigma_i \Sigma_j \underline{U}_{ij} \underline{a}_i^* \underline{a}_j^* (a_i . a_j)$$

Table 4.19 : Crystal data and details of the crystallographic analysis for $[Mo_2(\mu\text{-abipy})(O_2CCH_3)_3] \cdot C_3H_6O$

Formula	$Mo_2C_{25}H_{27}N_3O_7$
Molecular mass ($g.mol^{-1}$)	673.384
Crystal system	Monoclinic
Space group	$P\ 2_1/c$
a (Å)	8.536(4)
b (Å)	17.882(26)
c (Å)	17.215(8)
α (°)	90
β (°)	91.90(5)
γ (°)	90
V ($Å^3$)	2626(4)
Z	4
D_c ($g.cm^{-3}$)	1.70
F (000)	1352
λ (Mo - K_α) (Å)	0.71069
Scan mode	ω - 2θ
ω scan angle	$0.80 + 0.35\tan\theta$
Horizontal aperture width (mm)	$2.7 + 0.1\tan\theta$
Scattering range (°)	$2 \leq \theta \leq 30$
μ (cm^{-1})	9.881
Absorption corrections	Semi empirical
Measured intensities	4539
Unique intensities	2996
Unique intensities [$I > 3\sigma(I)$]	2151
Structure solution	Direct and Fourier methods
Weighting scheme	$1/[(\sigma^2(F) + 0.01F^2)]$
$R = \Sigma(F_o\text{-}F_c)/\Sigma F_o$	0.0784
$R_w = \Sigma_w{}^{1/2}(F_o\text{-}F_c)/\Sigma_w{}^{1/2}F_o$	0.0881
$(\Delta/\sigma)_{max}$	0.604
$\Delta\rho_{max}(eÅ^{-3})$	1.980
Number of parameters	173

Table 4.20 : Interatomic distances (Å) for $[Mo_2(\mu\text{-abipy})(O_2CCH_3)_3] \cdot C_3H_6O$

Mo(1)-Mo(2)	2.094(2)	Mo(1)-N(1)	2.399(14)
Mo(1)-N(2)	2.156(13)	Mo(1)-O(1)	2.110(11)
Mo(1)-O(3)	2.120(11)	Mo(1)-O(5)	2.126(11)
Mo(2)-N(3)	2.086(12)	Mo(2)-O(2)	2.131(12)
Mo(2)-O(4)	2.095(13)	Mo(2)-O(6)	2.097(12)
N(1)-C(1)	1.38(2)	N(1)-C(5)	1.36(2)
N(2)-C(6)	1.34(2)	N(2)-C(10)	1.39(2)
N(3)-C(10)	1.35(2)	N(3)-C(11)	1.43(2)
O(1)-C(17)	1.25(2)	O(2)-C(17)	1.27(2)
O(3)-C(19)	1.28(2)	O(4)-C(19)	1.27(2)
O(5)-C(21)	1.27(2)	O(6)-C(21)	1.26(2)
C(1)-C(2)	1.37(3)	C(2)-C(3)	1.35(3)
C(3)-C(4)	1.36(3)	C(4)-C(5)	1.39(2)
C(5)-C(6)	1.48(2)	C(6)-C(7)	1.34(2)
C(7)-C(8)	1.42(2)	C(8)-C(9)	1.36(2)
C(9)-C(10)	1.43(2)	C(12)-C(13)	1.395(0)
C(12)-C(11)	1.395(0)	C(13)-C(14)	1.395(0)
C(14)-C(15)	1.395(0)	C(15)-C(16)	1.395(0)
C(16)-C(11)	1.395(0)	C(17)-C(18)	1.53(2)
C(19)-C(20)	1.47(3)	C(21)-C(22)	1.48(3)
O(1S)-C(2S)	1.24(3)	C(1S)-C(2S)	1.46(4)
C(2S)-C(3S)	1.48(4)		

Table 4.21 : Interatomic angles (°) for $[Mo_2(\mu\text{-abipy})(O_2CCH_3)_3] \cdot C_3H_6O$

Mo(2)-Mo(1)-N(1)	162.1(4)	Mo(2)-Mo(1)-N(2)	92.3(3)
N(1)-Mo(1)-N(2)	70.4(5)	Mo(2)-Mo(1)-O(1)	91.8(3)
N(1)-Mo(1)-O(1)	105.6(5)	N(2)-Mo(1)-O(1)	175.9(5)
Mo(2)-Mo(1)-O(3)	91.2(3)	N(1)-Mo(1)-O(3)	85.3(4)
N(2)-Mo(1)-O(3)	92.3(5)	O(1)-Mo(1)-O(3)	87.5(4)
Mo(2)-Mo(1)-O(5)	92.0(3)	N(1)-Mo(1)-O(5)	92.7(4)
N(2)-Mo(1)-O(5)	91.0(5)	O(1)-Mo(1)-O(5)	88.9(4)
O(3)-Mo(1)-O(5)	175.3(4)	Mo(1)-Mo(2)-N(3)	94.2(3)
Mo(1)-Mo(2)-O(2)	90.9(3)	N(3)-Mo(2)-O(2)	174.9(5)
Mo(1)-Mo(2)-O(4)	92.8(4)	N(3)-Mo(2)-O(4)	91.9(5)
O(2)-Mo(2)-O(4)	88.3(5)	Mo(1)-Mo(2)-O(6)	91.7(3)
N(3)-Mo(2)-O(6)	90.2(5)	O(2)-Mo(2)-O(6)	89.2(5)
O(4)-Mo(2)-O(6)	174.9(5)	Mo(1)-N(1)-C(1)	127.1(11)
Mo(1)-N(1)-C(5)	115.5(10)	C(1)-N(1)-C(5)	116.8(14)
Mo(1)-N(2)-C(6)	123.4(11)	Mo(1)-N(2)-C(10)	116.8(10)
C(6)-N(2)-C(10)	119.8(13)	Mo(2)-N(3)-C(10)	119.7(10)
Mo(2)-N(3)-C(11)	118.7(8)	C(10)-N(3)-C(11)	121.3(12)
Mo(1)-O(1)-C(17)	118.4(11)	Mo(2)-O(2)-C(17)	117.7(11)
Mo(1)-O(3)-C(19)	116.7(10)	Mo(2)-O(4)-C(19)	116.7(12)
Mo(1)-O(5)-C(21)	115.0(11)	Mo(2)-O(6)-C(21)	117.0(12)
N(1)-C(1)-C(2)	122(2)	C(1)-C(2)-C(3)	120(2)
C(2)-C(3)-C(4)	120(2)	C(3)-C(4)-C(5)	120(2)
N(1)-C(5)-C(4)	122(2)	N(1)-C(5)-C(6)	113.8(14)
C(4)-C(5)-C(6)	125(2)	N(2)-C(6)-C(5)	116.4(14)
N(2)-C(6)-C(7)	122(2)	C(5)-C(6)-C(7)	121(2)
C(6)-C(7)-C(8)	121(2)	C(7)-C(8)-C(9)	118(2)
C(8)-C(9)-C(10)	120(2)	N(2)-C(10)-N(3)	116.9(14)
N(2)-C(10)-C(9)	118.9(14)	N(3)-C(10)-C(9)	124.2(14)
C(13)-C(12)-C(11)	120.0(0)	C(12)-C(13)-C(14)	120.0(0)
C(13)-C(14)-C(15)	120.0(0)	C(14)-C(15)-C(16)	120.0(0)
C(15)-C(16)-C(11)	120.0(0)	N(3)-C(11)-C(12)	122.8(6)
N(3)-C(11)-C(16)	117.2(6)	C(12)-C(11)-C(16)	120.0(0)
O(1)-C(17)-O(2)	121(2)	O(1)-C(17)-C(18)	121(2)
O(2)-C(17)-C(18)	118(2)	O(3)-C(19)-O(4)	123(2)
O(3)-C(19)-C(20)	117(2)	O(4)-C(19)-C(20)	121(2)

Table 4.21/ Cont.

O(5)-C(21)-O(6)	124(2)	O(5)-C(21)-C(22)	118(2)
O(6)-C(21)-C(22)	117(2)	O(1S)-C(2S)-C(1S)	126(3)
O(1S)-C(2S)-C(3S)	117(3)	C(1S)-C(2S)-C(3S)	116(3)

Table 4.22 : Fractional coordinates ($x10^4$) and equivalent isotropic thermal factors ($Å^2$, $x10^3$) for $[Mo_2(\mu\text{-abipy})(O_2CCH_3)_3] \cdot C_3H_6O$

	x/a	y/b	z/c	U_{eq}
Mo(1)	2021(2)	1969(1)	4282(1)	25
Mo(2)	1524(2)	3107(1)	4415(1)	26
N(1)	2423(14)	665(8)	4553(9)	31(3)
N(2)	1051(14)	1694(8)	5386(9)	28(3)
N(3)	506(14)	2968(7)	5490(8)	22(3)*
O(1)	3009(13)	2156(7)	3192(7)	34(3)*
O(2)	2504(14)	3351(7)	3321(8)	39(3)*
O(3)	4299(13)	2117(6)	4787(7)	31(3)*
O(4)	3725(15)	3328(7)	4940(8)	41(3)*
O(5)	-177(13)	1769(6)	3702(7)	33(3)*
O(6)	-677(14)	2984(7)	3852(7)	35(3)*
C(1)	3300(20)	166(10)	4138(11)	39(4)*
H(1)	3806(20)	346(10)	3602(11)	46(12)*
C(2)	3532(21)	-556(11)	4377(12)	43(5)*
H(2)	4155(21)	-941(11)	4015(12)	76(12)*
C(3)	3008(22)	-780(12)	5071(12)	48(5)*
H(3)	3263(22)	-1339(12)	5277(12)	76(12)*
C(4)	2125(20)	-307(10)	5497(11)	35(4)*
H(4)	1655(20)	-491(10)	6040(11)	76(12)*
C(5)	1884(17)	422(9)	5246(9)	22(4)*
C(6)	1010(18)	997(9)	5672(10)	28(4)*
C(7)	337(19)	839(10)	6347(11)	31(4)*
H(5)	393(19)	277(10)	6576(11)	76(12)*
C(8)	-475(18)	1398(9)	6755(10)	35(4)*
H(6)	-1130(18)	1258(9)	7261(10)	76(12)*
C(9)	-427(21)	2112(10)	6486(11)	33(4)*
H(7)	-984(21)	2553(10)	6803(11)	76(12)*
C(10)	386(18)	2278(9)	5795(9)	25(4)*
C(12)	650(12)	3734(5)	6690(6)	36(4)*
C(13)	280(12)	4395(5)	7072(6)	43(5)*
C(14)	-626(12)	4940(5)	6690(6)	51(6)*

Table 4.22/ Cont.

C(15)	-1161(12)	4823(5)	5925(6)	39(4)*
C(16)	-790(12)	4162(5)	5542(6)	30(4)*
C(11)	115(12)	3617(5)	5925(6)	27(4)*
H(8)	1351(12)	3312(5)	6986(6)	76(12)*
H(9)	694(12)	4485(5)	7664(6)	76(12)*
H(10)	-913(12)	5452(5)	6986(6)	76(12)*
H(11)	-1862(12)	5245(5)	5629(6)	76(12)*
H(12)	-1205(12)	4072(5)	4950(6)	76(12)*
C(17)	3018(19)	2807(10)	2931(10)	29(4)*
C(18)	3747(19)	2980(9)	2152(10)	31(4)*
H(13)	4449(19)	2673(9)	1751(10)	76(12)*
H(14)	4460(19)	3404(9)	2438(10)	76(12)*
H(15)	2777(19)	3242(9)	1839(10)	76(12)*
C(19)	4649(21)	2775(10)	5030(11)	31(4)*
C(20)	6232(27)	2881(15)	5379(15)	63(7)*
H(16)	6541(27)	3466(15)	5422(15)	76(12)*
H(17)	6997(27)	2605(15)	4983(15)	76(12)*
H(18)	6358(27)	2625(15)	5946(15)	76(12)*
C(21)	-1046(23)	2338(11)	3621(12)	37(5)*
C(22)	-2603(28)	2244(14)	3224(15)	56(6)*
H(19)	-2679(28)	1673(14)	3022(15)	76(12)*
H(20)	-2556(28)	2617(14)	2731(15)	76(12)*
H(21)	-3621(28)	2375(14)	3555(15)	76(12)*
O(1S)	3883(22)	5553(12)	7414(13)	105(7)*
C(1S)	-4949(37)	4413(18)	6957(18)	109(10)*
H(1S)	-5906(37)	4060(18)	7128(18)	76(12)*
H(2S)	-5161(37)	4980(18)	7141(18)	76(12)*
H(3S)	-3868(37)	4214(18)	7227(18)	76(12)*
C(2S)	4215(31)	5125(16)	6879(17)	76(8)*
C(3S)	3733(37)	5353(19)	6077(19)	109(11)*
H(4S)	4162(37)	4788(19)	6016(19)	76(12)*
H(5S)	4655(37)	5744(19)	5953(19)	76(12)*
H(6S)	2751(37)	5441(19)	5676(19)	76(12)*

*** isotropic temperature factor.**

$\underline{U}_{eq} = 1/3\ \Sigma_i \Sigma_j \underline{U}_{ij}\, \underline{a}_i^*\, \underline{a}_j^*\, (a_i \cdot a_j)$

Table 4.23 : Crystal data and details of the crystallographic analysis for $[Rh_2(\mu\text{-abipy})(O_2CCH_3)_3(NCPh)]$

Formula	$Rh_2C_{29}H_{27}N_4O_6$
Molecular mass ($g.mol^{-1}$)	733.367
Crystal system	Monoclinic
Space group	Cc
a (Å)	42.438(11)
b (Å)	8.458(3)
c (Å)	19.259(6)
α (°)	90
β (°)	115.81(2)
γ (°)	90
V ($Å^3$)	6223(4)
Z	8
D_c ($g.cm^{-3}$)	1.57
F (000)	3176
λ (Mo - K_α) (Å)	0.71069
Scan mode	ω - 2θ
ω scan angle	0.38 + 0.35tanθ
Horizontal aperture width (mm)	2.7 + 0.1tanθ
Scattering range (°)	$2 \leq \theta \leq 30$
μ (cm^{-1})	10.066
Absorption corrections	Semi empirical
Measured intensities	5892
Unique intensities	3621
Unique intensities [$I > 3\sigma(I)$]	2589
Structure solution	Direct and Fourier methods
Weighting scheme	$1/[(\sigma^2(F) + 0.006F^2)]$
$R = \Sigma(F_o\text{-}F_c)/\Sigma F_o$	0.0595
$R_w = \Sigma_w ½(F_o\text{-}F_c)/\Sigma_w ½F_o$	0.0646
$(\Delta/\sigma)_{max}$	1.392
$\Delta\rho_{max}(eÅ^{-3})$	1.533
Number of parameters	376

Table 4.24 : Interatomic distances (Å) for $[Rh_2(\mu\text{-abipy})(O_2CCH_3)_3(NCPh)]$

Rh(1)-Rh(2)	2.399(1)	Rh(1)-N(1)	2.190(10)
Rh(1)-N(2)	1.975(10)	Rh(1)-O(1)	2.051(9)
Rh(1)-O(3)	2.059(9)	Rh(1)-O(5)	2.033(8)
Rh(2)-N(3)	2.037(10)	Rh(2)-N(4)	2.256(11)
Rh(2)-O(2)	2.076(8)	Rh(2)-O(4)	2.027(9)
Rh(2)-O(6)	2.026(8)	N(1)-C(1)	1.34(2)
N(1)-C(5)	1.34(2)	N(2)-C(6)	1.39(2)
N(2)-C(10)	1.37(2)	N(3)-C(10)	1.34(2)
N(3)-C(11)	1.389(14)	N(4)-C(23)	1.14(2)
O(1)-C(17)	1.258(14)	O(2)-C(17)	1.278(14)
O(3)-C(19)	1.30(2)	O(4)-C(19)	1.23(2)
O(5)-C(21)	1.270(14)	O(6)-C(21)	1.268(14)
C(1)-C(2)	1.38(2)	C(2)-C(3)	1.37(2)
C(3)-C(4)	1.36(2)	C(4)-C(5)	1.41(2)
C(5)-C(6)	1.46(2)	C(6)-C(7)	1.39(2)
C(7)-C(8)	1.34(2)	C(8)-C(9)	1.35(2)
C(9)-C(10)	1.44(2)	C(12)-C(13)	1.395(0)
C(12)-C(11)	1.395(0)	C(13)-C(14)	1.395(0)
C(14)-C(15)	1.395(0)	C(15)-C(16)	1.395(0)
C(16)-C(11)	1.395(0)	C(17)-C(18)	1.51(2)
C(19)-C(20)	1.50(2)	C(21)-C(22)	1.48(2)
C(23)-C(24)	1.42(2)	C(25)-C(26)	1.395(0)
C(25)-C(24)	1.395(0)	C(26)-C(27)	1.395(0)
C(27)-C(28)	1.395(0)	C(28)-C(29)	1.395(0)
C(29)-C(24)	1.395(0)		

Table 4.25 : Interatomic angles (°) for $[Rh_2(\mu\text{-abipy})(O_2CCH_3)_3(NCPh)]$

Rh(2)-Rh(1)-N(1)	169.0(3)	Rh(2)-Rh(1)-N(2)	91.4(3)
N(1)-Rh(1)-N(2)	78.5(4)	Rh(2)-Rh(1)-O(1)	88.0(2)
N(1)-Rh(1)-O(1)	102.1(4)	N(2)-Rh(1)-O(1)	179.3(3)
Rh(2)-Rh(1)-O(3)	86.5(3)	N(1)-Rh(1)-O(3)	97.8(4)
N(2)-Rh(1)-O(3)	90.8(4)	O(1)-Rh(1)-O(3)	89.6(4)
Rh(2)-Rh(1)-O(5)	88.3(2)	N(1)-Rh(1)-O(5)	87.4(3)
N(2)-Rh(1)-O(5)	89.6(4)	O(1)-Rh(1)-O(5)	90.0(4)
O(3)-Rh(1)-O(5)	174.8(3)	Rh(1)-Rh(2)-N(3)	86.4(3)
Rh(1)-Rh(2)-N(4)	176.3(3)	N(3)-Rh(2)-N(4)	95.1(4)
Rh(1)-Rh(2)-O(2)	87.3(2)	N(3)-Rh(2)-O(2)	173.5(4)
N(4)-Rh(2)-O(2)	91.3(4)	Rh(1)-Rh(2)-O(4)	88.8(2)
N(3)-Rh(2)-O(4)	88.2(4)	N(4)-Rh(2)-O(4)	94.6(4)
O(2)-Rh(2)-O(4)	90.0(4)	Rh(1)-Rh(2)-O(6)	87.5(2)
N(3)-Rh(2)-O(6)	92.1(4)	N(4)-Rh(2)-O(6)	89.1(4)
O(2)-Rh(2)-O(6)	89.3(4)	O(4)-Rh(2)-O(6)	176.3(3)
Rh(1)-N(1)-C(1)	128.7(9)	Rh(1)-N(1)-C(5)	110.6(8)
C(1)-N(1)-C(5)	119.0(12)	Rh(1)-N(2)-C(6)	118.6(9)
Rh(1)-N(2)-C(10)	120.0(7)	C(6)-N(2)-C(10)	121.5(11)
Rh(2)-N(3)-C(10)	122.7(9)	Rh(2)-N(3)-C(11)	119.2(8)
C(10)-N(3)-C(11)	118.0(10)	Rh(2)-N(4)-C(23)	174.9(12)
Rh(1)-O(1)-C(17)	121.0(8)	Rh(2)-O(2)-C(17)	119.9(8)
Rh(1)-O(3)-C(19)	119.9(8)	Rh(2)-O(4)-C(19)	120.4(8)
Rh(1)-O(5)-C(21)	118.7(7)	Rh(2)-O(6)-C(21)	119.8(7)
N(1)-C(1)-C(2)	122(2)	C(1)-C(2)-C(3)	121(2)
C(2)-C(3)-C(4)	116.6(14)	C(3)-C(4)-C(5)	122(2)
N(1)-C(5)-C(4)	119.3(14)	N(1)-C(5)-C(6)	117.5(11)
C(4)-C(5)-C(6)	123.2(14)	N(2)-C(6)-C(5)	113.5(12)
N(2)-C(6)-C(7)	119.2(14)	C(5)-C(6)-C(7)	127.3(13)
C(6)-C(7)-C(8)	120.0(13)	C(8)-C(9)-C(10)	119.5(13)
N(2)-C(10)-N(3)	118.9(11)	N(2)-C(10)-C(9)	117.4(11)
N(3)-C(10)-C(9)	123.6(12)	C(13)-C(12)-C(11)	120.0(0)
C(12)-C(13)-C(14)	120.0(0)	C(13)-C(14)-C(15)	120.0(0)
C(14)-C(15)-C(16)	120.0(0)	C(15)-C(16)-C(11)	120.0(0)
N(3)-C(11)-C(12)	120.0(6)	N(3)-C(11)-C(16)	119.9(6)
C(12)-C(11)-C(16)	120.0(0)	O(1)-C(17)-O(2)	123.5(12)

Table 4.25/ Cont.

O(1)-C(17)-C(18)	118.8(12)	O(2)-C(17)-C(18)	117.7(12)
O(3)-C(19)-O(4)	124.1(12)	O(3)-C(19)-C(20)	114.7(13)
O(4)-C(19)-C(20)	121.2(13)	O(5)-C(21)-O(6)	125.3(11)
O(5)-C(21)-C(22)	117.5(11)	O(6)-C(21)-C(22)	117.2(11)
C(26)-C(25)-C(24)	120.0(0)	C(26)-C(27)-C(28)	120.0(0)
C(27)-C(28)-C(29)	120.0(0)	C(28)-C(29)-C(24)	120.0(0)
C(23)-C(24)-C(25)	122.0(6)	C(23)-C(24)-C(29)	117.8(6)
C(25)-C(24)-C(29)	120.0(0)		

Table 4.26 : Fractional coordinates ($x10^4$) and equivalent isotropic thermal factors ($Å^2$, $x10^3$) for $[Rh_2(\mu\text{-abipy})(O_2CCH_3)_3(NCPh)]$

	x/a	y/b	z/c	U_{eq}
Rh(1)	6829	6111(1)	359(1)	37
Rh(2)	6246	6725(1)	179(1)	36
N(1)	7357(2)	5208(13)	677(6)	49(3)
N(2)	6942(2)	5145(12)	1373(6)	39(2)
N(3)	6399(3)	5938(14)	1278(6)	52(3)
N(4)	5686(3)	7179(14)	-48(7)	55(3)
O(1)	6705(2)	7107(12)	-700(5)	52(2)
O(2)	6151(2)	7534(11)	-913(5)	50(2)
O(3)	6968(2)	8310(11)	860(5)	55(2)
O(4)	6417(2)	8905(11)	619(5)	49(2)
O(5)	6646(2)	3990(10)	-156(5)	43(2)
O(6)	6107(2)	4520(10)	-260(5)	46(2)
C(1)	7539(3)	5179(19)	256(9)	61(4)
H(1)	7455(3)	5915(19)	-251(9)	109(12)*
C(2)	7828(4)	4225(22)	445(13)	87(6)
H(2)	7964(4)	4198(22)	84(13)	109(12)*
C(3)	7946(4)	3290(24)	1087(13)	89(6)
H(3)	8176(4)	2556(24)	1254(13)	109(12)*
C(4)	7763(4)	3344(20)	1514(11)	80(5)
H(4)	7847(4)	2639(20)	2032(11)	109(12)*
C(5)	7464(3)	4304(16)	1308(8)	47(3)
C(6)	7259(3)	4364(15)	1751(8)	53(3)
C(7)	7351(4)	3754(17)	2482(9)	59(4)
H(5)	7599(4)	3154(17)	2774(9)	109(12)*
C(8)	7131(4)	3902(19)	2811(8)	56(4)
H(6)	7209(4)	3421(19)	3382(8)	109(12)*
C(9)	6819(3)	4647(17)	2455(7)	53(3)
H(7)	6650(3)	4778(17)	2740(7)	109(12)*
C(10)	6710(3)	5250(15)	1687(7)	41(3)
C(12)	6131(3)	7524(10)	1914(6)	69(5)
C(13)	5889(3)	7679(10)	2222(6)	76(5)
C(14)	5687(3)	6384(10)	2231(6)	72(5)

Table 4.26/ Cont.

C(15)	5727(3)	4934(10)	1933(6)	73(5)
C(16)	5969(3)	4779(10)	1625(6)	55(4)
C(11)	6170(3)	6074(10)	1616(6)	47(3)
H(8)	6287(3)	8526(10)	1907(6)	109(12)*
H(9)	5858(3)	8801(10)	2452(6)	109(12)*
H(10)	5501(3)	6504(10)	2469(6)	109(12)*
H(11)	5571(3)	3932(10)	1940(6)	109(12)*
H(12)	5999(3)	3657(10)	1394(6)	109(12)*
C(17)	6401(3)	7610(15)	-1112(8)	44(3)
C(18)	6325(5)	8346(18)	-1881(9)	67(4)
H(13)	6046(5)	8450(18)	-2066(9)	109(12)*
H(14)	6373(5)	7738(18)	-2319(9)	109(12)*
H(15)	6440(5)	9510(18)	-1791(9)	109(12)*
C(19)	6731(4)	9239(14)	887(8)	50(4)
C(20)	6866(5)	10795(17)	1280(10)	75(5)
H(16)	6675(5)	11080(17)	1490(10)	109(12)*
H(17)	6843(5)	11619(17)	831(10)	109(12)*
H(18)	7126(5)	10873(17)	1748(10)	109(12)*
C(21)	6327(3)	3647(15)	-358(7)	40(3)
C(22)	6203(3)	2076(16)	-716(9)	54(4)
H(19)	6398(3)	1454(16)	-831(9)	109(12)*
H(20)	5987(3)	2399(16)	-1255(9)	109(12)*
H(21)	6111(3)	1320(16)	-392(9)	109(12)*
C(23)	5411(4)	7382(17)	-107(8)	51(4)
C(25)	4842(2)	8724(12)	-779(5)	62(4)
C(26)	4511(2)	9061(12)	-833(5)	69(4)
C(27)	4398(2)	8341(12)	-328(5)	86(6)
C(28)	4617(2)	7285(12)	230(5)	84(6)
C(29)	4949(2)	6949(12)	283(5)	72(5)
C(24)	5061(2)	7669(12)	-222(5)	50(4)
H(22)	4929(2)	9281(12)	-1170(5)	109(12)*
H(23)	4341(2)	9878(12)	-1264(5)	109(12)*
H(24)	4142(2)	8601(12)	-369(5)	109(12)*
H(25)	4530(2)	6728(12)	620(5)	109(12)*
H(26)	5119(2)	6132(12)	715(5)	109(12)*

Table 4.26/ Cont.

*** isotropic temperature factor.**

$$\underline{U}_{eq} = 1/3\ \Sigma_i \Sigma_j \underline{U}_{ij}\, \underline{a}_i^{*}\, \underline{a}_j^{*}\, (a_i \cdot a_j)$$

Appendix A

General experimental details

A1) Instrumentation

Carbon, hydrogen and nitrogen analysis were performed by the Microanalytical Laboratory of the Chemistry Department at the University of Natal in Pietermaritzburg and by Galbraith Laboratories, Knoxville, Tennessee, U.S.A. Infrared spectra were recorded on a Shimadzu FT-1400 infrared spectrometer. ^{1}H and ^{13}C NMR spectra were recorded on a Gemini 200 MHz spectrometer. Deuterated solvents were employed in all cases. Mass spectra were recorded on a Hewlet-Packard Gas Chromatographic-Mass Spectrometer (HP5988A). Absorbtion spectra were recorded on a Shimadzu UV-2101PC UV-Vis Scanning Spectrophotometer.

A2) Experimental techniques

All reactions, unless otherwise stated, were performed under an atmosphere of dry nitrogen gas, using standard Schlenk techniques. All solvents were freshly distilled and dried prior to use, using standard proceedures[35]. In the case of the molybdenum work both methanol and acetone were freeze-thawed under argon prior to their use.

A3) Crystal structure determination

a) Data collection:

The intensities of the reflections were measured at 22°C with an Enraf-Nonius CAD-4 diffractometer using graphite monochromated Mo-Kα radiation.

Cell constants were obtained by fitting the setting angles of 25 high-order reflections (θ >12°). Three standard reflections were measured every hour to check any possible decomposition of the crystal. An ω-2θ scan with a variable speed up to a maximum of 5.49°.min^{-1} was used. The ω-

angle changed as a_θ, b_θ, a_h and b_h were determined for each crystal by a critical evaluation of peak shape for several reflections with different values of θ using the program OTPLOT (Omega-Theta plot; Enraf-Nonius diffractometer control program, 1988). Where applicable, a linear decay correction was applied using the mean value linear curves fitted through three intensity control reflections, measured at regular time intervals. Data were corrected for Lorentz and polarization effects, and where possible for absorbtion by the psi-scan (semi empirical) method[67].

b) Structural solution refinement:

Direct methods or the Patterson function where used to solve the phase problem. Once a suitable phasing model was found, successive applications of Fourier and difference Fourier techniques allowed the location of the remaining non-hydrogen atoms. Hydrogen atoms were not located in any of the structures reported in this thesis. Weighted full-matrix least-squares methods were always used to refine the structure; the weighting scheme was chosen so as to find the smallest variation of the mean value of $\omega(F_o-F_c)^2$ as a function of the magnitude of F_o . R, R_w and the weighting scheme are defined as follows:

$$= \frac{\Sigma \left| F_O - F_C \right|}{\Sigma \left| F_O \right|} \quad , \quad R_W = \frac{\Sigma \omega^{1/2} \left| F_O - F_C \right|}{\Sigma \omega^{1/2} \left| F_O \right|}$$

and $\omega = 1.0/ [\theta^2(F) + gF^2]$, where g is a variable.

Scattering factor data were taken from "International Tables for X-ray Crystallography", Kynoch Press, Birmingham, Vol. 4 (1974), pp94,149. For all the structure solution calculations, the programs SHELX-76 [68] and SHELX-86[69] were employed. Mean plane and torsion angle calculations were performed using the programs PLANE and TORSION of the SDS package[70]. Plotting of structures was performed using the program ORTEP-II [71] while the tabulation of fractional coordinates, thermal parameters, interatomic distances and angles was achieved using the program TABLES [72].

Appendix B

Sources of chemicals

B1) Commercially available chemicals:

The following chemicals were all purchased from the indicated supplier and were all used without further purification.

I) Chemicals obtained from **SAARchem**.:
Aniline, piperidine, PCl_5, $MgSO_4$, $K_3[Fe(CN)_6]$, H_2O_2, acetic anhydride.

ii) Chemicals obtained from **Fluka**:
2,2'-bipyridine, $RuCl_3 \cdot 3H_2O$, MeI, HPF_6, $Cu(ClO_4)_2 \cdot 6H_2O$, benzonitrile.

iii) Chemicals obtained from **Strem Chemicals**:
$Mo(CO)_6$, $Ru_3(CO)_{12}$.

iv) Chemicals obtained from **E.Merk**:
$POCl_3$, glacial acetic acid.

v) Chemicals obtained from **Acros**:
N-methylaniline.

B2) Chemicals synthesised by published methods:

The following chemicals were synthesised by literature methods:

Compound	Literature references
$[Cu(MeCN)_4](PF_6)$	64
$[\{Ru_2(CO)_4(O_2CCH_3)_2\}_n]$	38
$[Ru_2(O_2CCH_3)_4Cl]_n$	42
$[Mo_2(O_2CCH_3)_4]$	65
6-chloro-2,2'-bipyridine	34
2,2'-bipyridin-6-one	66

In the preparation of 2,2'-bipyridin-6-one, purification of the N-oxide by HPLC was found to be unnecessary, instead recrystallisation of the N-oxide from ether-petroleum ether 60-80°C gave sufficiently pure material. In the preparation of $[Ru_2(O_2CCH_3)_4Cl]_n$ best results were achieved by using a large excess of acetic anhydride and heating the reaction mixture of $RuCl_3 \cdot 3H_2O$, glacial acetic acid and acetic anhydride to 150°C.

B3) Other sources:

Dr. C.Raab for his kind donation of $[Rh_2(O_2CCH_3)_4]$.

Appendix C

Calculation of the minimum distance of the α-protons from the copper atom in $[Cu(\eta^2\text{-pipbipy})_2]^+$

Assumption : the minimum distance of the α-protons from the copper atom illustrated in Fig. A can be calculated by assuming symmetrical rotation of the piperidyl group about the N3-C10 axis.

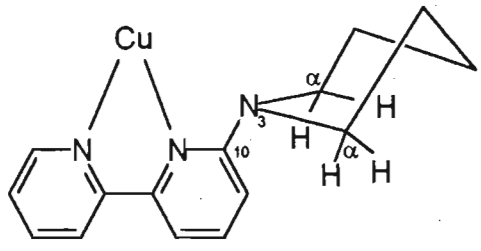

Fig. A

Hypothesis: the minimum distance of any H_α from Cu is achieved when Cu, C10, N3 and H_α are coplanar.

Proof: Consider Fig.B:

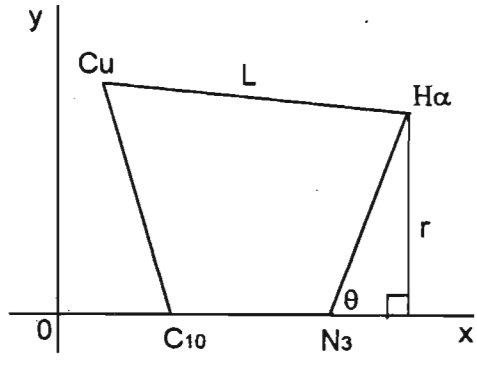

Fig. B

The distance L between Cu and H_α for a cartesian set of axes (x, y, z) is given by the general equation:

$$L = [\,(x_{Cu} - x_{H\alpha})^2 + (y_{Cu} - y_{H\alpha})^2 + (z_{Cu} - z_{H\alpha})^2\,]^{1/2}$$

$$= [(x_{Cu})^2 - 2(x_{Cu})(x_{H\alpha}) + (x_{H\alpha})^2 + (y_{Cu})^2 - 2\,(y_{Cu})(y_{H\alpha}) + (y_{H\alpha})^2 + (z_{Cu})^2$$

$$- 2(z_{Cu})(z_{H\alpha}) + (\,z_{H\alpha})^2\,]^{1/2} \qquad \text{— (1)}$$

The H_α atom is free to rotate about the C10-N3 axis by an angle θ subtended at N3. Since rotation is by definition about the x-axis, the $x_{H\alpha}$ coordinate is constant and only the $y_{H\alpha}$ and $z_{H\alpha}$ coordinates of H_α are variable. The R.H.S. of eqn. **1** becomes:

$$[\ \underset{\text{const.}}{(x_{Cu})^2} - \underset{\text{const.}}{2(x_{Cu})(x_{H\alpha})} + \underset{\text{const.}}{(x_{H\alpha})^2} + \underset{\text{const.}}{(y_{Cu})^2} - \underset{\text{var.}}{2\,(y_{Cu})(y_{H\alpha})} + \underset{\text{var.}}{(y_{H\alpha})^2} + \underset{\text{const.}}{(z_{Cu})^2}$$

$$\underset{\text{var.}}{- 2(z_{Cu})(z_{H\alpha})} + \underset{\text{var.}}{(\ z_{H\alpha})^2}\ ]^{1/2}$$

If Cu, C10, and N3 lie in the z plane where $z = 0$, then the R.H.S. of eqn. **1** becomes :

$$[\ \text{const.} + (y_{H\alpha})^2 + (z_{H\alpha})^2 - 2(y_{Cu})(y_{H\alpha})\ ]^{1/2}$$

Since $(y_{H\alpha})^2 + (z_{H\alpha})^2 = r^2 = \text{const.}$

The R.H.S. of eqn **1** becomes :

$$L = [\ \text{const.} - 2(y_{Cu})(y_{H\alpha})\ ]^{1/2}$$

By inspection of Fig. B y_{Cu} is always in the same quadrant as $y_{H\alpha}$ and will have the same sign. Thus L is smallest when $y_{H\alpha}$ is maximum which will occur when H_α is in the same plane as Cu, C10 and N3.

Calculation of minimum H_α-Cu distance.

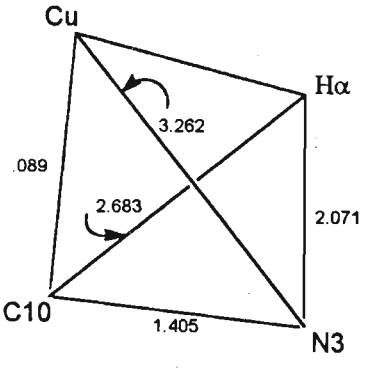

Fig. C

In Fig. C the Cu, C10, N3 and H_α atoms are coplanar and all lengths are given in Å. The H_α-N3 and H_α-C10 distances are the average distances of the four α-protons from N3 and C10 respectively. The distances between atoms were calculated using the eqn.[73] :

$$\text{distance} = [\ (\Delta xa)^2 + (\Delta yb)^2 + (\Delta zc)^2 + 2ab\Delta x\Delta y\cos\gamma + 2ac\Delta x\Delta z\cos\beta + 2bc\Delta y\Delta z\cos\alpha\ ]^{1/2}$$

where Δx, Δy, Δz are fractional coordinates obtained from Table 3.10 and a, b, c, α, β and γ are the unit cell parameters listed in Table 3.9.

Let the angle Cu-C10-N3 = ϕ

$$\text{then } \cos\phi = (a^2 - b^2 - c^2) / (-2bc) = [\ (3.262)^2 - (3.089)^2 - (1.405)^2\ ] / -2(3.089)(1.405)$$
$$= 0.100848$$
$$\therefore\ \phi = 84.212°$$

Let the angle H_α-C10-N3 = ψ

$$\text{then } \cos\psi = [\ (2.071)^2 - (2.683)^2 - (1.405)^2\ ] / -2(2.683)(1.405)$$
$$= 0.64775$$
$$\therefore\ \psi = 49.628°$$

Let the angle Cu-C10-H_α = ω

$$\text{then } \omega = \phi - \psi = 84.212° - 49.628°$$
$$= 34.584°$$

$$\text{then the Cu-}H_\alpha\text{ distance} = (\ b^2 + c^2 - 2bc\cos\omega\ )^{1/2}$$
$$= [\ (3.089)^2 + (2.683)^2 - 2(3.089)(2.683)\text{Cos}(34.584°)\ ]^{1/2}$$
$$= \underline{1.759\ \text{Å}}$$

References

1. F.A. Cotton and R.A. Wilkinson, in *'Multiple Bonds Between Metal Atoms'* , 2nd Ed ., Clarendon Press, Oxford (1993) .
2. A.R. Chakravarty, F.A. Cotton, and E.S. Shamshoum, *Inorg. Chem.*, 1984, **23**, 4216.
3. F.A. Cotton, R.H. Niswander, and J.C. Sekutowski, *Inorg. Chem.*, 1978, **17**, 3541.
4. F.A. Cotton, C.E. Rice, and G.W. Rice, *J. Am. Chem. Soc.*, 1977, **99**, 4704.
5. S.N. Ketkar and M. Fink, *J. Am. Chem. Soc.*, 1985, **107**, 338.
6. F.A. Cotton, P.E. Fanwick, R.H. Niswander, and J.C. Sekutowski, *J. Am. Chem. Soc.*,1978, **100**, 4725.
7. W. Clegg, C.D. Garner, L. Akhter, and M.H. Al-Samman, *Inorg. Chem.*, 1982, **22**, 2466.
8. F.A. Cotton, L.R. Falvello, S. Han, and W. Wang, *Inorg. Chem.*, 1983, **22**, 4106.
9. F.A. Cotton and T.R. Felthouse, *Inorg. Chem.*, 1981, **20**, 584.
10. J.L. Bear, C.-L. Yao, L.-M. Liu, F.J. Capdevielle, J.D. Korp, T.A. Albright, S.-K. Kang, and K.M. Kadish, *Inorg. Chem.*, 1989, **28**, 1254.
11. A.R. Chakravarty, F.A. Cotton, and D.A. Tocher, *Inorg. Chem.*, 1985, **24**, 172.
12. H.J. McCarthy and D.A. Tocher, *Polyhedron*, 1992, **11**, 13.
13. P.L. Andreu, J.A. Cabeza, V. Riera, Y. Jeannin, and D. Miguel, *J. Chem. Soc. Dalton Trans.*, 1990, 2201.
14. W. Clegg, L. Akhter and C. D. Garner, *J. Chem. Soc., Chem. Comm.*, 1984, 101.
15. A.J. Blake, R.O. Gould, J.M. Rowson, and R.E.P. Winpenny, *J. Chem. Soc. Dalton Trans.*, 1994, 2005.
16. A.R. Chakravarty, F.A. Cotton, and D.A. Tocher, *Inorg. Chem.*, 1984, **23**, 4030.
17. L.Steven Hollis and S.J. Lippard, *Inorg. Chem.*, 1983, **22**, 2708.
18. K.W. Henderson, R.E. Mulvey, W. Clegg, and P.A. O'Neil, *J. Organomet. Chem.*, 1992, **439** , 237 .
19. E.C. Morrison, C.A. Palmer, and D.A. Tocher, *J. Organomet. Chem.*, 1988, **349**, 403.
20. A.R. Chakravarty, F.A. Cotton, and E.S. Shamshoum, *Inorg Chim Acta*, 1984, **86**, 5.
21. F.A. Cotton G.E. Lewis, and G.N. Mott, *Inorg. Chem.*, 1983, **22**, 378.
22. A.R. Chakravarty and F.A. Cotton, *Inorg. Chim. Acta*, 1985, **105**, 19.
23. M.F. Summers, P. J. Toscano, N. Bresciani-Pahor, G. Nardin, L. Randaccio and L. G. Marzilli, *J. Am. Chem. Soc.*, 1983, **105**, 6259.
24. D.X. West, S.F. Pavkovic, and J.N. Brown, *Acta Cryst.* 1980, **B36**, 143.
25. A.R. Chakravarty, F.A. Cotton, and D.A. Tocher, *Organomet.*, 1985, **4**, 863.
26. A.T. Baker, W.R. Tikkanen, W.C. Kaska, and P.C. Ford, *Inorg. Chem.*, 1984, **23**, 3254.

27. E. Binamira-Soriaga, S. Sprouse, R. Watts, W. Kaska, *Inorg. Chim. Acta*, 1984, **84**, 135.

28. W.R. Tikkanen, E. Binamira-Soriaga, W.C. Kaska, and P.C. Ford, *Inorg. Chem.*, 1984, **23**, 141.

29. J.R. Pugh, M.R.M. Bruce, B.P. Sullivan, T.J. Meyer, *Inorg. Chem.*, 1991, **30**, 86.

30. C.M. Bollinger, N. Story, B.P. Sullivan, T. J. Meyer, *Inorg. Chem.*, 1988, **27**, 4582.

31. F.A. Cotton and G. Wilkinson, in *'Advanced Inorganic Chemistry'*, 3rd Ed., John Wiley and sons, USA, 1966.

32. F.H. Burstall, *J. Chem. Soc.*, 1938,1662.

33. B.E. Halcrow and W.O. Kermack, *J. Chem. Soc.*, 1946,155.

34. J.S. Field, R.J. Haines, C.J. Parry, and S.H. Sookraj , *S. Afr. J. Chem.*, 1993, **46**, 70.

35. D.D. Perrin, W.L.F. Amarego, D.R. Perrin, in *'Purification of Laboratory Chemicals'*, 2nd Ed., Pergamon Press, New York, 1980.

36. L.L. Merrit, E.D. Shroeder, *Acta Cryst.*, 1956, **9**, 801.

37. J.S. Field, R.J. Haines, C.J. Parry and S.H. Sookraj, *Polyhedron*, 1993, **12**, 2425.

38. G.R. Crooks, B.F.G. Johnson, J. Lewis, I.G.Williams and G. Gamlen, *J. Chem. Soc.*(A), 1969, 2761

39. S.J. Sherlock, M. Cowie, E. Singleton and M.M de V.Steyn, *J. Organomet. Chem.*, 1989, **361**, 353.

40. M. Mintert and W.S. Sheldrick, *J. Chem. Soc. Dalton Trans.*, 1995, 2663.

41. P.L Andreu, J.A. Cabeza, G.A. Carriedo, V. Riera, S. García-Granda, J.F. Van der Maelen and G. Mori, *J. Organomet. Chem.*,1991, **421**, 305.

42. T.A. Stephenson and G. Wilkinson, *J. Inorg. Nucl. Chem.*, 1966, **28**, 2285.

43. M. Mintert and W.S. Sheldrick, *Inorg. Chim. Acta*, 1995, **236**, 13.

44. M. Mintert and W.S. Sheldrick, *Inorg. Chim. Acta*, 1994, **219**, 23.

45. A.R. Chakravarty , F.A. Cotton , and D.A. Tocher , *Inorg. Chem.*, 1985 , **24**, 1263.

46. J.A. Cabeza, C. Landazuri, L.A. Oro, A. Tiripicchio and M. Tiripicchio-Camellini, *J. Organomet. Chem.*, 1987, **C16**, 322.

47. S.J. Sherlock, M. Cowie, E. Singleton and M.M de V.Steyn, *Organometallics*, 1988, 7, 1663.

48. M. Spohn, T. Vogt and J. Strühle, *Z. Naturforsch.* B, 1986, **41**, 1373.

49. H. Schumann, J. Opitz and J. Pickardt, *J.Organomet. Chem.*, 1977, **128**, 253.

50. M. Mintert and W.S. Sheldrick, *Chem. Ber.*, 1996, **129**, 683.

51. D.M. Baird, K.Y. Shih, J.H. Welch and R.D. Bereman, *Polyhedron*, 1989, **8**, 2359.

52. D.M. Collins, F.A. Cotton and C.A. Murillo, *Inorg. Chem.*, 1976, **15**, 1861.

53. F.A. Cotton and J. Norman Jr., *J. Am.Chem. Soc.*, 1972, **94**, 5697.

54. T.R. Felthouse. *Prog. Inorg. Chem.*, 1982, **29**, 73.

55. E.B. Boyer and S.D. Robinson, *Cood. Chem. Rev.*, 1983, **50** 109.

56. E.B. Boyer and S.D. Robinson, *Platinum Met. Rev.*, 1982, *26*, 65.

57. I.B. Baranovskii, *Russ. J. Inorg. Chem.*, 1982, **27**, 759.

58. C.-L. Yao, K.H. Park, A.R. Khokhar, M.-J. Jun, and J.L. Bear, *Inorg. Chem.*, 1990, **29**, 4033.

59. W. Clegg, *Acta Crystallogr.*, 1980, **B36**, 2437.

60. A.J. Deeming, M.N.N. Meah, H.M. Dawes and M.B. Hursthouse, *J. Organmet. Chem.*, 1986, **C25**, 299.

61. D.A. Tocher and J.L. Tocher, *Inorg. Chim. Acta*, 1985, **104**, L15.

62. E. Binamira-Soriaga, N.L. Keder and W.C. Kaska, *Inorg. Chem.*, 1990, **29**, 3167.

63. The Chemical Society London, in ` *Interatomic Distances Supplement*', Special Publication No.18, Eyre and Spottiswoode Ltd, Kent (1965).

64. G.J. Kubas, *Inorg. Syn.*,1979, **19**, 90.

65. A.B. Brignole and F. A. Cotton, *Inorg. Synth.*,1972, **13**, 81.

66. D.B. Moran, G.O. Morton and J.D. Albright, *J. Heterocyclic Chem.*, 1986, **23**, 1071.

67. A.C.T. North, D.C. Philips and F.S. Mathews, *Acta Crystallogr., Sect. A.*, 1968, **24**, 351.

68. G. Sheldrick, SHELX-76, Program for Crystal Structure Determination, University of Cambridge, 1976.

69. G. Sheldrick, SHELX-86, Program for Crystal Structure Determination, University of Göttingen, 1976.

70. Structure Determination Package, B.A. Frenze and Associates Inc., College Station, Texas 77480, U.S.A.; and Enraf-Nonius, Delft, Holland, 1985.

71. C. Johnson, ORTEP-II, A Fortran Thermal Ellipsoid Programme for Crystal Structure Illustrations, Oak Ridge National Laboratory, Tennessee, 1976.

72. D. Liles, TABLES, Program for Tabulation of Crystallographic Data, Council for Scientific and Industrial Research (pretoria), 1988.

73. G.H. Stout and L.H. Jensen in `*X-ray Sructure Determination- A practical Guide*', 1968, Macmillan Publishing Co., New York, U.S.A.